

THE UNIVERSITY OF MICHIGAN
ANN ARBOR, MICHIGAN

FINAL REPORT

FOR

RESEARCH AND DEVELOPMENT ON HIGH-POWER CRESTATRONS

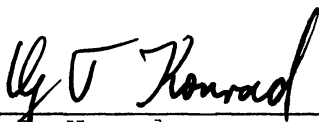
FOR THE 100-300 MC FREQUENCY RANGE

This report covers the period July 1, 1960 to December 31, 1965

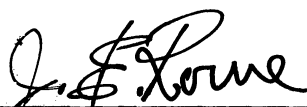
Electron Physics Laboratory
Department of Electrical Engineering

By: G. T. Konrad

Approved by:



G. T. Konrad
Project Engineer



J. E. Rowe, Director
Electron Physics Laboratory

Project 03783

NAVY DEPARTMENT BUREAU OF SHIPS
ELECTRONICS DIVISION
CONTRACT NO. Nobsr-81403
PROJECT SERIAL NO. SF0100 201
TASK NO. 9294

September, 1965

ABSTRACT

Research and development work on VHF Crestatrons is described. Design parameters for both 100- and 1000-watt, cw, electrostatically focused tubes are presented. The 100-watt tube is described in much more detail, because it was completely tested. Details of the cold-test work, beam analyzer tests on the electron gun and focusing system, beam transmission tests and r-f tests are described fully.

Digital computer programs are described, which were developed for the analysis of electrostatically focused beam systems. The gun region as well as the electrostatic focusing region can be analyzed. The designs of two $P_{\mu} = 20$ guns are checked with these computer programs.

The details of design, construction and performance evaluation of a series of magnetically focused traveling-wave tubes for the 100-300 mc frequency region are presented. These tubes yield a minimum of 100 watts, cw at a minimum of 10 db gain throughout this frequency region. The three tubes to be delivered to the Navy were built so as to meet environmental specifications. Results of the environmental tests are presented.

TABLE OF CONTENTS

| | <u>Page</u> |
|--|-------------|
| ABSTRACT | iii |
| LIST OF ILLUSTRATIONS | vii |
| LIST OF TABLES | xii |
| LIST OF PUBLICATIONS | xiii |
| PERSONNEL | xiv |
| <u>PART I</u> | |
| 1. INTRODUCTION | 2 |
| 2. ELECTROSTATICALLY FOCUSED 100-WATT VHF AMPLIFIERS | 3 |
| 2.1 Design Parameters for the Electrostatically Focused Crestatrons | 3 |
| 2.1.1 Helix Design | 4 |
| 2.1.2 Electron Gun Design | 6 |
| 2.1.3 Focusing System Design | 9 |
| 2.1.4 Beam Collector Design | 11 |
| 2.2 Cold Test Results | 11 |
| 2.3 Beam Analyzer Tests on the $P_{\mu} = 4.46$ Hollow Beam Gun | 14 |
| 2.4 Electrostatic Focusing Tests | 22 |
| 2.5 Digital Computer Calculations on the $P_{\mu} = 4.46$ Gun and Focusing System | 24 |
| 2.6 Performance of the 100-Watt Electrostatically Focused Tube | 29 |
| 3. HIGH PERVEANCE HOLLOW-BEAM GUN STUDIES | 37 |
| 3.1 Design of Two $P_{\mu} = 20$ Guns | 37 |
| 3.2 Beam Analyzer Tests of the 1.076 Inch Diameter, $P_{\mu} =$ 20 Gun | 41 |
| 4. SUMMARY AND CONCLUSIONS | 43 |
| 5. RECOMMENDATIONS FOR FUTURE WORK | 45 |

| | <u>Page</u> |
|---|-------------|
| <u>PART II</u> | |
| 1. INTRODUCTION | 47 |
| 2. ELECTROSTATICALLY FOCUSED TUBES | 50 |
| 2.1 Electrical Design of Electrostatically Focused Tubes | 50 |
| 2.1.1 Collector Design | 50 |
| 2.1.2 Electron Guns | 52 |
| 2.1.3 R-f Match | 57 |
| 2.2 Mechanical Design | 57 |
| 3. PHASE I -- 100-WATT MAGNETICALLY FOCUSED CRESTATRON FEASIBILITY STUDIES | 63 |
| 3.1 TW-143 | 63 |
| 3.1.1 Electrical Design | 65 |
| 3.1.2 Mechanical Design | 78 |
| 3.1.3 Experimental Results | 78 |
| 3.2 TW-147 | 84 |
| 3.2.1 Electrical Design | 89 |
| 3.2.2 Mechanical Design | 90 |
| 3.2.3 Experimental Results | 90 |
| 4. PHASE II -- DEVELOPMENT OF DELIVERABLE 100-WATT MAGNETI- CALLY FOCUSED CRESTATRON | 97 |
| 4.1 Electrical Design of TW-148 | 99 |
| 4.1.1 R-f Circuit | 99 |
| 4.1.2 Electron Gun | 100 |
| 4.1.3 R-f Match | 101 |
| 4.2 Mechanical Design | 103 |
| 4.3 Focusing Methods | 104 |
| 4.3.1 Periodic Permanent Magnets | 104 |
| 4.3.2 Straight Permanent Magnets | 106 |
| 4.3.3 Solenoids | 108 |
| 4.4 Test Results | 108 |
| 5. SUMMARY AND CONCLUSIONS | 124 |
| 6. RECOMMENDATIONS | 132 |

| | <u>Page</u> |
|---|-------------|
| APPENDIX A. TENTATIVE SPECIFICATIONS FOR TW-148 | 133 |
| APPENDIX B. VIBRATION TESTS | 134 |
| APPENDIX C. SHOCK TESTS | 140 |
| APPENDIX D. R-F TEST SETUP | 145 |

LIST OF ILLUSTRATIONS

PART I

| <u>Figure</u> | | <u>Page</u> |
|---------------|--|-------------|
| 2.1 | Diagram of the $P_{\mu} = 4.46$ Gun with an Einzel Lens. | 7 |
| 2.2 | Photograph of the $P_{\mu} = 4.46$ Gun. | 8 |
| 2.3 | Electrostatic Focusing Scheme. | 10 |
| 2.4 | Phase Velocity as a Function of Frequency for the 100-Watt Electrostatically Focused Crestatron Helix. | 12 |
| 2.5 | Synchronous Voltage, Dielectric Loading Factor and Insertion Loss for the 100-Watt Electrostatically Focused Crestatron Helix. | 13 |
| 2.6 | Impedance as a Function of Frequency for the 100-Watt Electrostatically Focused Crestatron Helix. | 15 |
| 2.7 | Schematic Diagram of Gridded Beam Collector. | 17 |
| 2.8 | $P_{\mu} = 4.46$ Gun Mounted in the Beam Analyzer. | 18 |
| 2.9 | Comparison of Beam Profiles as a Function of Lens Voltage at a Distance of 0.150 Inch from the Final Gun Anode. | 19 |
| 2.10 | Comparison of Beam Profiles as a Function of Anode-Collector Spacing, d . (Lens Voltage = -900 Volts) | 20 |
| 2.11 | Beam Spread as a Function of Distance from the Final Gun Anode. (Lens Voltage = -900 Volts) | 21 |
| 2.12 | Schematic Diagram of the Focusing Tester. | 23 |
| 2.13 | Optimum Transmission for the Condition $V_{D_1} - V_o = V_o - V_{D_2}$. ($V_{D_1} = V_{D_3}$, $V_{D_2} = V_{D_4} = V_{D_5} = V_{D_6}$) | 25 |
| 2.14 | Electron Trajectories in the Gun Region. | 27 |
| 2.15 | Electron Trajectories in the Electrostatic Focusing Region. (Helix Voltage = V_o Volts) | 28 |
| 2.16 | Electrostatically Focused Crestatron. | 30 |
| 2.17 | Test Area for the Electrostatically Focused Crestatron. | 31 |

| <u>Figure</u> | | <u>Page</u> |
|--------------------|--|-------------|
| 2.18 | Small-Signal Electronic Gain vs. Frequency. | 32 |
| 2.19 | Saturation Gain for $V_K = -1800$ Volts. ($I_K = 90$ ma) | 33 |
| 2.20 | Beam Transmission vs. P_{out} for $V_K = -1800$ Volts. | 35 |
| 2.21 | Gain vs. P_{out} for $V_K = -1800$ Volts. ($I_K = 90$ ma) | 36 |
| 3.1 | Trajectory Plot for Large Diameter $P_\mu = 20$ Gun. ($J_o = 3.722 \cdot 10^3$ Amp/m ² , $P_\mu = 17.97$, $2r = 1.076$ Inch) | 39 |
| 3.2 | Trajectory Plot for Small Diameter $P_\mu = 20$ Gun. ($J_o = 7.203 \cdot 10^3$ Amp/m ² , $P_\mu = 19.573$, $2r = 0.660$ Inch) | 40 |
| 3.3 | Beam Profiles as a Function of Lens Voltage at a Distance of 0.10 Inch from the Last Gun Anode. | 42 |
| <u>PART II</u> | | |
| 2.1 | Subassemblies for 100-Watt Tube. | 51 |
| 2.2 | Typical Beam Contours. 1 Kilowatt Tube. ($V = 1000$ Volts). | 53 |
| 2.3 | Typical Beam Contours. 1 Kilowatt Tube. ($V = 4000$ Volts). | 53 |
| 2.4 | Beam Contours. (100-Watt Tube). | 54 |
| 2.5 | Collector Area as a Function of Electrode Potential. (1 Kilowatt Tube). | 54 |
| 2.6 | Electron Trajectories in Collector Region. | 55 |
| 2.7 | 4.46 Micropervance Electron Gun Configuration. | 55 |
| 2.8 | Tangential Transition. | 58 |
| 2.9 | VSWR of Single Transition. | 59 |
| 2.10 | VSWR of Two-Transition System. | 59 |
| 2.11 | Envelope Forming Furnace. | 62 |
| 3.1 | Detailed Assembly Drawing of Gun | 69 |

| <u>Figure</u> | | <u>Page</u> |
|---------------|--|-------------|
| 3.2 | Photos of the Electron Beam from the Gun Tester. | 69 |
| 3.3 | Voltage Reflection (VSWR vs. L/λ). | 73 |
| 3.4 | VSWR Versus Frequency for Tube No. 3. | 74 |
| 3.5 | R-f Match of the Coupled Helix. | 76 |
| 3.6 | Comparison of Insertion Losses. | 76 |
| 3.7 | Configuration of Folded Helix Matching Section. | 77 |
| 3.8 | VSWR of Folded Helix Match. | 77 |
| 3.9 | Cross Section of Coupled-Helix Tube. | 79 |
| 3.10 | Power Out of Tube No. 4 (100-300 mc). | 83 |
| 3.11 | Performance Characteristics of Tube No. 4 (400-1000 mc). | 83 |
| 3.12 | Power Out of Tube No. 7. | 85 |
| 3.13 | Power Out of Tube No. 8. | 85 |
| 3.14 | Power Output of TWT-143-A-10. | 86 |
| 3.15 | Power Output of TWT-143-A-9. (I_K) = 400 ma. | 86 |
| 3.16 | Small-Signal Response vs. Frequency, TWT-143-A-9 Power Output vs. Frequency at 1 Watt Drive which is 3 to 6 db Below Saturating Drive Level. | 87 |
| 3.17 | Power Output Characteristics of TWT-143-A-14. (I_K = 300 ma). | 87 |
| 3.18 | Power Output Characteristics of TWT-143-A-14. (I_K = 400 ma). | 88 |
| 3.19 | Power Output vs. Power Input TWT-143-A-18. | 88 |
| 3.20 | TW-147 Cross-Section View. | 91 |
| 3.21 | VSWR and Insertion Loss vs. Frequency TW-147-1. | 92 |
| 3.22 | VSWR and Insertion Loss vs. Frequency TW-147-2. | 92 |
| 3.23 | Power Output vs. Power Input TW-147-1. | 93 |
| 3.24 | Power Output vs. Power Input TW-147-2. | 93 |
| 3.25 | Maximum Power Output and Saturated Gain vs. Frequency TW-147-3. | 95 |

| <u>Figure</u> | | <u>Page</u> |
|---------------|--|-------------|
| 3.26 | Small-Signal Synchronous Voltage -- Low Beam Current TW-147-3. | 95 |
| 3.27 | Power Output and Gain vs. Frequency -- Medium Current TW-147-3. | 96 |
| 4.1 | TW-148 100-Watt Magnetically Focused Crestatron. | 98 |
| 4.2 | TW-148 Electron Gun Cross Section. | 102 |
| 4.3 | TW-148 Cross Section. | 105 |
| 4.4 | Outline of Estimated Permanent Magnet Required to Focus TW-148. | 107 |
| 4.5 | TW-148 Solenoid, Type 9. | 109 |
| 4.6 | Power Output vs. Frequency with 7 Watts Input Drive; TW-148-2. | 111 |
| 4.7 | Power Output vs. Frequency for TW-148-2R; 7-Watt and 30-Watt Drives. | 111 |
| 4.8 | Power Output vs. Power Input Before Environmental Tests; TW-148-3R. | 113 |
| 4.9 | Power Output vs. Power Input After Vibration; TW-148-3R. | 113 |
| 4.10 | Power Output vs. Power Input After Vibration and Shock Tests; TW-148-3R. | 114 |
| 4.11 | Power Output vs. Frequency at 10-Watts Drive; TW-148-3R. | 114 |
| 4.12 | Maximum Power Output vs. Frequency - Optimum Drive Power; TW-148-3R. | 115 |
| 4.13 | $P_{o\max}$ vs. f TW-148-4. | 115 |
| 4.14 | P_o vs. P_{in} , Filtered, TW-148-4R. | 117 |
| 4.15 | P_o vs. P_{in} , Unfiltered, TW-148-4R. | 117 |
| 4.16 | $P_{o\max}$ vs. f - TW-148-4R. | 118 |
| 4.17 | Gain vs. f ., Filtered, TW-148-4R. | 118 |
| 4.18 | Gain vs. f ., Unfiltered, TW-148-4R. | 120 |
| 4.19 | $P_{o\max}$ vs. f TW-148-5RR. | 120 |

| <u>Figure</u> | | <u>Page</u> |
|---------------|---|-------------|
| 4.20 | Gain vs. f TW-148-5RR. | 121 |
| 4.21 | $P_{O_{max}}$ vs. f TW-148-5RRR. | 121 |
| 4.22 | P_O vs. P_{in} , Filtered, TW-148-5RRR. | 122 |
| 4.23 | P_O vs. P_{in} , Unfiltered, TW-148-5RRR. | 122 |
| 4.24 | Gain vs. f, Filtered, TW-148-5RRR. | 123 |
| 4.25 | Gain vs. f, Unfiltered, TW-148-5RRR. | 123 |
| 4.26 | Output Signals with One Frequency Input, Saturating. | 125 |
| 4.27 | Output Signals with Two Frequency Inputs, Both Frequencies Saturating. | 126 |
| 4.28 | Output Signals with Two Frequency Inputs, Only One Frequency Saturating. | 127 |
| 4.29 | $P_{O_{max}}$ vs. f TW-148-6. | 128 |
| 4.30 | P_O vs. P_{in} , Filtered, TW-148-6. | 128 |
| 4.31 | P_O vs. P_{in} , Unfiltered, TW-148-6. | 129 |
| 4.32 | Gain vs. f, Filtered, TW-148-6. | 129 |
| 4.33 | Gain vs. f, Unfiltered, TW-148-6. | 129 |
| B.1 | Control Accelerometer. | 137 |
| B.2 | Vibration Levels. | 138 |
| C.1 | Shock Test. | 143 |
| D.1 | Crestatron D-c Power Supply Requirements. | 145 |
| D.2 | Crestatron R-f Test Equipment (100-300 mc). | 146 |

LIST OF TABLES

PART I

| <u>Table</u> | | <u>Page</u> |
|--------------|--|-------------|
| 2.1 | Design Parameters | 4 |
| 2.2 | General Design Values | 5 |
| 2.3 | Gun Requirements | 6 |
| 2.4 | Beam and Focusing Parameters | 9 |
| 3.1 | Parameters for $P_{\mu} = 20$ Gun (1.076 Inch Diameter Beam) | 37 |
| 3.2 | Parameters for $P_{\mu} = 20$ Gun (0.806 Inch Diameter Beam) | 38 |

PART II

| | | |
|-----|---|----|
| 3.1 | Electrical and Physical Data of Tubes Constructed | 80 |
|-----|---|----|

LIST OF PUBLICATIONS

Technical Report

C. Yeh, "Helix Couplers for Linear-Beam Devices", Tech. Report No. 50, September, 1961.

Journal Article

C. Yeh, "Helix Couplers for Linear-Beam Devices", Trans. PGED-IRE, vol. ED-9, pp. 69-75; January, 1962.

PERSONNEL

THE UNIVERSITY OF MICHIGAN

| <u>Faculty and Principal Engineers</u> | | <u>Time Worked In</u> <u>Man Months</u> * |
|--|------------------------------|--|
| W. Dow | Professors | .06 |
| J. Rowe | | 3.16 |
| C. Yeh | | 11.26 |
| R. Lomax | Assistant Professor | .89 |
| J. Boers | Associate Research Engineers | 7.88 |
| G. Konrad | | 18.26 |
| <u>Engineering Assistance</u> | | 45.38 |
| <u>Service Personnel</u> | | 174.52 |

* Time Worked is based on 172 hours per month.

PART I

The University of Michigan Work

by

G. T. Konrad

FINAL REPORT
FOR
RESEARCH AND DEVELOPMENT ON HIGH-POWER CRESTATRONS
FOR THE 100-300 MC FREQUENCY RANGE

1. Introduction

Contract NObsr-81403 consisted of a research and development program on high-power 100-300 mc Crestatrons. Originally the aim had been to construct both a 100-watt and a 1000-watt electrostatically focused tube in as compact packages as possible. Both tubes were to have operated cw; the lower power tube was to have been the driver for the higher power tube. The choice of two tubes was dictated by the desire to have tubes of a reasonable length for this frequency range.

A portion of the development phase of this program was subcontracted to Bendix Research Laboratories with the approval of the Bureau of Ships. Bendix was to deliver to the Navy, through The University of Michigan, several tubes of each kind for evaluation.

After this program had been well under way, it was agreed, by consultation with the Navy, that system requirements would not permit use of the electrostatically focused tubes due to their length and the increase in complexity of the system. The additional power supplies necessary for operation of the electrostatically focused tubes more than offset the saving in size and weight of the tubes due to the elimination of magnetic focusing. Thus a major redirection of effort became necessary on this program.

Under the new approach The University of Michigan continued gun studies and improvements on electrostatic focusing systems from a basic research standpoint. Bendix Research Laboratories, on the other hand, devoted its time to the construction of compact 100-watt Crestatrons employing magnetic focusing. At the end of this program, three tubes meeting electrical and environmental specifications were constructed and delivered to the Navy.

This report covers The University of Michigan work consisting of research on electrostatic focusing systems, hollow-beam guns and the design of the original Crestatrons. This work is described in Part I of this report. Part II of this report was submitted by Bendix Research Laboratories and covers the work done on the magnetically focused tubes, which were ultimately delivered to the Bureau of Ships.

2. Electrostatically Focused 100-Watt VHF Amplifiers

2.1 Design Parameters for the Electrostatically Focused Crestatrons.

The Crestatron is a high-frequency traveling-wave amplifier operating in the beating-wave regime. Its chief advantages are a short physical length and a high operating efficiency over a fairly wide frequency band. The device has only moderate gain; thus an attenuator is not necessary to keep the tube stable. In view of these facts, it is apparent that a Crestatron should be well suited for amplification of long wavelength signals. The following goals were set for the design of the 100-watt and 1000-watt Crestatrons.

Table 2.1

Design Parameters

| | <u>100-Watt Tube</u> | <u>1000-Watt Tube</u> |
|---------------------|-------------------------|------------------------------------|
| Frequency Range | 100-300 mc | 100-300 mc |
| Power Output | 100 watts, cw | 1000 watts, cw |
| Gain | 10-12 db | 10-12 db |
| Efficiency | 30-40 percent | 30-40 percent |
| Type of Focusing | Electrostatic | Electrostatic |
| Type of R-f Circuit | Helix | Helix |
| Cooling | Air-Cooled Collector | Air- or Water- Cooled Collector |

2.1.1 Helix Design. For Crestatron operation over a substantial frequency region, it is necessary to keep the value of b constant and slightly larger than the value of b where the growth factor, x_1 , becomes a minimum. This requires low dispersion and small impedance variation for the r-f structure across the frequency band of interest.

In order to design the helix, one chooses first a reasonable efficiency for the tube, and then a beam power and perveance can be computed. If the frequency range and beam power are known, a low-frequency ka can be chosen. An inside circuit diameter, which should permit a reasonable current density, is then determined. Since a representative value of the quantity $1+Cb$ for most Crestatrons with hollow beams is near 1.5, a low-frequency γa , which should lie between 0.5 and 1.0, can be determined. It is possible to make an estimate of the DLF from experience, and then the phase velocity can be plotted as a function of frequency. If the beam geometry has been chosen, C and b can be

calculated. The latter quantity should be between 2.5 and 3.5 for Crestatron operation. The exact value of b depends on QC , which can be calculated at this stage of the design procedure. The maximum Crestatron gain is determined from C , QC and b . The helix length can be calculated by setting $CN_g \approx 0.35$ at the low-frequency end. From this the efficiency and gain can be determined for different drive levels throughout the frequency band. The values shown in Table 2.2 were determined by this procedure.

Table 2.2
General Design Values

| | <u>100-Watt Tube</u> | <u>1000-Watt Tube</u> |
|---------------------|----------------------|-----------------------|
| Low Frequency ka | 0.04 | 0.04 |
| Beam Power | 400 watts | 4000 watts |
| Operating Voltage | 1520 volts | 4000 volts |
| Perveance | 4.46 microperv | 4.46 microperv |
| Mean Helix Radius | 0.752 inch | 0.752 inch |
| Wire Diameter | 0.100 inch | 0.150 inch |
| Helix Pitch | 0.307 inch | 0.445 inch |
| Mid-Band Frequency | 200 mc | 200 mc |
| Mid-Band γ_a | 1.29 | 0.94 |
| Mid-Band v_p/C | 0.062 | 0.085 |
| Mid-Band DLF | 0.78 | 0.78 |
| Mid-Band Impedance | 140 ohms | 210 ohms |
| Mid-Band C | 0.162 | 0.190 |
| Mid-Band b | 2.72 | 2.47 |
| Mid-Band QC | 0.24 | 0.27 |
| Interaction Length | 18 inches | 28 inches |

2.1.2 Electron Gun Design. Since both of the tubes require a hollow-beam gun, it was decided to use the same gun in the two tubes, but to operate at different voltages in the two cases. Thus only one gun design effort was necessary and the same gun points could be used for the two tubes. Two types of guns were considered, namely, a simple triode gun and one which had a convergent Einzel lens. The design of the former was handled by Bendix Research Laboratories and will be described in Part II of this report. Even though the triode gun is simpler from a structural point of view, it was decided to use the other type of gun in the early experiments, because it permits much greater versatility in the control of the beam entrance conditions.

The design of the gun was straightforward. Use was made of an electrolytic tank in arriving at the electrode geometries. Figure 2.1 shows a schematic diagram of the gun, while Fig. 2.2 shows a photograph with the final anode removed for a better view of the internal electrode arrangement. In Table 2.3 the gun requirements for the two tubes are summarized.

Table 2.3

Gun Requirements

| | <u>100-Watt Tube</u> | <u>1000-Watt Tube</u> |
|------------------|---------------------------|---------------------------|
| Voltage | 1520 volts | 4000 volts |
| Current | 0.253 amp | 1.080 amp |
| Perveance | 4.46 microperv | 4.46 microperv |
| Beam Thickness | 0.080 inch | 0.080 inch |
| Mean Beam Radius | 0.538 inch | 0.538 inch |
| Current Density | 0.150 amp/cm ² | 0.613 amp/cm ² |

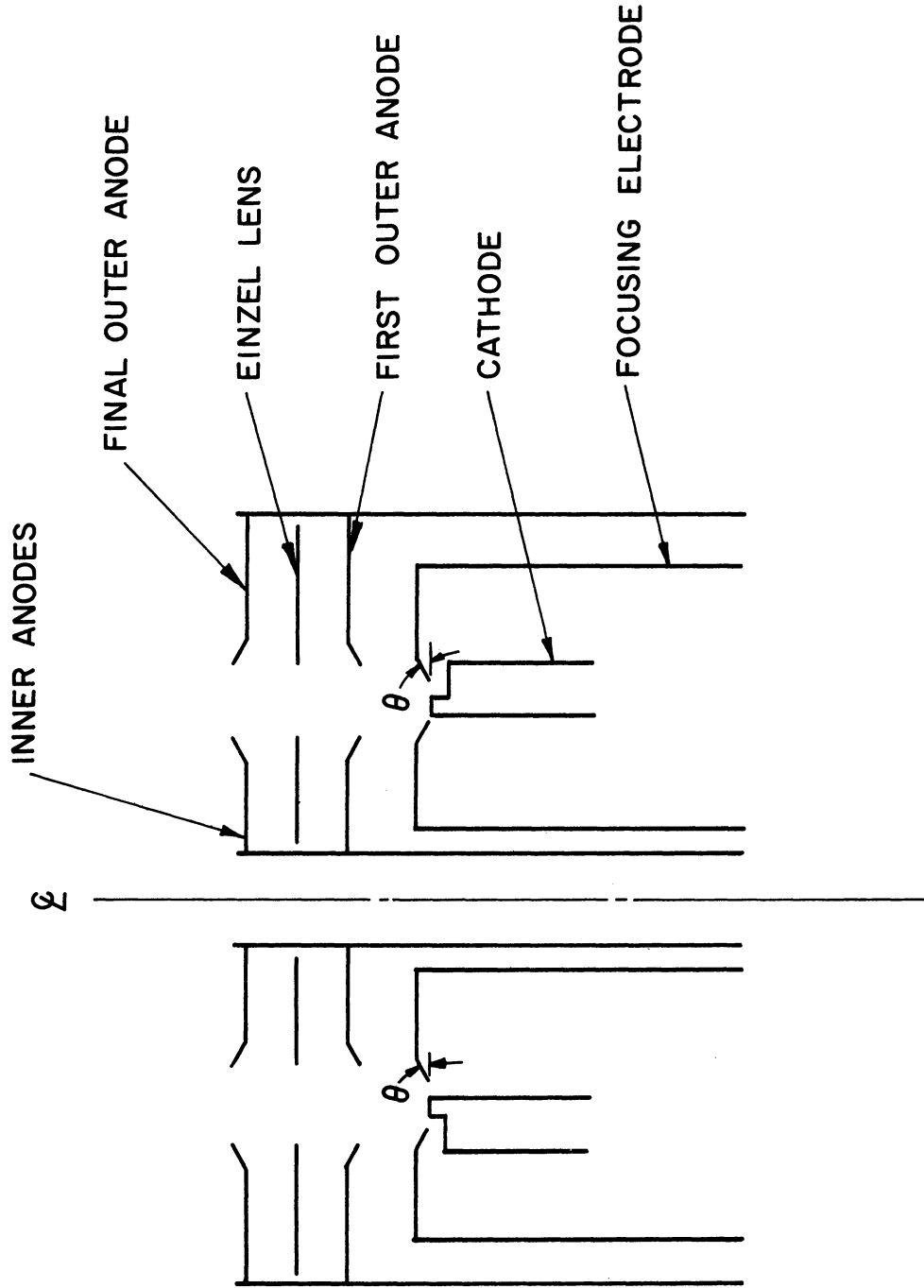


FIG. 2.1 DIAGRAM OF THE $P_{\mu} = 4.46$ GUN WITH AN EINZEL LENS.

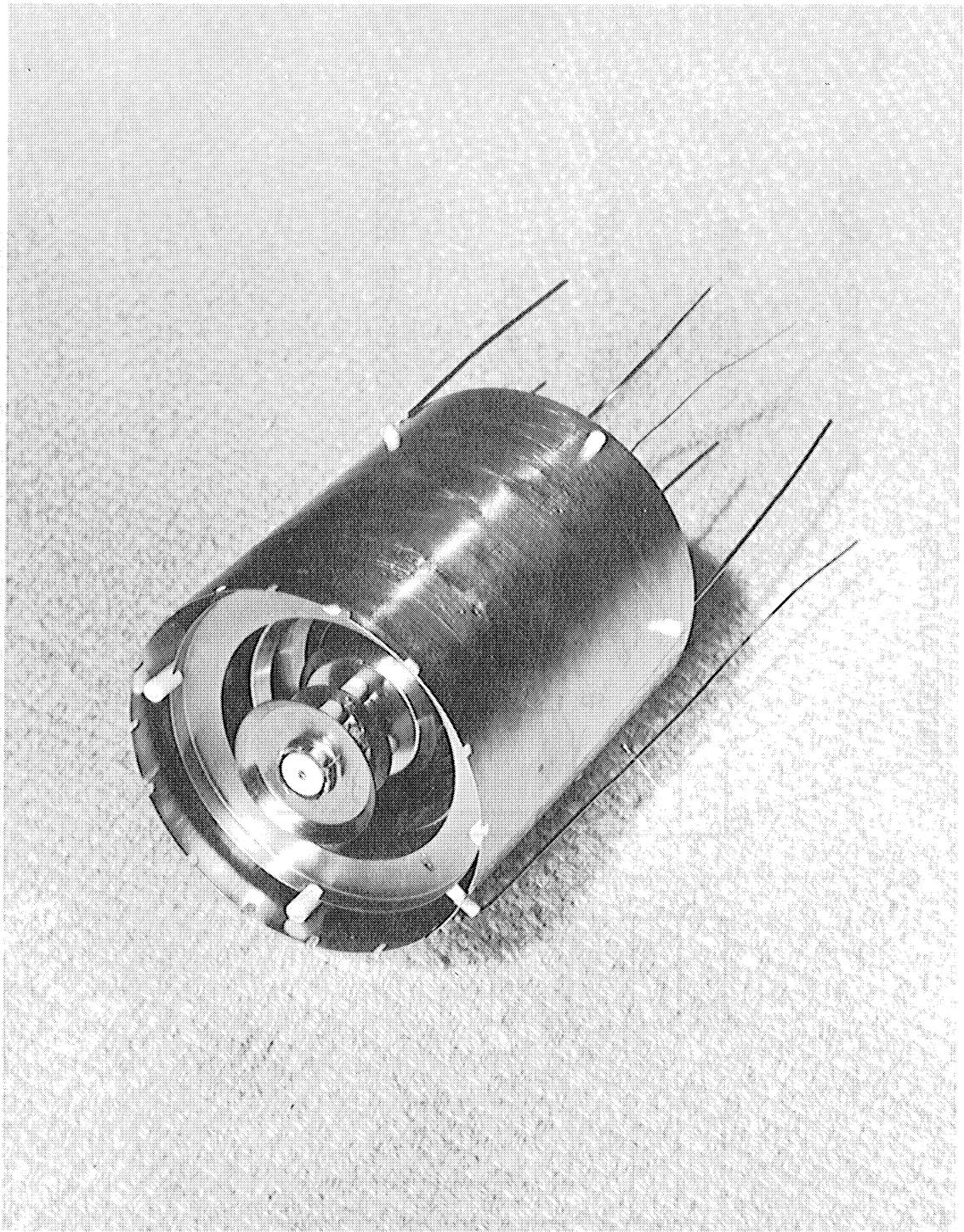


FIG. 2.2 PHOTOGRAPH OF THE $P_{\mu} = 4.46$ GUN.

2.1.3 Focusing System Design. The electrostatic focusing scheme utilized in these tubes was very similar to that described by Johnson¹, the main difference being that in these Crestatrons the focusing structure was in the center of the hollow beam, and the helix was placed around the outside of the beam. A schematic diagram of the arrangement is shown in Fig. 2.3.

The focusing disks were stacked on the centering structure, which was so arranged that alternate disks could be held at potentials above and below the beam voltage. This, in conjunction with the fact that the helix potential was slightly below the mean potential of the focusing disks, permitted the beam to be focused all the way to the collector end of the tube.

By use of Johnson's curves the focusing voltages necessary could be computed. For a beam thickness of 0.080 inch and a perveance of 4.46 microperv the operating parameters given in Table 2.4 were obtained.

Table 2.4

Beam and Focusing Parameters

| | <u>100-Watt Tube</u> | <u>1000-Watt Tube</u> |
|---------------------------------|----------------------|-----------------------|
| Beam Voltage (U_0) | 1520 volts | 4000 volts |
| Circuit Voltage (U_-) | 1488 volts | 3880 volts |
| High Focusing Voltage (V_+) | 2075 volts | 5420 volts |
| Low Focusing Voltage (V_-) | 965 volts | 2580 volts |
| Perveance | 4.46 microperv | 4.46 microperv |
| Mean Beam Radius | 0.538 inch | 0.538 inch |

1. Johnson, C. C., "Periodic Electrostatic Focusing of a Hollow Electron Beam", Trans. PGED-IRE, vol. ED-5, No. 4, pp. 233-243; October, 1958.

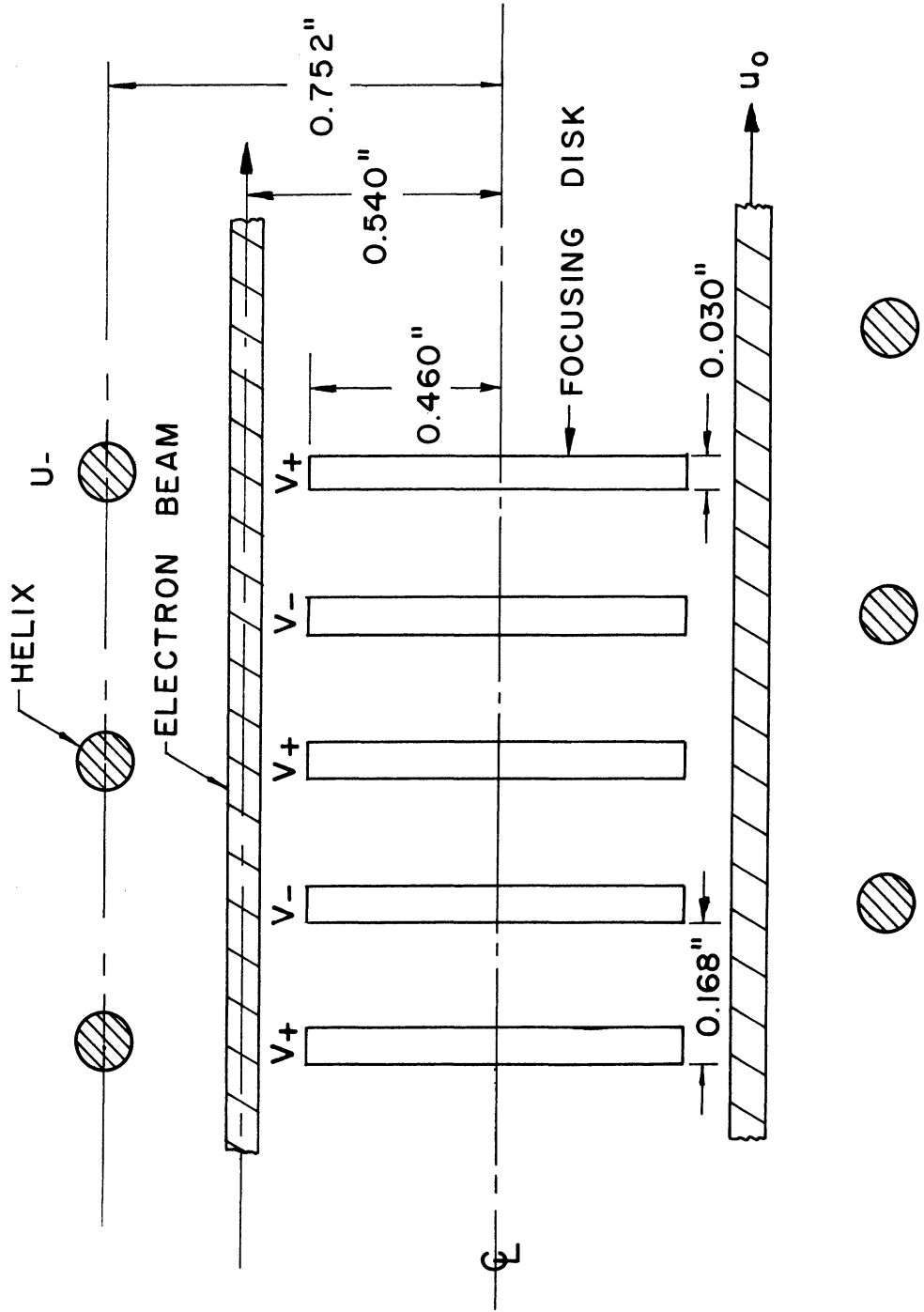


FIG. 2.3 ELECTROSTATIC FOCUSING SCHEME.

Table 2.4 (contd.)

| | <u>100-Watt Tube</u> | <u>1000-Watt Tube</u> |
|-----------------------------|----------------------|-----------------------|
| Beam Thickness | 0.080 inch | 0.080 inch |
| Beam Current | 0.263 amp | 1.080 amp |
| Focusing Pitch | 0.168 inch | 0.168 inch |
| Thickness of Focusing Disks | 0.030 inch | 0.030 inch |

2.1.4 Beam Collector Design. The design of the collectors for both tubes was worked out by Bendix Research Laboratories. This work is described in Part II of this report.

2.2 Cold Test Results. Extensive cold tests were conducted on the helix for the 100-watt tube so that the operating parameters computed for the tube could be checked. Figure 2.4 shows the phase velocity as a function of frequency obtained from measurements of the guide-wavelength, λ_g , on the helix. These measurements were obtained by moving a shorting plunger along the helix and observing the movement of the VSWR minima at the input to the helix. Two cases were considered. One was for the structure without either a metallic shield surrounding the helix or a conducting rod along the center, while the other was for the helix with a surrounding conducting shield of $b/a = 1.65$, where b is the shield radius and a is the mean helix radius. Both cases are shown in Fig. 2.4.

It should be added that before this data could be obtained coupled-helix couplers had to be built for this tube. This type of coupling was chosen because it is by far the most versatile coupling method for an experimental tube, even though other methods may be expected to yield lower insertion losses and a somewhat better match. The coupled-helix couplers were so made that they fit closely around the tube envelope and thus

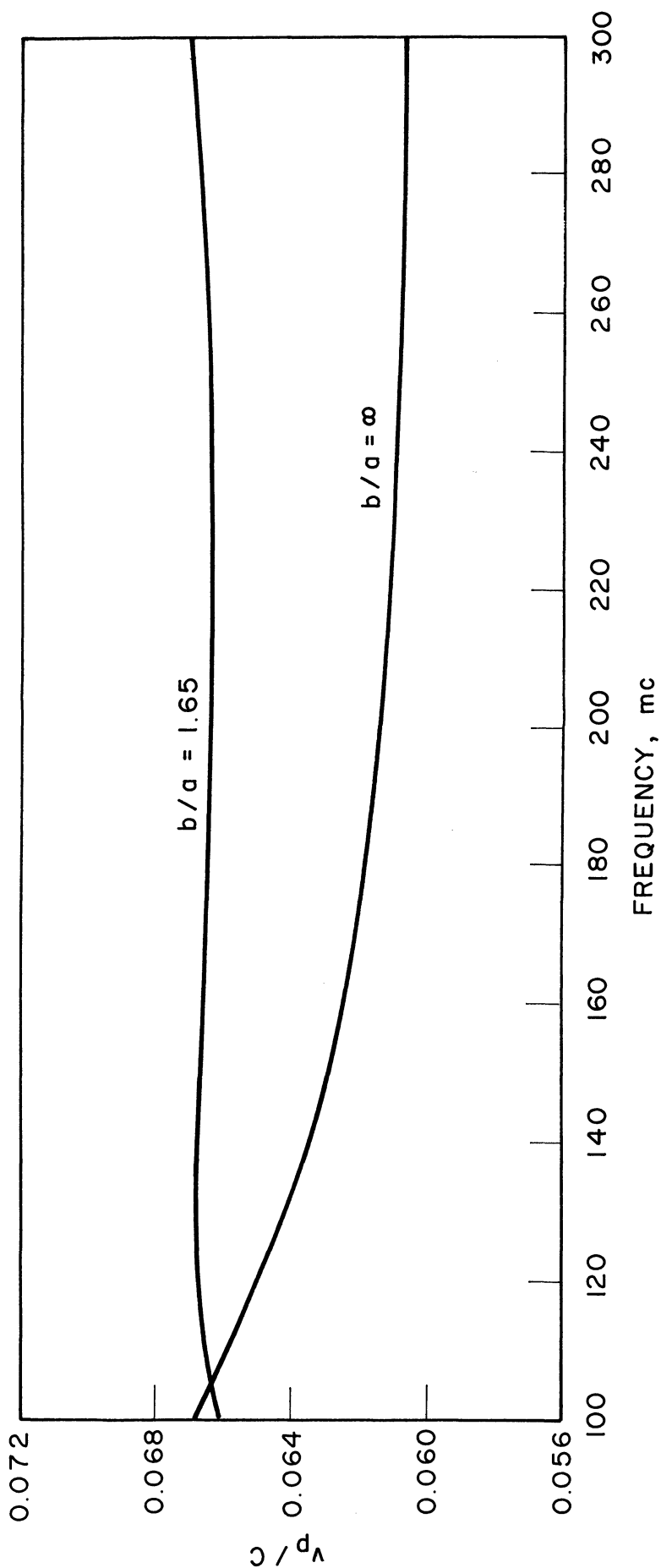


FIG. 2.4 PHASE VELOCITY AS A FUNCTION OF FREQUENCY FOR THE 100-WATT ELECTROSTATICALLY FOCUSED CRESTATRON HELIX.

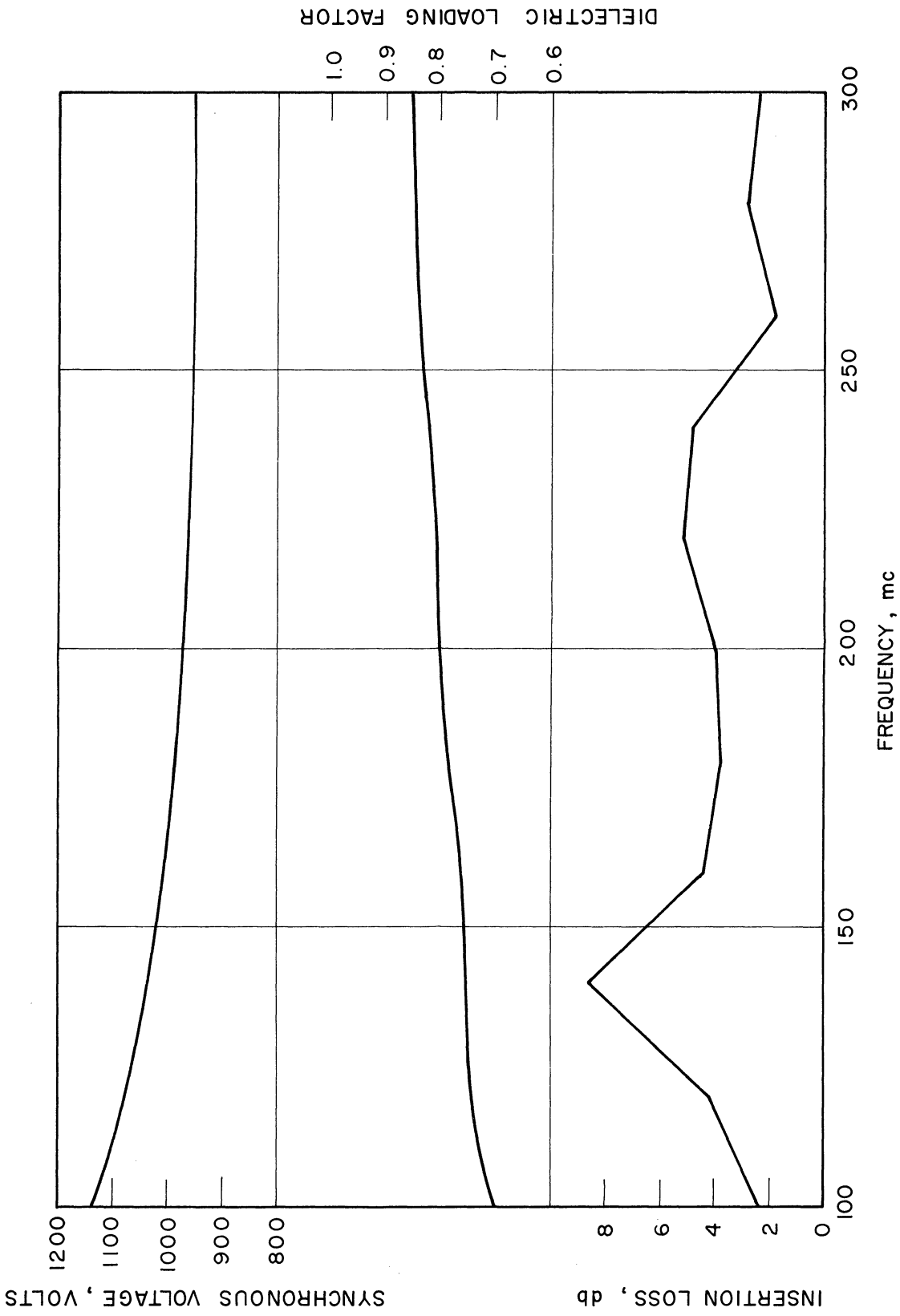


FIG. 2.5 SYNCHRONOUS VOLTAGE, DIELECTRIC LOADING FACTOR AND INSERTION LOSS FOR THE 100-WATT ELECTRO-STATICALLY FOCUSED CRESTATRON HELIX.

afforded a means of tube support. The details of these couplers have been described in the various progress reports on this program.

From a knowledge of the phase velocity the synchronous voltage and the DLF were computed and plotted as a function of frequency, as shown in Fig. 2.5. The dielectric loading is seen not to be very severe, even for these low frequencies, where the fields extend far out from the helix wire. Figure 2.5 also shows the insertion loss of the completed 100-watt tube with the focusing structure along the center of the helix. The helix was 18 inches long and the loss curve of Fig. 2.5 includes the losses due to the two coupled-helix couplers. Since the helix loss was measured to be in the range of 0.75 to 1.00 db, it may be seen that the major portion of the loss was due to the couplers. Thus it appears that the couplers each contributed from 1 to 2 db of loss throughout the frequency range, except near 140 mc, where the loss was higher.

The impedance variation for the helix is shown in Fig. 2.6. The values of impedance were calculated at the mean beam radius, assuming that no conducting elements were present at the center of the helix. This explains the discrepancy between the two curves in Fig. 2.6. In order to measure the impedance of the completed tube by the Kompfner dip method, the focusing structure had to be along the axis of the helix. Hence the impedance at the beam radius was lower, as shown.

All the cold tests described were done on the 100-watt tube helix. Similar work had been started for the 1000-watt tube helix just as the redirection of effort on this program became effective. Hence the work on that helix was terminated before the tests were completed.

2.3 Beam Analyzer Tests on the $P_{\mu} = 4.46$ Hollow Beam Gun. As mentioned previously, it was decided to make use of a hollow-beam gun with an Einzel lens. This lens helped greatly in controlling the beam

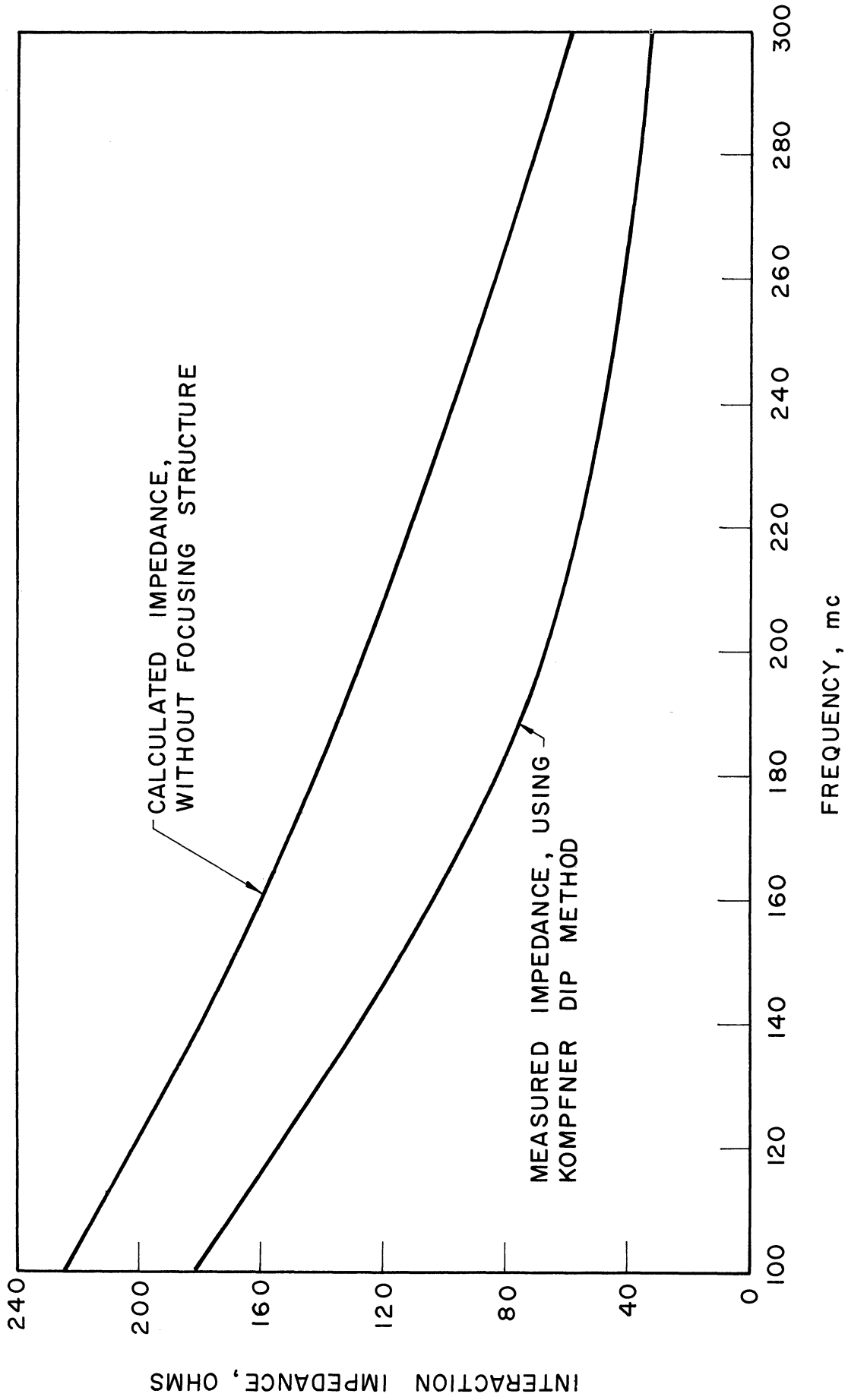


FIG. 2.6 IMPEDANCE AS A FUNCTION OF FREQUENCY FOR THE 100-WATT ELECTROSTATICALLY FOCUSED CRESTATRON HELIX.

characteristics at the entrance to the focusing structure. As the experiments showed very conclusively, good beam control at the beginning of the electrostatic focusing region was the most important single factor in successful focusing along the length of the tube.

The gun tests were conducted over a fairly long period of time in order to refine the gun as much as possible. A demountable beam analyzer was used for this purpose. The gun was attached to a movable post inside a vacuum chamber. Directly above the gun was a stationary collector with a pin-hole sampling collector built into it. The collector also had several grids in front of it which could be biased for suppression of secondary electrons. The arrangement is shown in the form of a diagram in Fig. 2.7. In Fig. 2.8 is shown a photograph of the gun mounted in the beam analyzer. The collector shown here is slightly different from the one in Fig. 2.7. This latter collector contains a Faraday cage with deflection plates. By this means it was possible to determine the radial velocity components in addition to the current density at any point within the beam.

A typical set of beam contours is shown in Fig. 2.9. Note that the lens is very effective in controlling the thickness of the beam. In Fig. 2.10 a series of beam contours is shown as one moves farther away from the gun. As is expected, the beam spreads out due to space-charge effects. This spreading is shown more clearly in Fig. 2.11, which was obtained from a set of contours such as those shown in Fig. 2.10.

Before a well-behaved beam, such as shown in these curves, could be obtained, many trial and error experiments were required. One lengthy set of experiments determined the optimum angle θ in Fig. 2.1. Even though this angle did not have much effect on the behavior of the beam at the

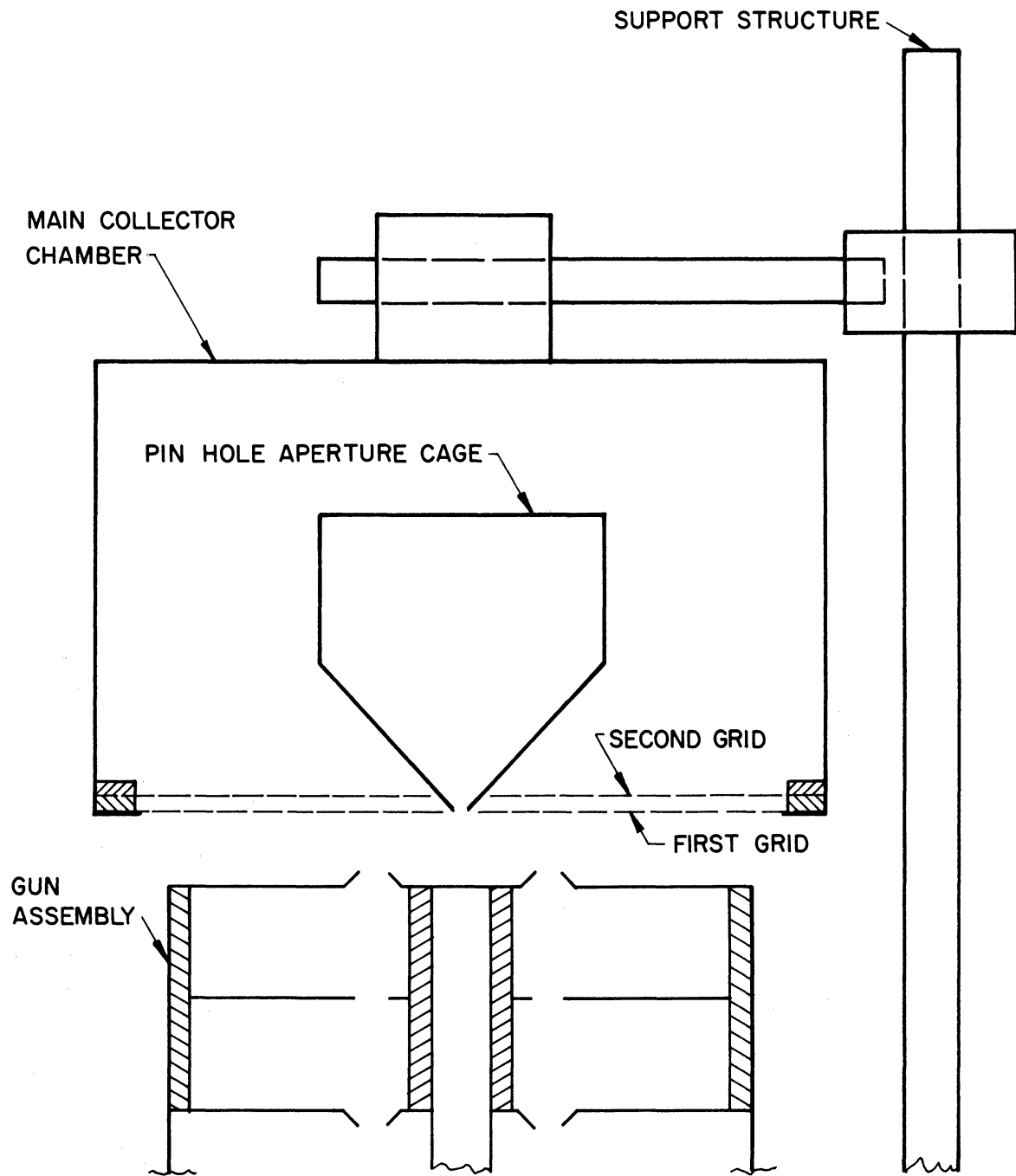


FIG. 2.7 SCHEMATIC DIAGRAM OF GRIDDED BEAM COLLECTOR.

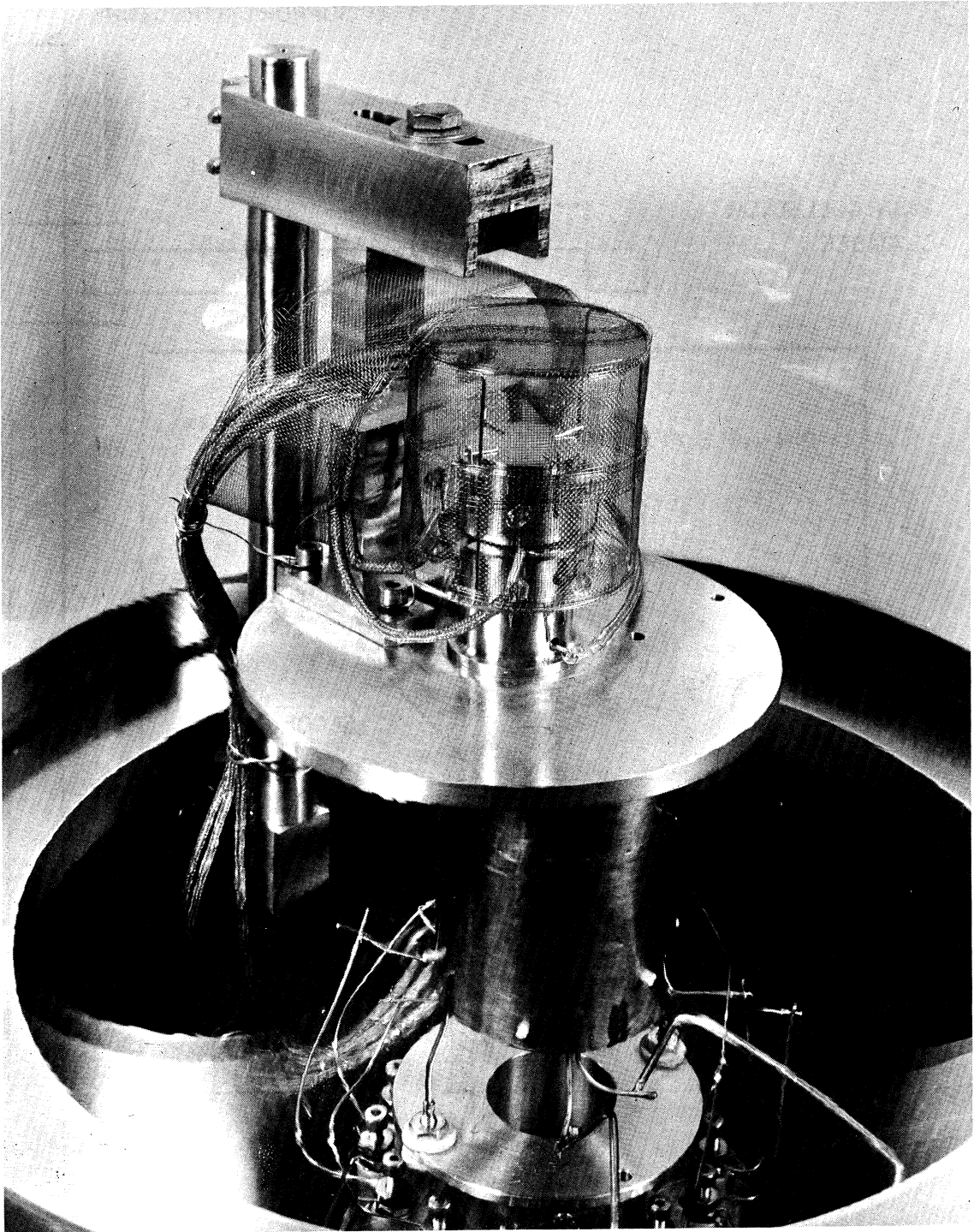


FIG. 2.8 $P_{\mu} = 4.46$ GUN MOUNTED IN THE BEAM ANALYZER.

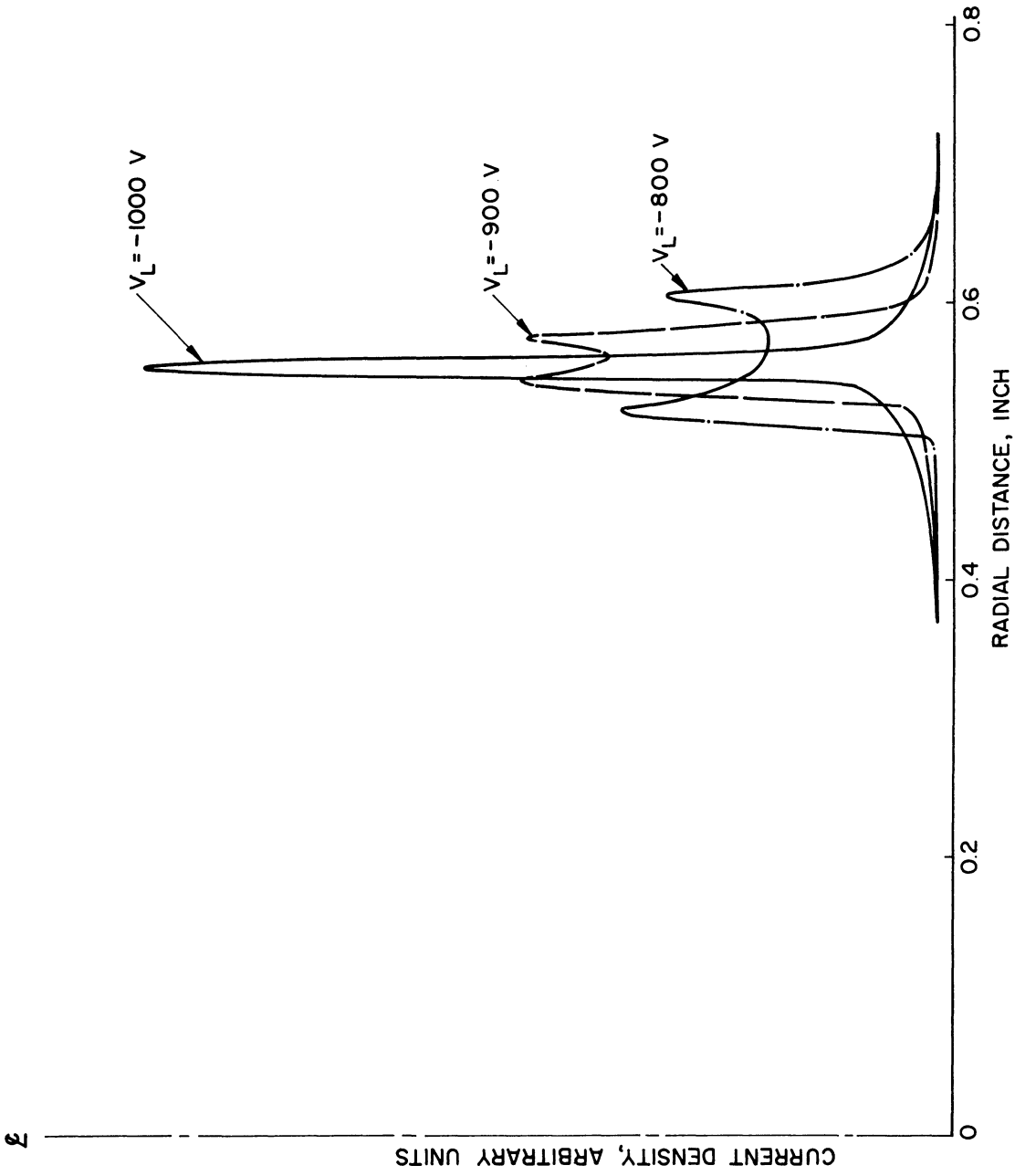


FIG. 2.9 COMPARISON OF BEAM PROFILES AS A FUNCTION OF LENS VOLTAGE AT A DISTANCE OF 0.150 INCH FROM THE FINAL GUN ANODE.

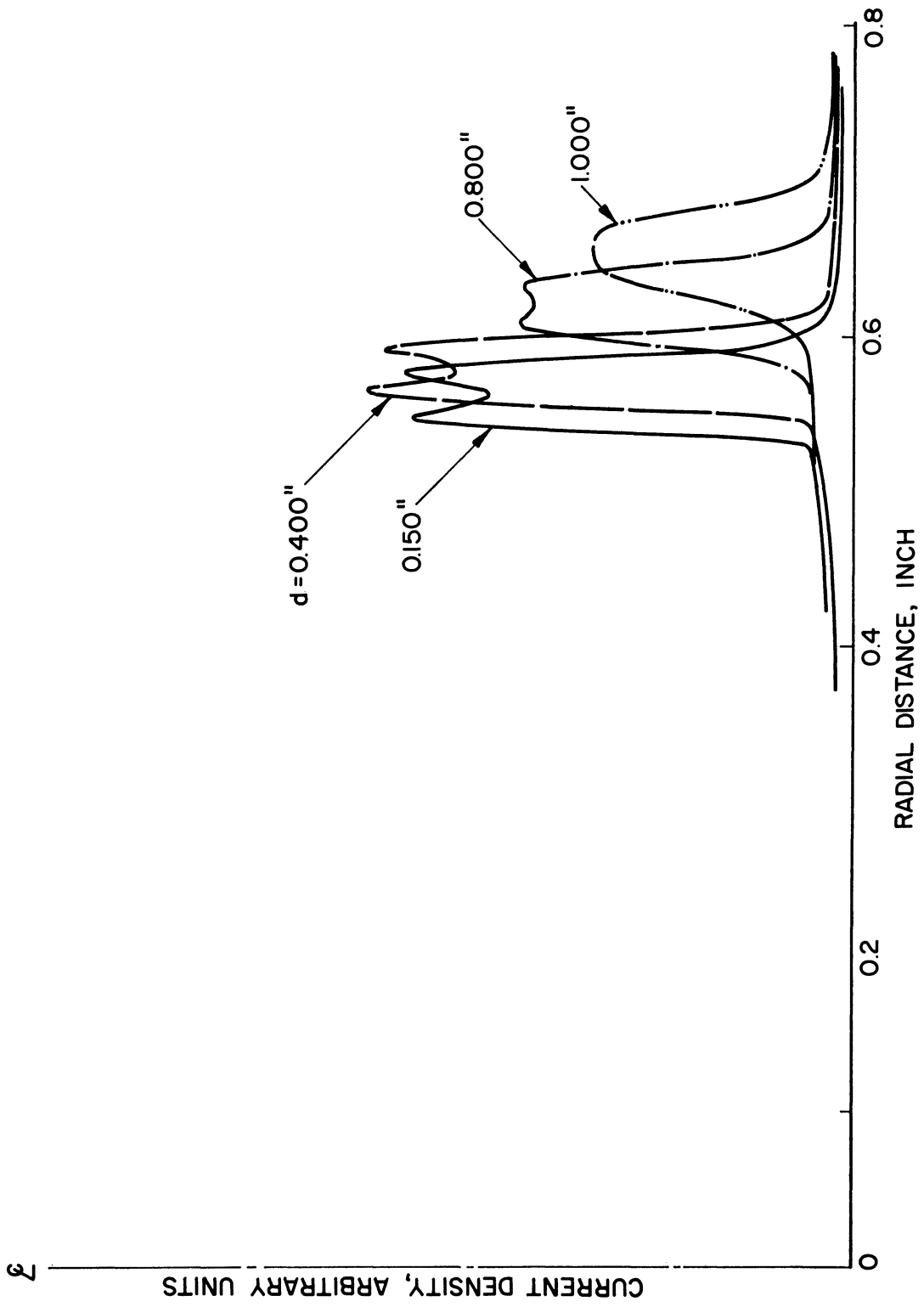


FIG. 2.10 COMPARISON OF BEAM PROFILES AS A FUNCTION OF ANODE-COLLECTOR SPACING, d. (LENS VOLTAGE = -900 VOLTS)

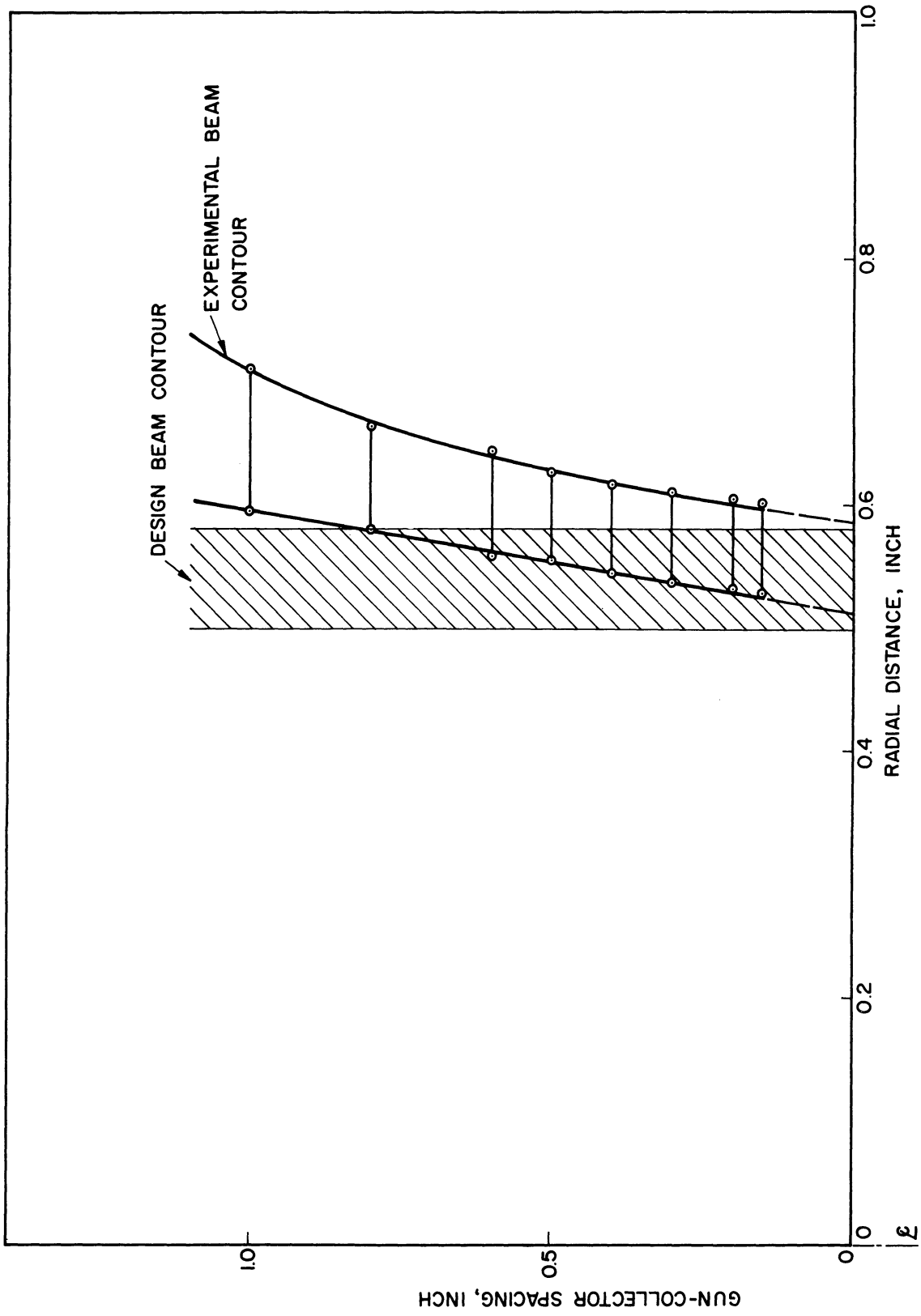


FIG. 2.11 BEAM SPREAD AS A FUNCTION OF DISTANCE FROM THE FINAL GUN ANODE.
(LENS VOLTAGE = -900 VOLTS)

entrance to the focusing structure, it did have a marked effect on the beam interception within the gun. Eventually θ was chosen to be approximately 34 degrees.

2.4 Electrostatic Focusing Tests. In order to evaluate the electrostatic focusing scheme more effectively than was possible in a complete tube, the device depicted in Fig. 2.12 was constructed. The gun was mounted in the beam analyzer as for the gun tests. Instead of the sampling collector the series of six disks and an outer cylinder were placed directly above the gun. A lead was brought out of the chamber from each one of the disks so that they all could be biased independently. The beam was collected at the end of the focusing region, as shown in Fig. 2.12.

Several modes of operation were possible for the device. The most obvious one was such that D_1 , D_3 and D_5 were operated at the high focusing voltage and D_2 , D_4 and D_6 were at the low focusing voltage. Another method investigated was the one for which the high and low voltages were interchanged. As expected, this method did not work as well, but there was still more than 50 percent beam transmission to the collector.

The best method for beam transmission turned out to be the one cited first in the previous paragraph, but with each individual disk adjusted for an optimum voltage, which was close to the following:

$$V_{D_{\text{odd}}} - V_o = V_o - V_{D_{\text{even}}} \quad (2.1)$$

and

$$V_{D_{\text{odd}}} > V_{D_{\text{even}}} \quad , \quad (2.2)$$

where V_o is the beam voltage and $V_{D_{\text{odd}}}$ is the voltage on the odd numbered focusing disks and $V_{D_{\text{even}}}$ is the voltage on the even numbered ones. There

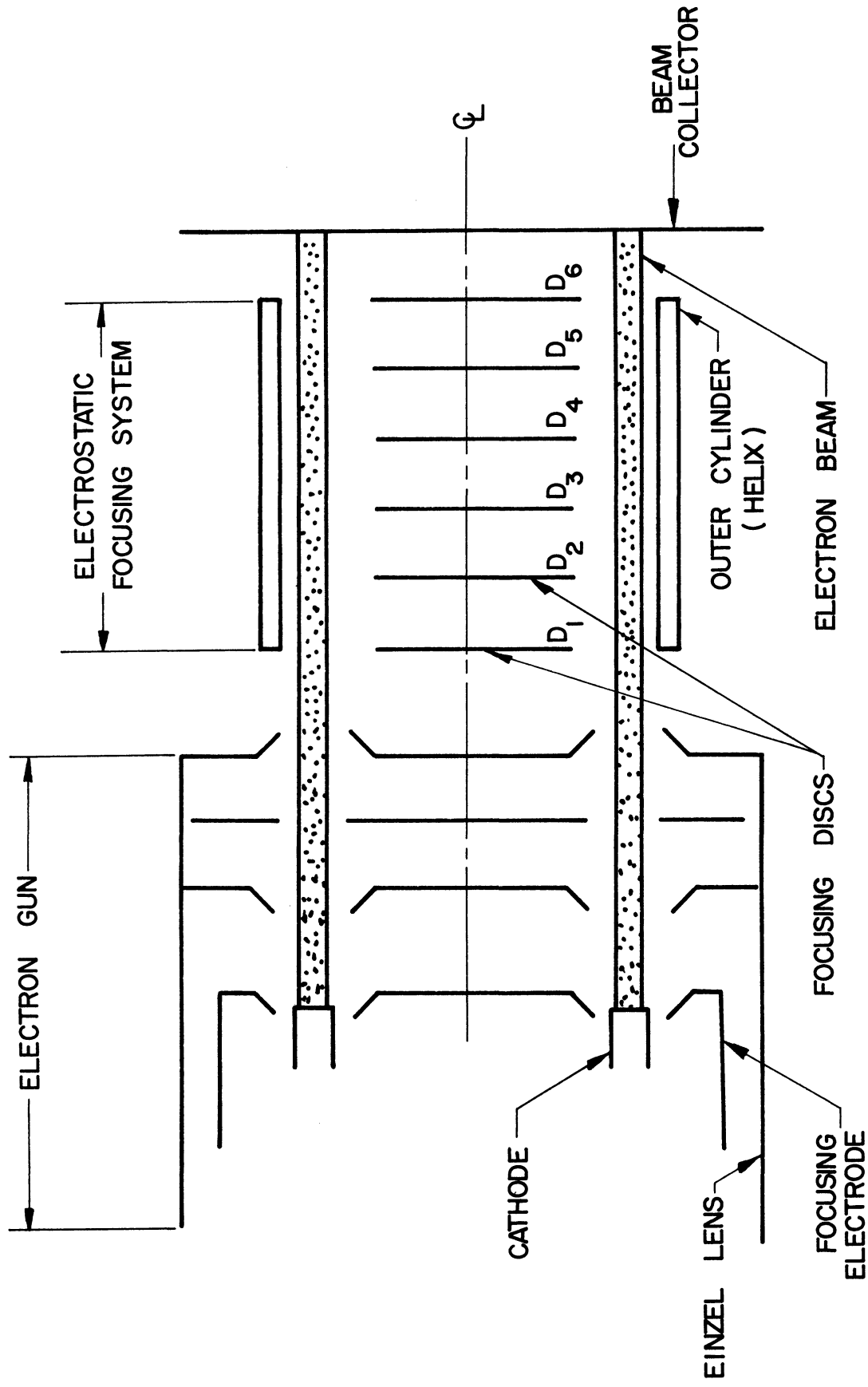


FIG. 2.12 SCHEMATIC DIAGRAM OF THE FOCUSING TESTER.

was one exception to this rule, however. It turned out that if D_5 was operated at the low focusing voltage, a slightly better beam transmission could be observed. This anomaly is believed to be due to an alignment error in the gun or focusing tester.

Figure 2.13 shows the transmission observed through the electrostatic focusing system alone and through the gun and focusing system combined. A relatively low voltage had to be used in order to eliminate electrical breakdown between individual parts in the focusing tester and to prevent overheating of the collector. Pulse operation was not possible due to a lack of a sufficient number of pulsers for operation of the disks. In Fig. 2.13 the gun transmission appears to be near 50 percent. This low a transmission is due to two factors. First, the gun transmission was always poor at lower voltages and improved markedly as the operating voltage of 1500 volts was approached. Second, at the stage in the program when these tests were conducted, the gun was not yet refined to the point where values of transmission near 90 percent were observed as was the case later.

2.5 Digital Computer Calculations on the $P_\mu = 4.46$ Gun and Focusing System. A digital computer program was developed, which was capable of analyzing the performance of any axially symmetric, electrostatically focused, hollow-beam electron flow system. The program was written in the Fortran programming system. The input to the computer consisted of the cathode current density, the scaled voltage, the scaled distance and the time increment for the trajectory calculation. Also required were the points for representing the electrode geometry. Output from the computer included the voltage and space-charge matrices and the final set of electron trajectories.

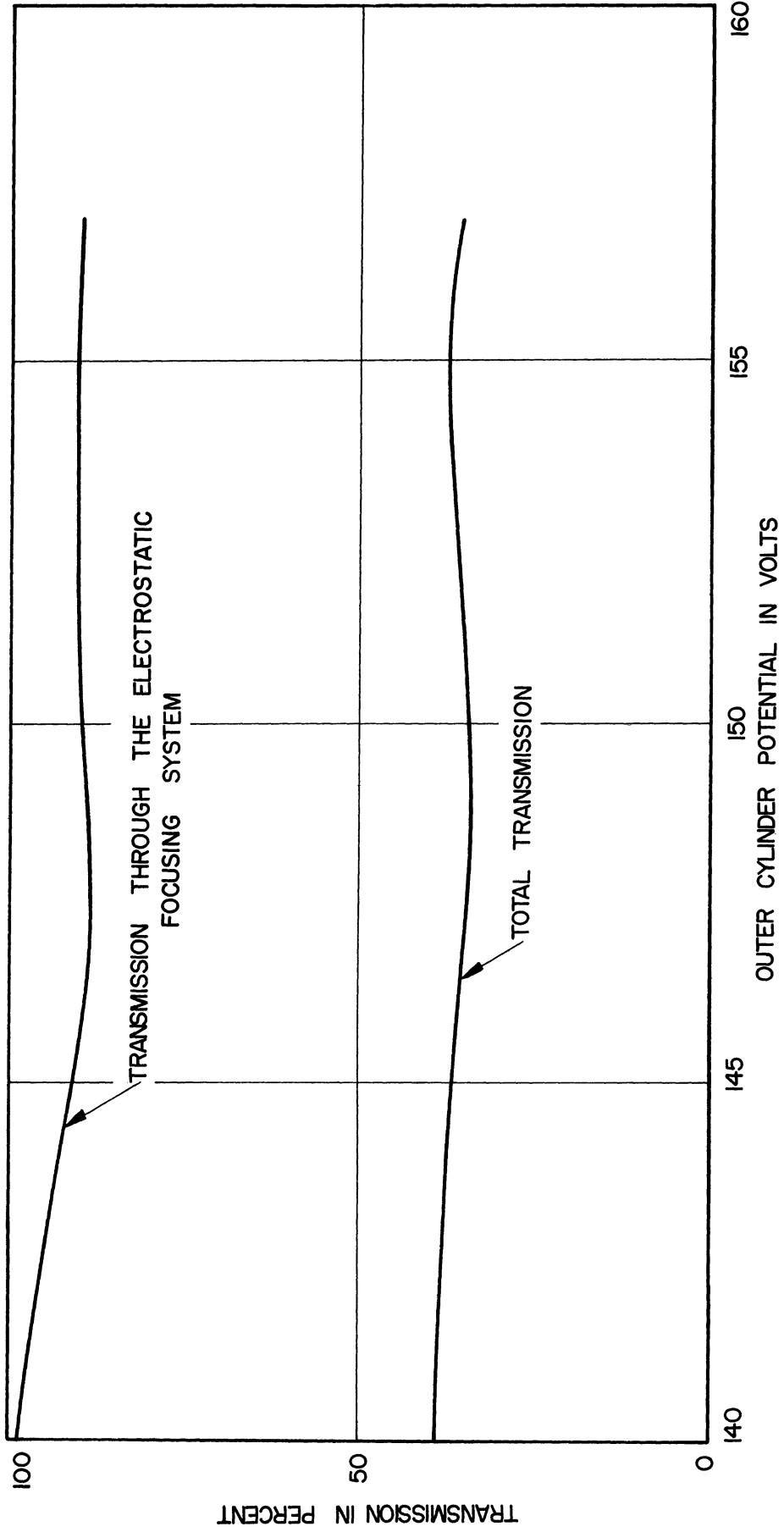


FIG. 2.13 OPTIMUM TRANSMISSION FOR THE CONDITION $V_{D_1} = V_0 = V_{D_2} \cdot (V_{D_1} = V_{D_3}, V_{D_2} = V_{D_4}, V_{D_3} = V_{D_5} = V_{D_6})$

For convenience the gun and focusing systems were analyzed separately because of program matrix limitations. A 120 x 100 point matrix was employed in each case. First the trajectories were found for the gun region, and then using this information consisting of velocities and potentials along the last gun electrode as input data for the second step, the trajectories were continued through the focusing structure to the collector.

Within the computer the electric fields were calculated by relaxation techniques applying Laplace's equation in the space-charge-free region and Poisson's equation in the beam region. The space-charge term in Poisson's equation was computed by summing the space-charge effects of electron trajectories traced through the gun. Direct interaction between electrons was not computed, but the space charge was higher in a region where the electron trajectories were close together and proportionately smaller where there were fewer electrons. The program alternately called for computation of electric field and trajectories (space charge) until two consecutive sets of trajectories essentially repeated themselves.

Figure 2.14 shows the trajectories in the final gun design. The effect of the Einzel lens, which was held at one fourth of the beam voltage, is clearly visible. The beam was still diverging after it left the final anode. The beam minimum occurred near the first focusing disk as it should for maximum beam transmission through the focusing structure. Figure 2.15 depicts the beam through the focusing structure. The trajectories shown here are a continuation of those shown in Fig. 2.14. It is apparent that the beam was spreading out and would strike the drift tube sooner or later. This problem could be circumvented if the drift tube were operated at approximately $(V_0 - 5)$ volts. Another computer run

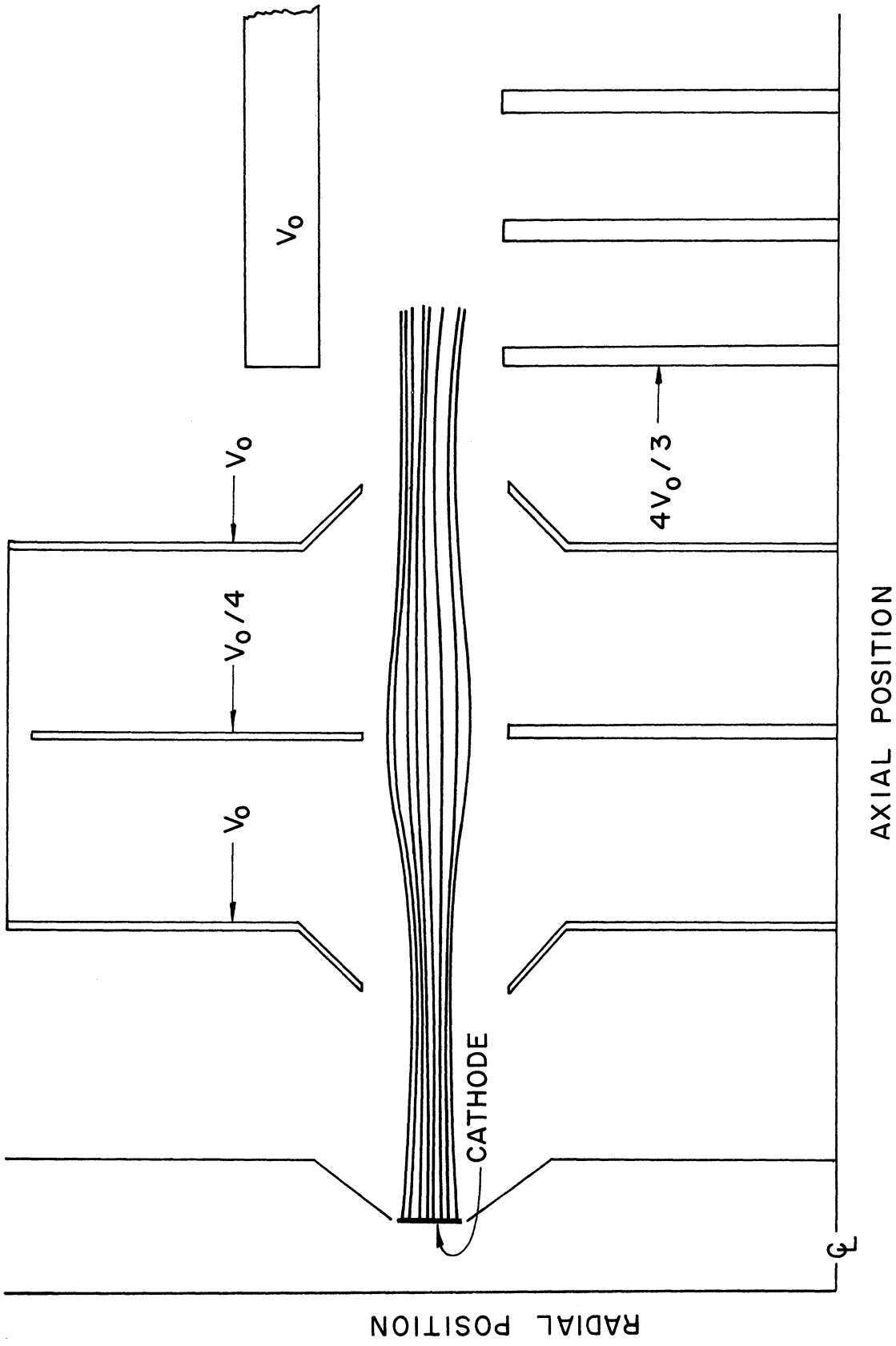


FIG. 2.14 ELECTRON TRAJECTORIES IN THE GUN REGION.

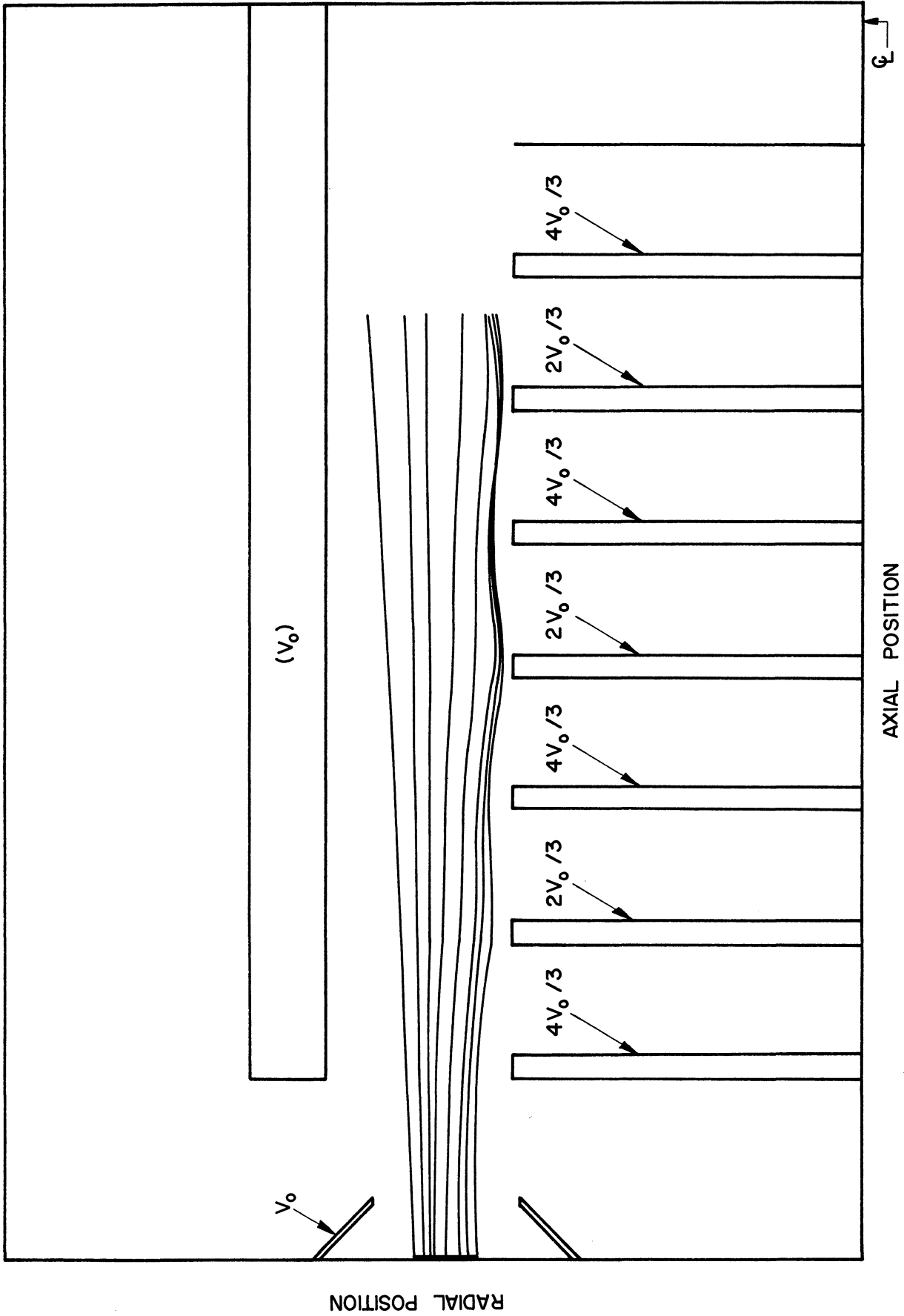


FIG. 2.15 ELECTRON TRAJECTORIES IN THE ELECTROSTATIC FOCUSING REGION. (HELIX VOLTAGE = V_0 VOLTS)

confirmed this. The slightly lower voltage imparted an inward force to the electrons along the outer beam edge, thus helping the beam to focus all the way to the collector.

2.6 Performance of the 100-Watt Electrostatically Focused Tube.

The pertinent design and operating parameters for this tube have already been listed in Sec. 2.1. The tube was built using a precision bore 7052 glass envelope. The gun and focusing structure were an integral unit and were held along the axis of the helix by supports within the gun bulb and within the collector. The helix was held in the glass envelope by means of sapphire rods. During the testing the tube was held in place by the two coupled-helix couplers. A 5 l/sec appendage pump was used at the gun end in order to insure a good vacuum in the tube throughout its life. The whole tube package is shown in Fig. 2.16. The test area for the tube, including power supplies, r-f driver equipment and measuring instruments may be seen in Fig. 2.17.

The insertion loss as a function of frequency for the 100-watt Crestatron was shown in Fig. 2.5. In the hot tests to be described in the following, the gain and power output values were corrected for this cold loss. Thus the values of electronic gain and actual power levels at the helix are shown in the figures.

Figure 2.18 shows the electronic gain as a function of frequency. It may be seen that the gain curves in the higher frequency band are fairly flat and hence a better tube performance is indicated in this range. A typical set of saturation curves for a number of frequencies is shown in Fig. 2.19. At this beam voltage of 1800 volts a maximum gain of 4.2 db was observed at 290 mc. In all cases the cathode current was between 80 and 90 ma. This is low by a factor of approximately three. Beam transmission tests on this tube without r-f drive revealed that as the cathode

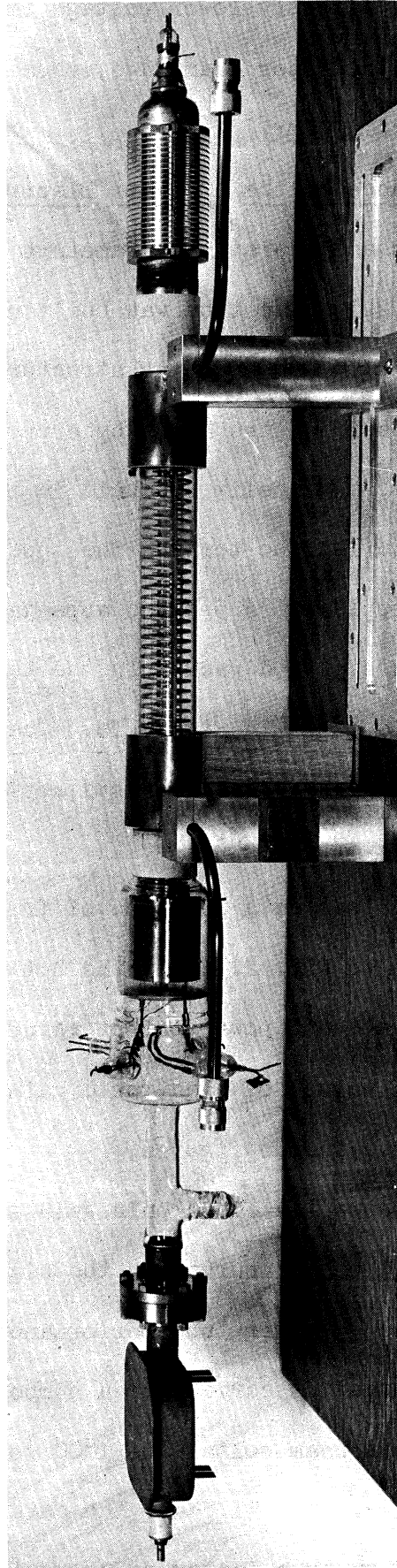


FIG. 2.16 ELECTROSTATICALLY FOCUSED CRESTATRON.

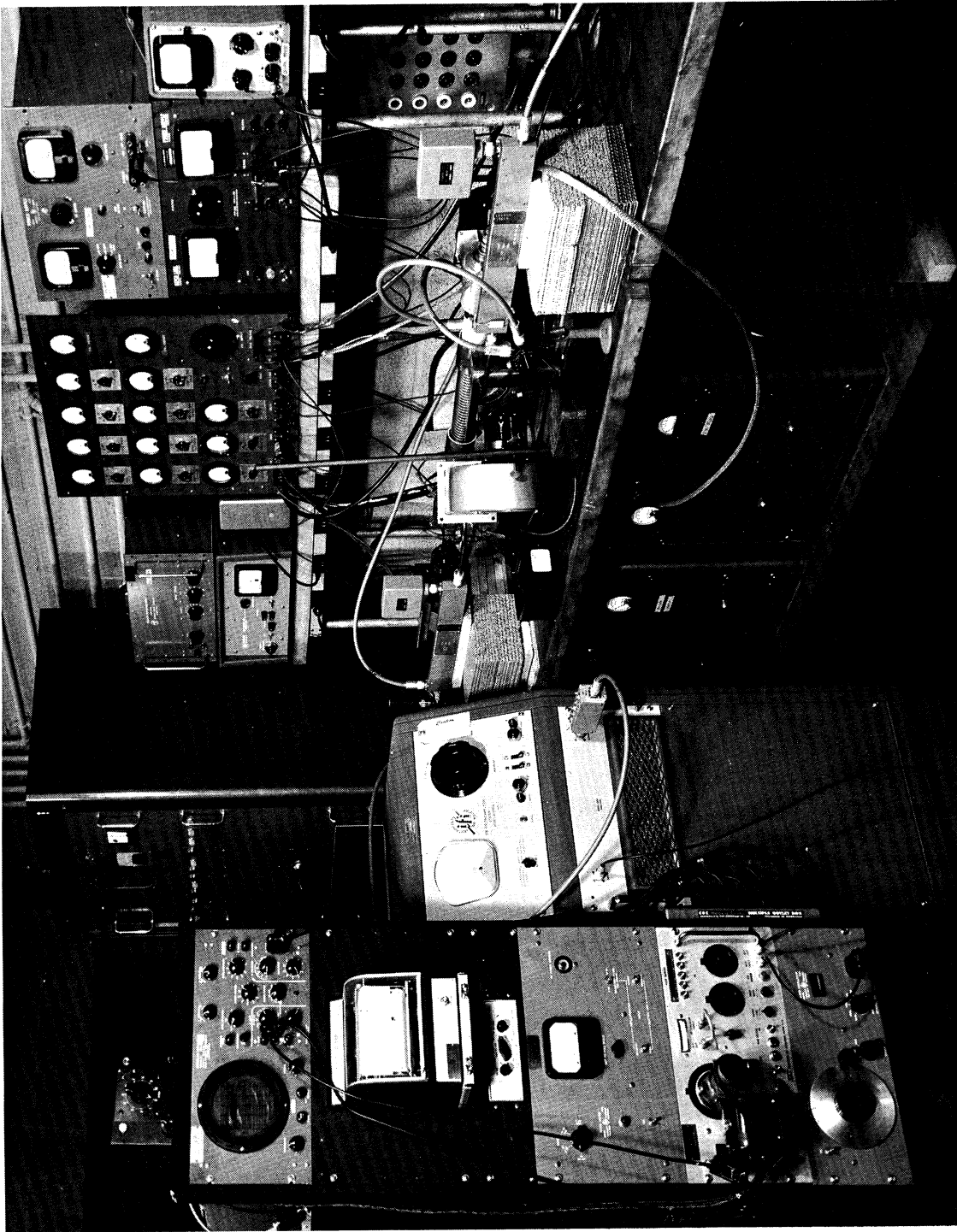


FIG. 2.17 TEST AREA FOR THE ELECTROSTATICALLY FOCUSED CRESTATRON.

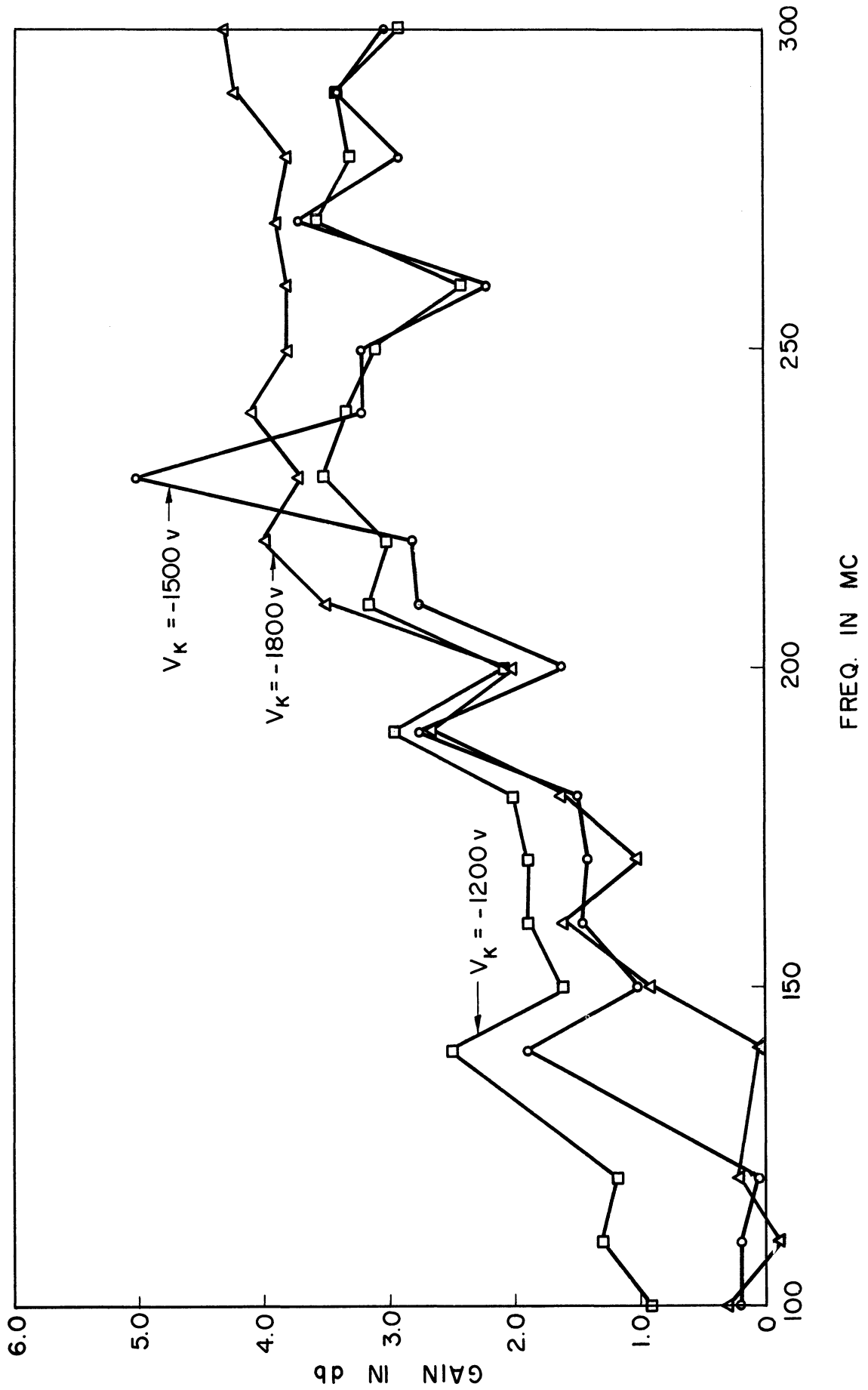


FIG. 2.18 SMALL-SIGNAL ELECTRONIC GAIN VS. FREQUENCY.

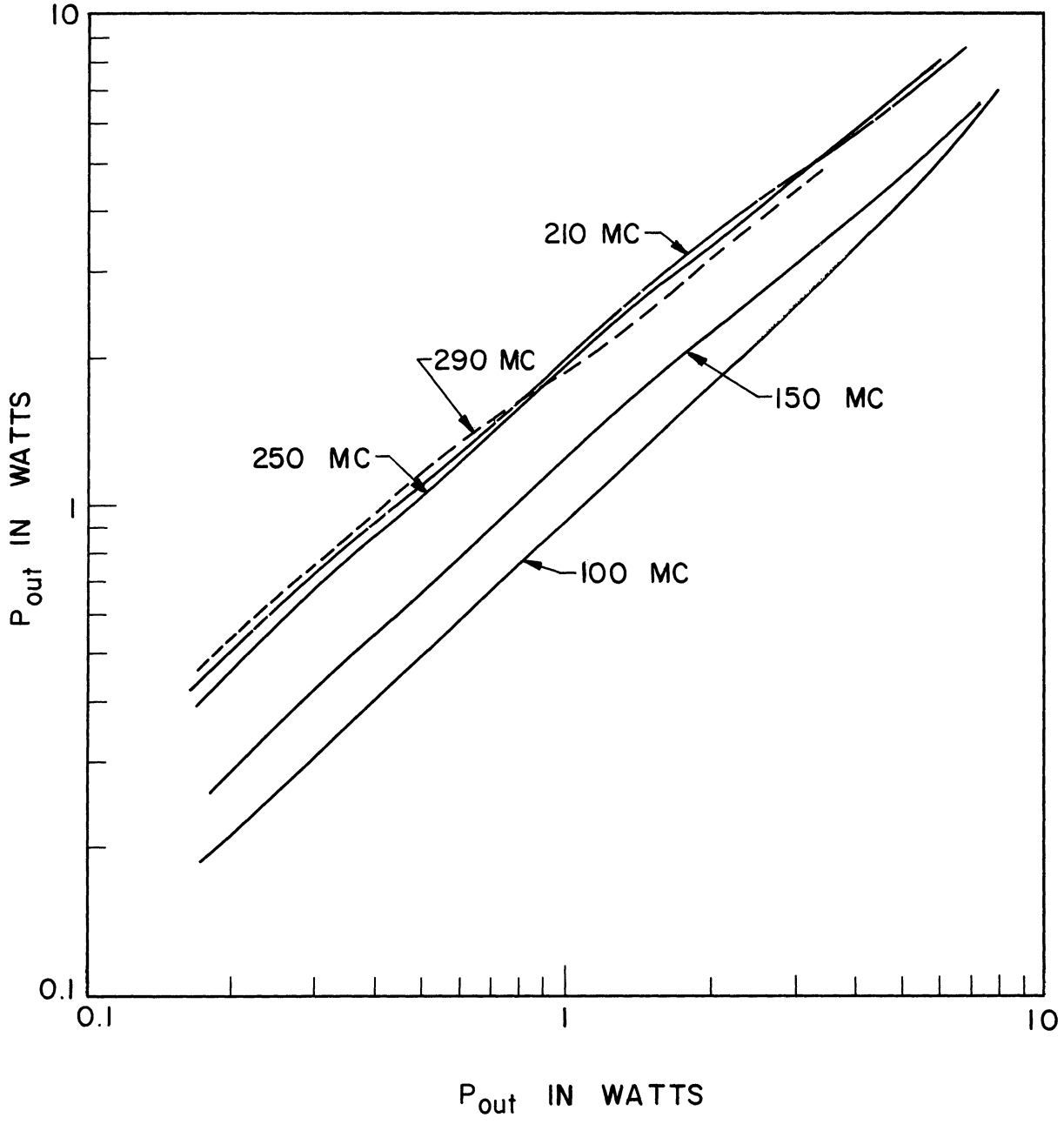


FIG. 2.19 SATURATION GAIN FOR $V_K = -1800$ VOLTS. ($I_K = 90$ ma)

current was increased, the collector current did not rise proportionately. In fact, the percentage of beam transmission to the collector dropped markedly for higher values of beam current. This fact prevented the tube from being operated at its design value of beam current. The low values of gain and power output shown in Figs. 2.18 and 2.19 can be directly attributed to the low cathode current limited by poor beam transmission.

Even though the digital computer results indicate that good beam transmission should be possible at the design value of beam current, there are in reality several factors which can cause serious difficulties. The most important one of these is due to thermal electrons, which cause beam broadening. Another factor, which could not be included in the computer program either, is secondary electron emission when the beam grazes the focusing disks. Both of these effects contributed in making the hollow electron beam much thicker than predicted. This manifested itself in the low beam transmission and hence in the low r-f gain observed.

As the r-f power in an electrostatically focused tube increases, the velocity distribution of the electrons within the beam becomes greater. Since the electrostatic focusing parameters depend quite critically on the beam voltage, it is obvious that the beam transmission deteriorates as the r-f drive is increased. This is shown in Fig. 2.20. The reason that the beam transmission is only between 30 and 40 percent even at low power levels is believed to be due to mechanical misalignments within the gun or the tube itself. Thus in an electrostatically focused tube the gain not only falls off due to saturation effects as the power level is increased, but it also falls off due to a lowering of collector current as a result of less effective focusing. Figure 2.21 shows this markedly.

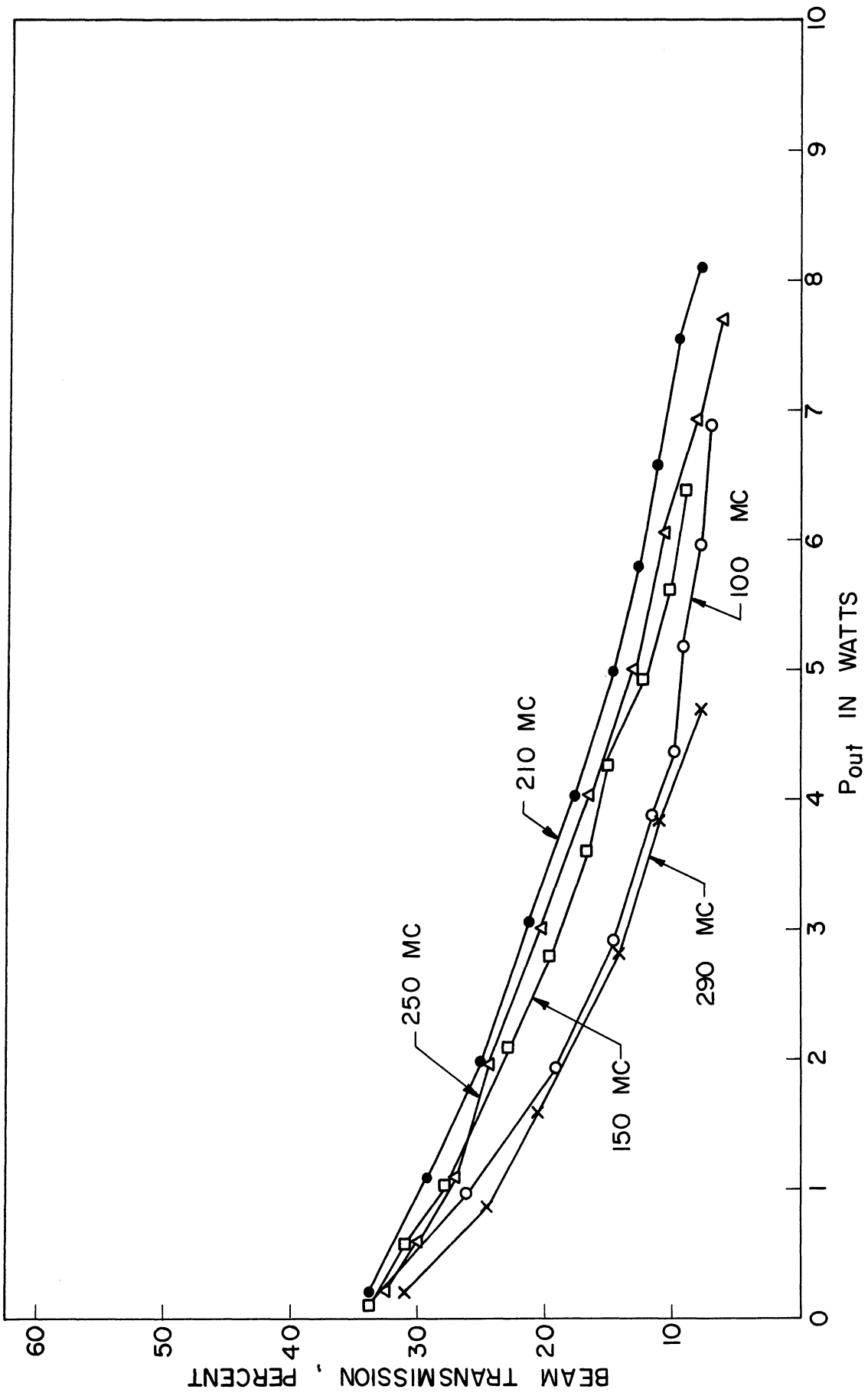


FIG. 2.20 BEAM TRANSMISSION VS. P_{out} for V_K = -1800 VOLTS.

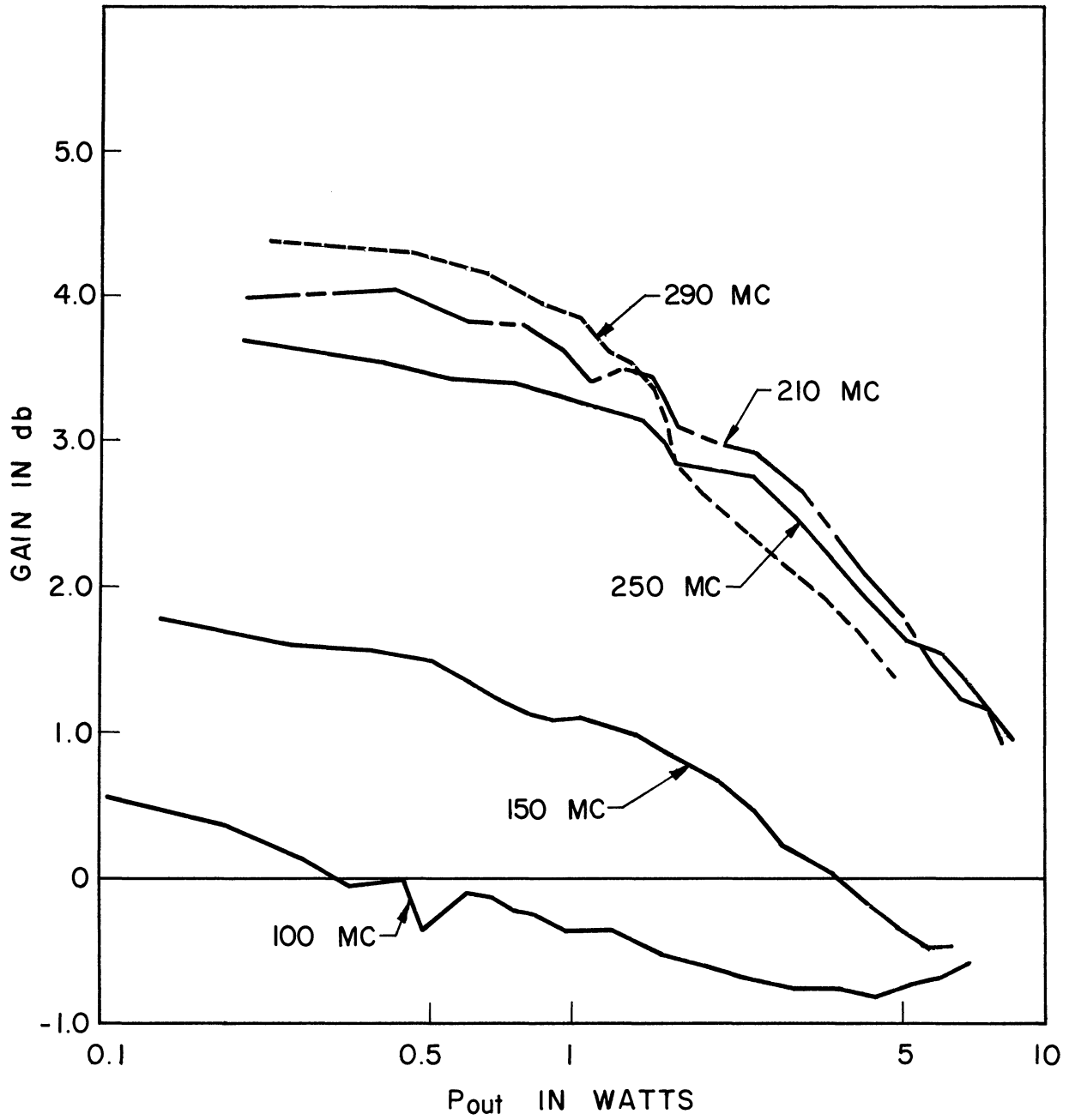


FIG. 2.21 GAIN VS. P_{out} FOR V_K = -1800 VOLTS. (I_K = 90 ma)

3. High Perveance Hollow-Beam Gun Studies

3.1 Design of Two $P_{\mu} = 20$ Guns. The computer program described in Section 2.5 revealed that it should be possible to focus electrostatically an electron beam of $P_{\mu} = 4.46$. The question then arose whether a higher current beam could be focused by the same means. Thus it was decided to work out a design which would yield a gun of $P_{\mu} = 20$, with an operating voltage of approximately 2000 volts, and a beam power near 3 kw. The gun geometry was so chosen that it could be incorporated into the 100-watt electrostatically focused Crestatron, if desired. Such a tube should then be able to deliver almost a kilowatt of r-f power. An Einzel lens was to be used in this gun also. The following parameters apply to this $P_{\mu} = 20$ gun.

Table 3.1

Parameters for $P_{\mu} = 20$ Gun
(1.076 Inch Diameter Beam)

| | |
|--------------------|---------------------------|
| Perveance | 20 microperv |
| Operating Voltage | 1860 volts |
| Operating Current | 1.61 amp |
| Beam Width | 0.080 inch |
| Mean Beam Diameter | 1.076 inch |
| Current Density | 0.673 amp/cm ² |

Note that for this gun the beam dimensions are the same as those for the $P_{\mu} = 4.46$ gun used in the electrostatically focused Crestatron.

In order to have available a higher current density gun to be used with a 1 kw magnetically focused tube, if the need should arise, another $P_{\mu} = 20$ gun was designed. The pertinent parameters are listed in Table 3.2.

Table 3.2

Parameters for $P_{\mu} = 20$ Gun
(0.806 Inch Diameter Beam)

| | |
|--------------------|--------------------------|
| Perveance | 20 microperv |
| Operating Voltage | 2000 volts |
| Operating Current | 1.79 amp |
| Beam Power | 3.58 kw |
| Current Density | 1.31 amp/cm ² |
| Beam Thickness | 0.080 inch |
| Mean Beam Diameter | 0.806 inch |

Both of these guns were designed with the help of an electrolytic tank in the usual way. The digital computer program was then applied and the electron trajectories plotted. Several modifications in the electrode geometry became necessary before a reasonably good beam could be obtained. For the larger diameter gun, for example, it was necessary to narrow the first anode aperture and to add lips to the center electrodes of the Einzel lens. The final gun design is shown in Fig. 3.1. Note that the beam is much less laminar than in the $P_{\mu} = 4.46$ gun. In addition the beam spreads much more quickly after leaving the final anode, due to the higher space-charge forces in this beam.

The smaller diameter gun was even more difficult to handle, as Fig. 3.2 should indicate. The lens electrode had to be shaped in the odd fashion shown in order to prevent both serious trajectory crossing and beam interception on the last anode. It was also found to be necessary to use a curved cathode surface in this gun, in order to impart an initial convergent force to the electrons. With a flat cathode

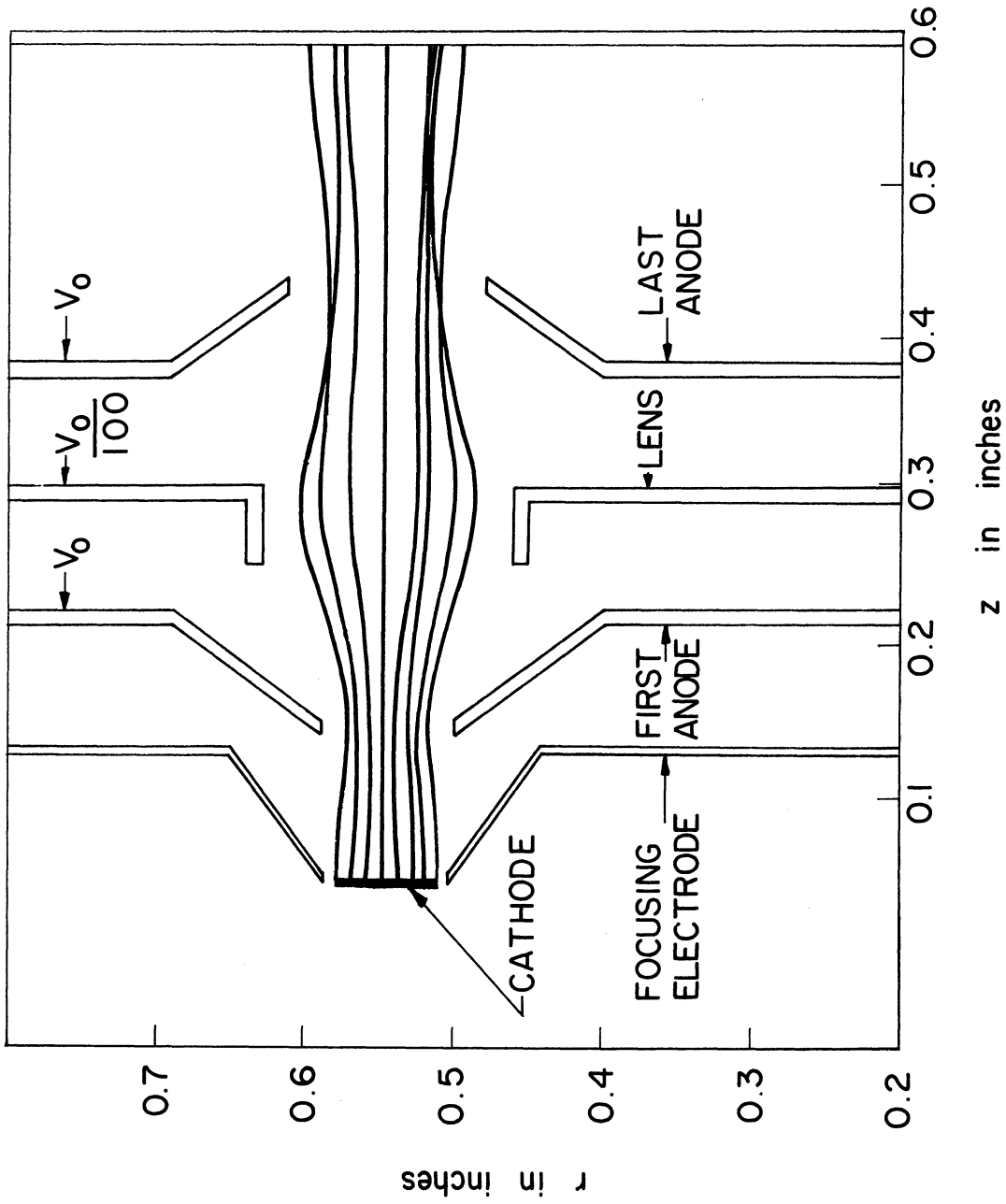


FIG. 3.1 TRAJECTORY PLOT FOR LARGE DIAMETER $P_\mu = 20$ GUN. ($J_0 = 3.722 \cdot 10^9$ AMP/ m^2 , $P_\mu = 17.97$,

$2r = 1.076$ INCH)

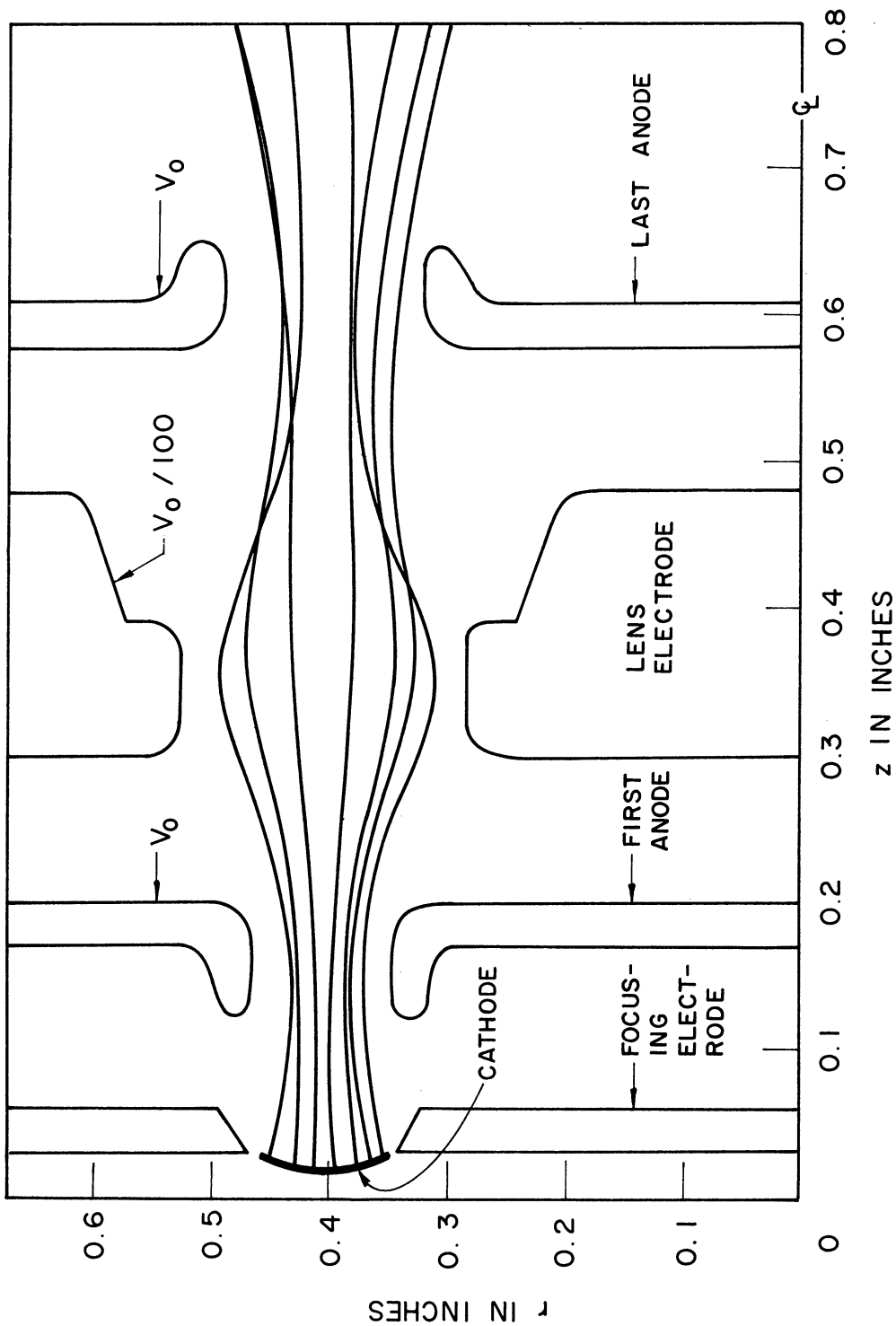


FIG. 3.2 TRAJECTORY PLOT FOR SMALL DIAMETER $P_{\mu} = 20$ GUN. ($J_0 = 7.203 \cdot 10^3$ AMP/ m^2 , $P_{\mu} = 19.573$,

$2r = 0.660$ INCH)

the outer electrons would always be intercepted either on the first anode or on the lens electrode.

A small axial magnetic field throughout the gun region was found to be very beneficial in keeping the beam laminar, however. In particular, for the gun shown in Fig. 3.2 a flat cathode and a lens electrode with straight sides could be used, if an axial magnetic field of approximately 200 gauss was used.

3.2 Beam Analyzer Tests of the 1.076 Inch Diameter, $P_{\mu} = 20$ Gun.

The first of the guns described in the previous section was constructed and mounted for testing in the beam analyzer. Various beam profiles were taken for different lens voltages and for several distances from the gun anode. Figure 3.3 is a typical set of curves. Even though the two cases shown appear not to be much different as far as beam profiles are concerned, the beam interception was much less with the lens voltage of -1455 volts applied, indicating that most of the interception occurs on the last anode. Other curves taken for this gun indicate that the beam spreads quite rapidly as it drifts away from the final anode. For example, at a distance approximately one inch from the gun, the beam is already twice as thick as at the exit. For a lens voltage of -1455 volts the beam appears to be approximately 0.1 inch thick when leaving the gun, as compared to the design value of 0.08 inch. This latter thickness could be obtained with a slightly larger lens voltage, but at the expense of somewhat poorer beam transmission. With secondary electrons returning from the collector suppressed by means of the grids in front of the collector surface shown in Fig. 2.7, a beam transmission through this gun of 80 to 90 percent was observed.

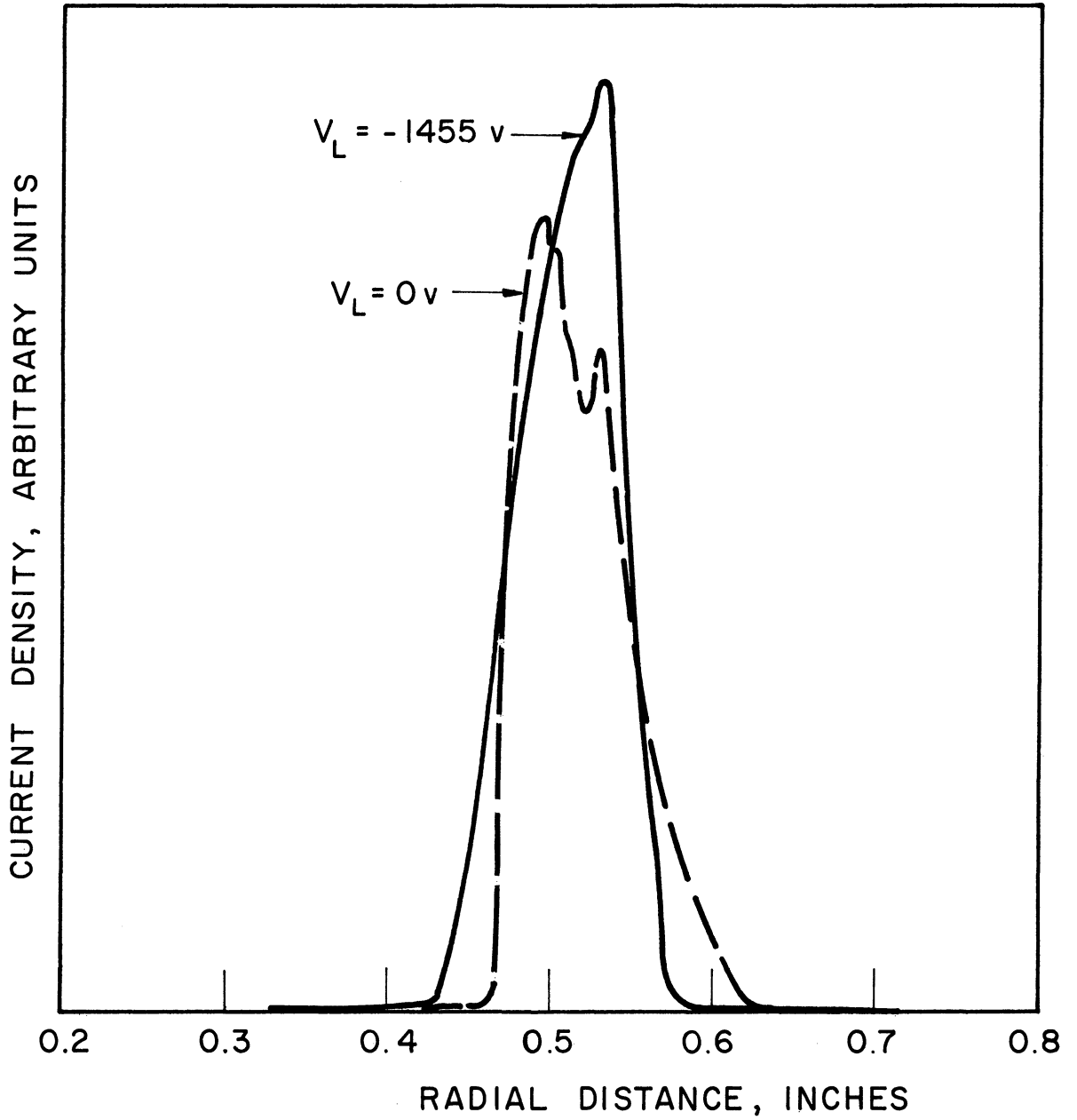


FIG. 3.3 BEAM PROFILES AS A FUNCTION OF LENS VOLTAGE AT A DISTANCE OF 0.10 INCH FROM THE LAST GUN ANODE.

From this data it can be concluded that it would be essential to start the electrostatic focusing fields as near to the gun as possible, if the beam is to be transmitted through a slow-wave structure for any reasonable distance. Once the space-charge forces have caused the beam to diverge substantially, it would no longer be possible to hold the beam together in a periodic electrostatic focusing system.

4. Summary and Conclusions

Two electrostatically focused Crestatrons were designed for the 100 to 300 mc frequency range. Both made use of a hollow electron beam obtained from identical $P_{\mu} = 4.46$ guns. One was designed for a power output of 100 watts, cw, while the other was designed for 1000 watts, cw.

Both tubes employed electrostatic focusing of the type where high voltage and low voltage disks alternated along the center of the hollow beam. A helix was used for the slow-wave circuit, and coupling onto and off of the r-f circuit was accomplished by a pair of coupled-helix couplers.

The lower power tube was constructed and tested. There were several basic limitations which prevented the tube from being operated at full power and with the designed gain:

A. Even though a digital computer analysis of the electron gun and the electrostatic focusing system indicated that the beam should be transmitted all the way to the collector, it was found in practice that beam broadening due to thermal electrons and the generation of a large number of secondary electrons when the primary beam grazed the focusing disks caused the beam transmission to be less than satisfactory.

B. There was a high probability that individual parts in the gun and the focusing system were not aligned perfectly, causing the beam to strike the focusing structure or the helix.

C. The electrostatic focusing system was too critically dependent on voltage. This resulted in poor beam focusing under large-signal operation, when the velocity spread in the electron beam was large.

As a result of the above limitations, the beam current had to be kept near 80 or 90 milliamperes, which was only approximately one third of the design value. Hence the small-signal gain was in the range of 3 to 4 db, and saturation took place at power levels near 10 watts.

The 100-watt tube development program was altered to require a short and compact magnetically focused tube for an entirely different reason than the shortcomings cited above. A size limitation was imposed by systems requirements. This brought about a new tube design. The details of this work are described fully in Part II of this report.

In addition to the tube work mentioned above, this program also included some studies on digital computer techniques for the analysis of axially symmetric, hollow-beam guns and electrostatic focusing systems. The program was developed to the point where electron trajectories could be plotted for any such system. Use was made of this program in checking the beam optics of the 100-watt electrostatically focused Crestatron and in predicting the performance of several other gun designs. Within the limitations of the program, which were cited at the appropriate places in this report, the agreement between the computer results and the experimental studies were generally good.

5. Recommendations for Future Work

A lot of time could have been saved in the trial and error work on both the experimental phase of the program and the computer analyses of the various gun-beam systems if a synthesis procedure using a digital computer program had been available. Therefore a program should be worked out that is able to determine the necessary electrode geometries for both generating the desired beam and electrostatically focusing it to the collector. It would be desirable to be able to include thermal velocity effects as well as velocity distributions in the electron beam due to the presence of r-f.

This is admittedly a very difficult proposition, but if it could be solved, tube designs using focusing systems of the type described here would become straightforward. Not only would such a program tell the designer what electrode geometries to use, but it would also yield a direct estimate on the limitations of such a design. The effects of r-f drive and beam perveance on the focusing problem could be estimated readily.

PART II

Bendix Corporation Work

by

K. C. Earl
J. G. Meeker
A. G. Peifer
J. W. Ross

DEVELOPMENT OF 100-WATT CRESTATRON AMPLIFIER FOR
OPERATION IN THE 100-300 MEGACYCLE
FREQUENCY RANGE

1. Introduction

This part of the report delineates the work accomplished by The Bendix Corporation, Research Laboratories Division, in assisting The University of Michigan in developing high-power broadband Crestatron tubes under Navy Contract NObsr-81403.

The program was divided into two parts. The first part was basically a research-type program which was undertaken to demonstrate the feasibility of employing electrostatic focusing in high-power VHF microwave amplifier tubes, while the second part concerned the development of a magnetically focused tube applicable to existing hardware.

The Bendix Research Laboratories Division's responsibilities under the first part of the program were as follows:

- A. Assist The University of Michigan in the initial electron gun design and determination of entrance conditions of the electron beam into the electrostatic focusing structure.
- B. Construct and test electron guns according to the designs.
- C. Design and test collector structures.
- D. Design and test coaxial line to helix r-f transitions.
- E. Provide an overall mechanical design.

F. Construct and deliver six laboratory engineering models of the 100-watt tube.

G. Construct and deliver three laboratory engineering models of the 1000-watt tube.

Two tubes, a 100-watt tube and a 1000-watt tube, were to be developed. Each tube was to be packaged in a glass envelope, electrostatically focused, and exhibit a gain of at least 10 db across the specified frequency band.

During the first year all subassemblies for the 100-watt tube were designed and tested. These components included the electron gun, collector, r-f structure, focusing structure, and r-f matching systems. In addition, the r-f structure and matches were completed for the 1000-watt tube. Construction was started on the first 100-watt tube, but the tube was not finished because of a change in program objectives.

During discussions with the Navy, it became apparent that the electrostatically focused tubes would be too large for existing hardware. In the interest of developing a tube directly applicable to existing hardware, the electrostatically focused tube was discontinued as a part of the Bendix Research Laboratories Division program in August 1961.

A new program to develop a magnetically focused 100-watt tube was then presented to the Navy. Work was started on this program 1 August 1962 and work on the 1000-watt was deferred until a later date. This redirected program, of eighteen months duration, was to culminate in the delivery of three tubes to the Navy.

The Bendix Research Laboratories Division assumed responsibility for all aspects of the magnetically focused tube program, except the basic

electrical design of the r-f structure which was a joint effort with The University of Michigan, who monitored the work as it progressed.

This redirected portion of the program was divided into two phases. Phase I concerned proving the feasibility of obtaining an output of 100 watts from a magnetically focused Crestatron tube capable of operating over the 100- to 300-megacycle frequency range. Operable tubes meeting the electrical and environmental requirements were to be fabricated during Phase II, and three such tubes delivered to the Navy.

Two series of tubes, TW-143 and TW-147, were fabricated under Phase I. The first tube was designated TW-143. This tube was designed as the smallest possible helical tube which would operate in the specified frequency range. The design goal was achieved by choosing a smaller than normal helix diameter for this frequency and power combination, with the intent of electronically tuning the tube to lower the operating frequency range. For large-signal operation, the r-f circuit would not operate as intended, because of phase-focusing effects which caused inverse saturation characteristics. Therefore, a new circuit was designed and designated TW-147. Three of these tubes were constructed and tested. The required power and large-signal gain were obtained over the specified frequency band, but some inverse saturation characteristics were still observed; therefore, the design was adjusted to obtain a tube with normal overload characteristics.

Effort during Phase II was primarily concerned with developing a mechanical design capable of meeting the environmental specifications. This design was designated TW-148. These tubes have equaled or exceeded the electrical and environmental specifications, and three such tubes were delivered, along with solenoids, to the Navy.

2. Electrostatically Focused Tubes

Based upon the original electrical design all parts for assembling a 100-watt tube were fabricated, and the subassemblies were nearly completed, as shown in Fig. 2.1. The mechanical design appeared feasible at this point in the program and cold tests indicated good r-f matches between coaxial lines and the helix.

A 7052 glass envelope was to be used for the first tube. Successful forming of 7052 precision glass envelopes was accomplished and considerable progress was made toward forming 1723 alumino-silicate glass envelopes.

It was concluded that the mechanical design was sound and cold test measurements indicated that the passive electrical characteristics were satisfactory.

2.1 Electrical Design of Electrostatically Focused Tubes. For convenience and clarity the tube design is discussed in terms of the collector, electron gun, and the r-f impedance transitions. The r-f circuit and focusing structure designs were the prime responsibility of The University of Michigan and are discussed in Part I of this report.

2.1.1 Collector Design. A hollow electron beam drifting between two concentric conducting cylinders, with the outer cylinder more positive, will experience diverging forces which tend to cause the beam to intercept the outer cylinder. The outer edge of the beam experiences forces from the space charge of the beam as well as the applied electric field between the two cylinders, which also acts on the inner edge of the beam. This model was analyzed using the method

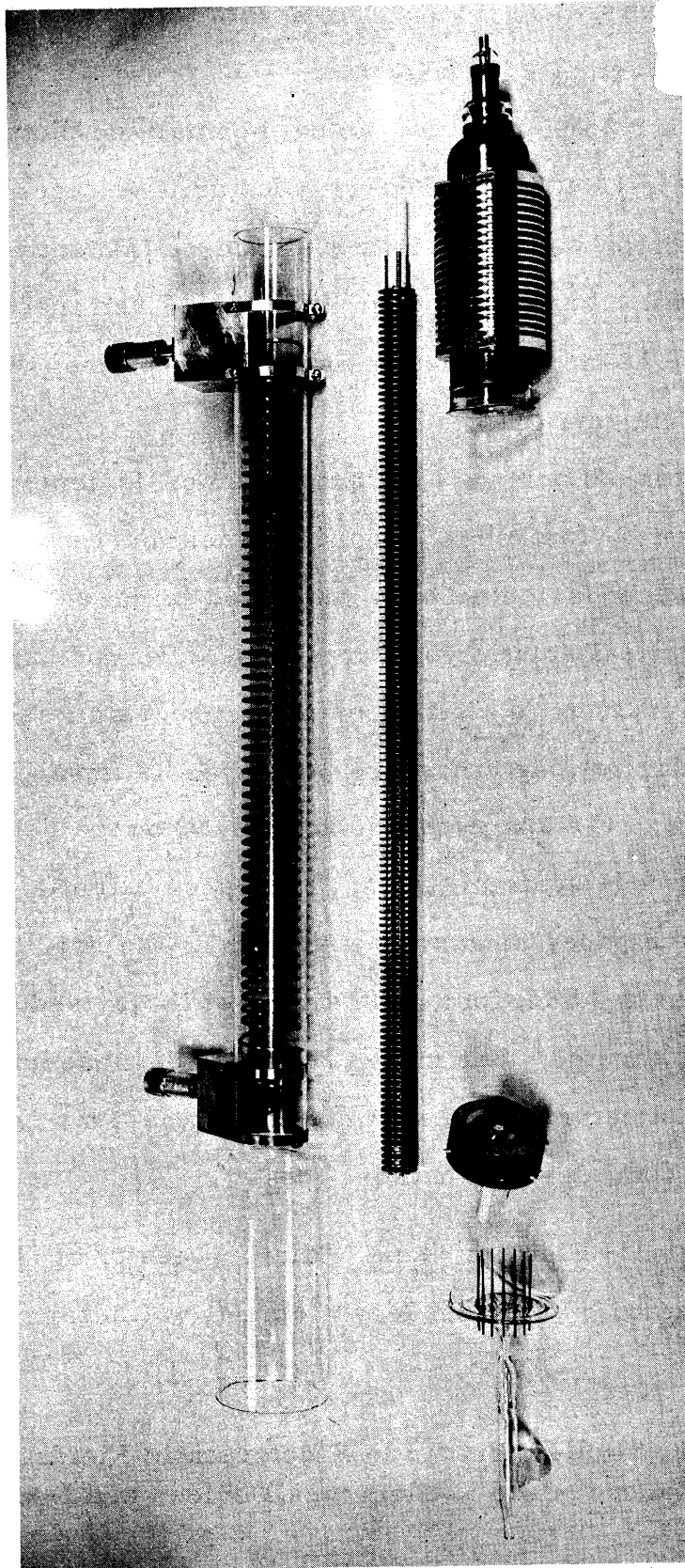


FIG. 2.1 SUBASSEMBLIES FOR 100-WATT TUBE

described by Lawrence A. Harris.¹ The model assumed axial symmetry, constant electron axial velocity, zero beam thickness (initially), and zero electron radial velocity (initially).

Figures 2.2 and 2.3 show typical normalized plots of the beam contours for the 1000-watt tube. Various drift voltages were considered, since the collector was to operate at depressed potentials. Similar plots for the 100-watt tube are shown in Fig. 2.4. From these plots the area over which the beam is collected can be determined. Figure 2.5 shows a plot of this information.

A depressed potential collector cannot, in general, be as simple as two concentric electrodes, because means must be provided for trapping any secondary electrons generated in the collector region. Since the analytical solution of complicated electrode arrangements is a very difficult problem, a digital computer program was used, with electrode configurations and space potentials as inputs, to derive data representative of the space-charge-free electron trajectories through the collector electrode configurations. The space potentials were determined from resistance paper measurements. Using the results from the analytical investigation as a guide, four geometries were devised and the electron trajectories computed. The most promising of these configurations and the electron trajectories are shown in Fig. 2.6. This configuration was chosen as the final design for these tubes.

2.1.2 Electron Guns. The University of Michigan developed an electron gun with an Einzel lens element, which formed the electron

1. Harris, L. A., "Hollow Beams in Electrostatic Fields," 1956 IRE Convention Record, Part 3, Electrons, Devices and Receivers, p. 11.

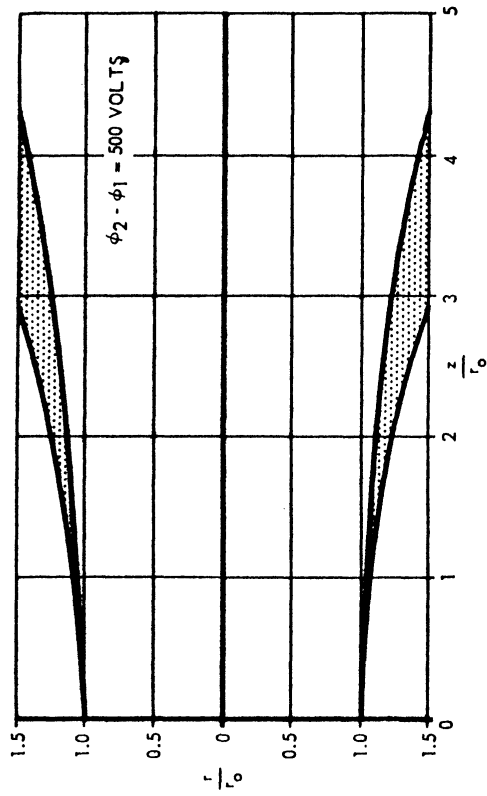
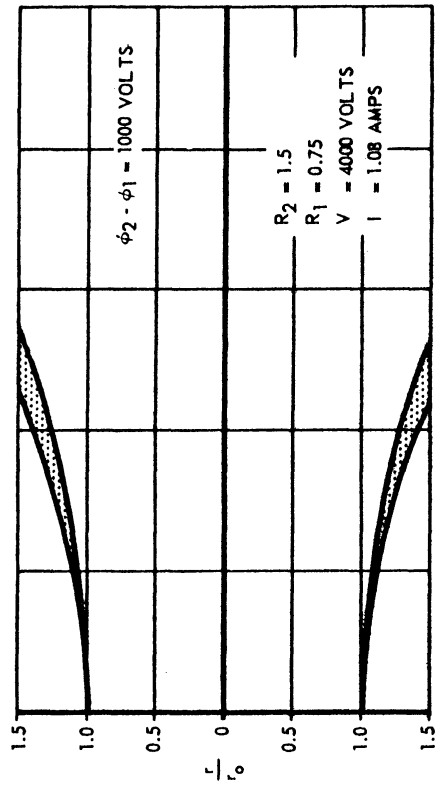


FIG. 2.3 TYPICAL BEAM CONTOURS.

1 KILOWATT TUBE. (V = 4000 VOLTS).

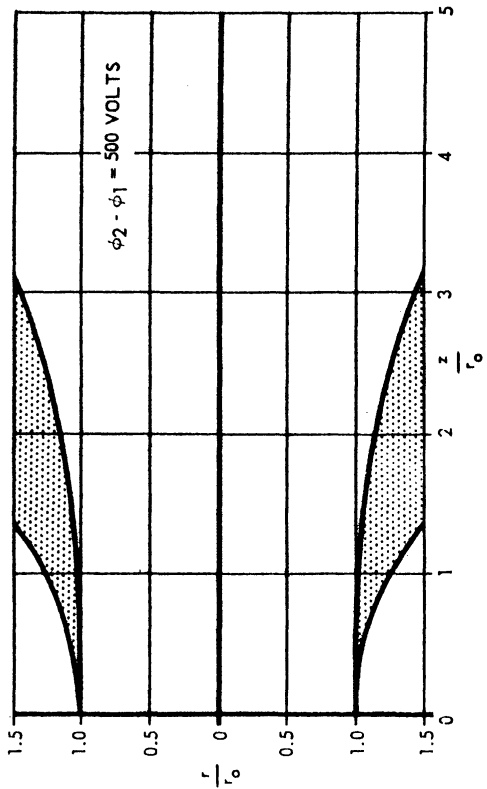
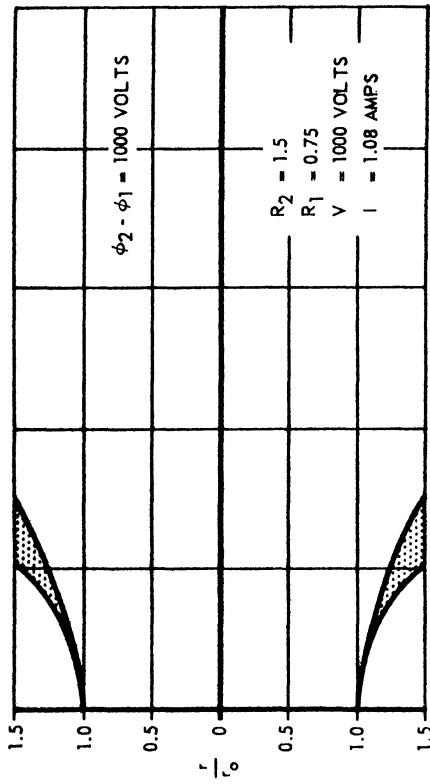


FIG. 2.2 TYPICAL BEAM CONTOURS.

1 KILOWATT TUBE. (V = 1000 VOLTS).

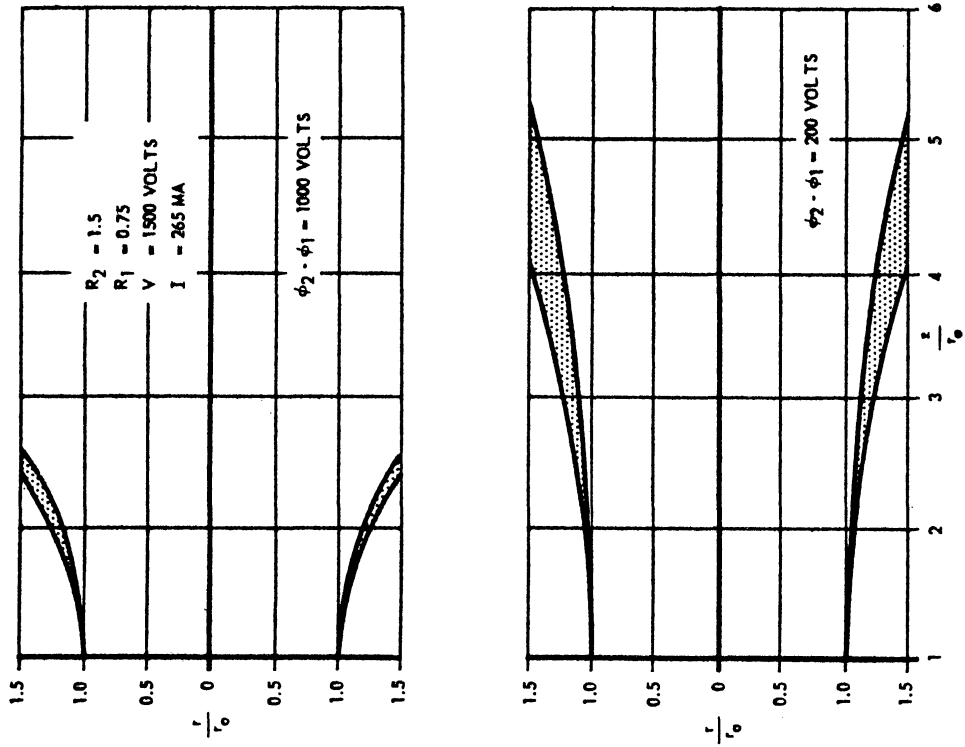


FIG. 2.4 BEAM CONTOURS.
(100-WATT TUBE).

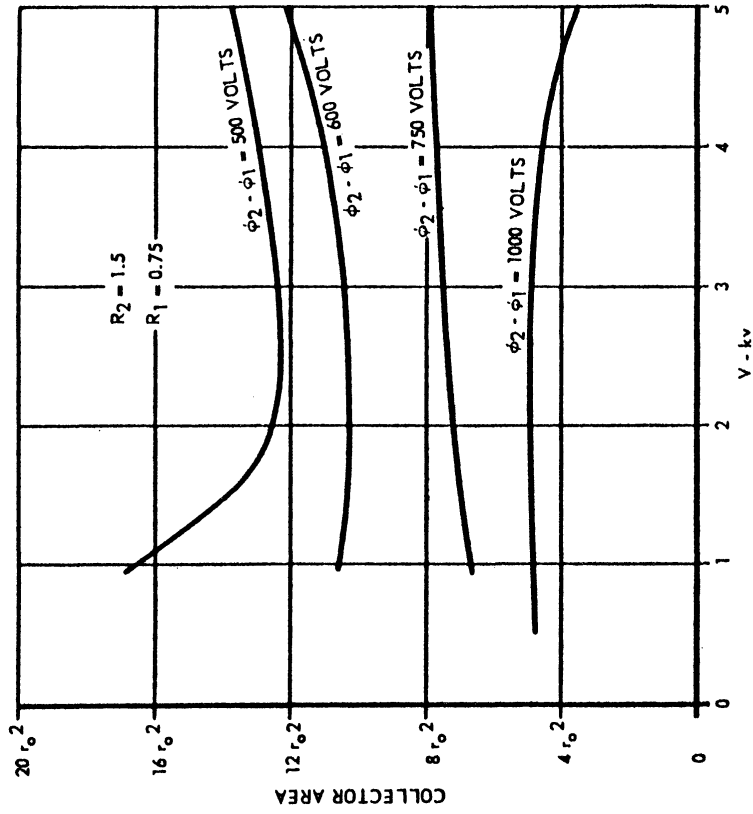


FIG. 2.5 COLLECTOR AREA AS A FUNCTION
OF ELECTRODE POTENTIAL.
(1 KILOWATT TUBE).

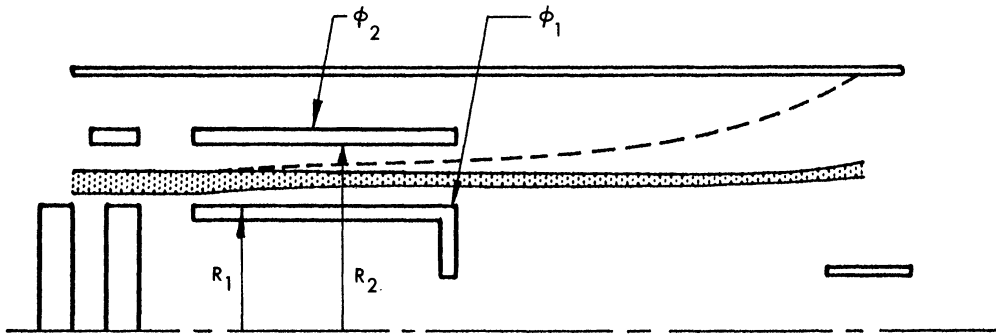


FIG. 2.6 ELECTRON TRAJECTORIES IN COLLECTOR REGION.

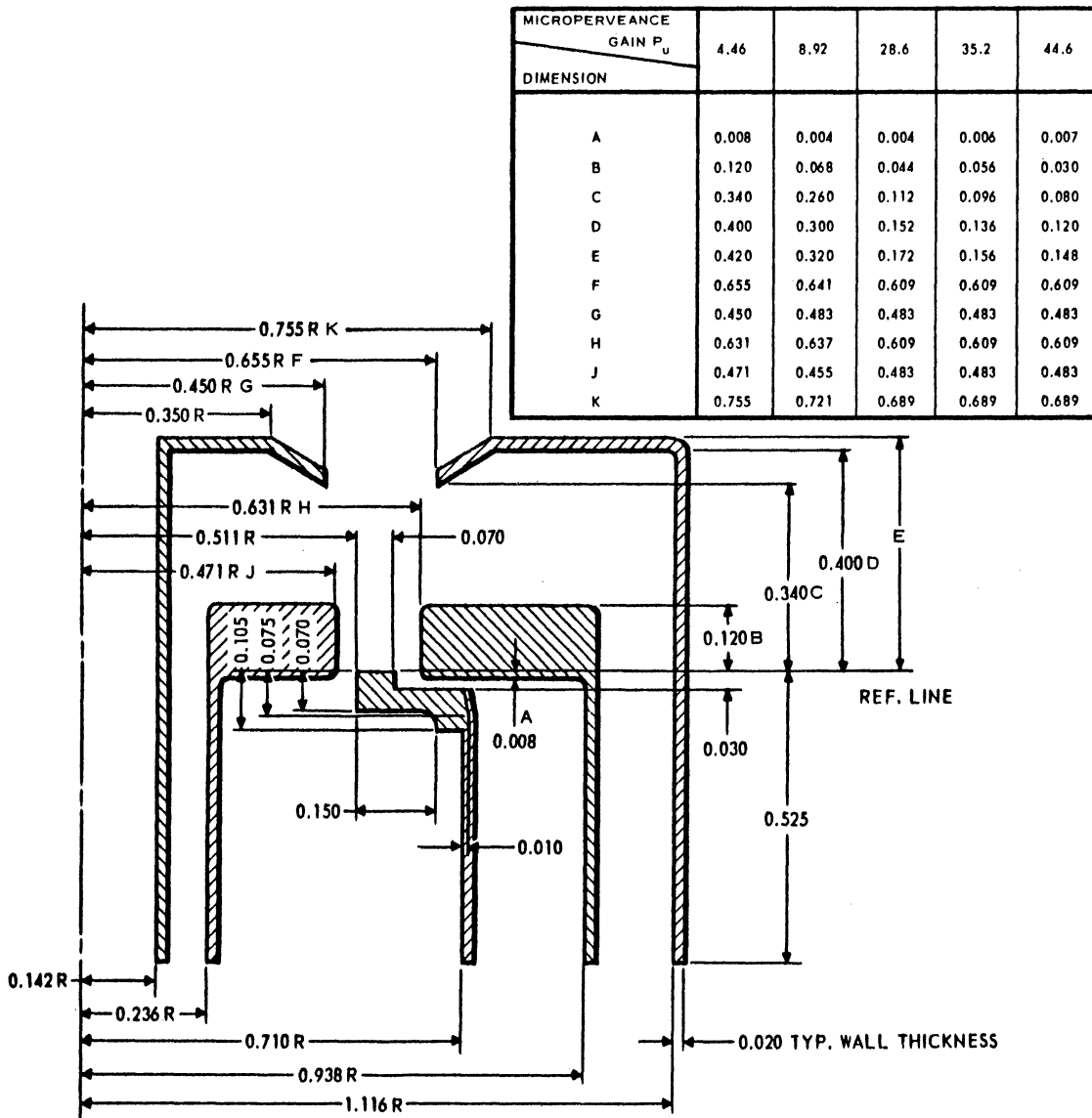


FIG. 2.7 4.46 MICROPERVEANCE ELECTRON GUN CONFIGURATION.

beam very accurately prior to the beam entrance into the electrostatic focusing structure. Although this gun was essential to the development of the focusing structure, it was believed that a triode gun (one focus electrode and one aperatured anode in addition to the cathode), would produce a sufficiently well-formed beam for this particular tube. The resulting simplification of the gun structure was considered worthwhile; therefore, the Bendix Research Laboratories Division undertook a program to design a triode gun for the tube.

A triode gun design for the 100-watt tube was derived by using an electrolytic tank to duplicate, as closely as possible, the potential profile of a space-charge-limited planar diode. The design parameters for the gun were as follows:

Grid Voltage = 0 (with respect to the cathode potential)

Anode Voltage = +1520 (with respect to the cathode potential)

Perveance = 4.46×10^{-6}

Total Current = 265 ma

Cathode Current Density = 0.15 amp/cm²

Beam Outer Radius = 0.581 inch

Beam Inner Radius = 0.511 inch

In an investigation of the limitations and advantages of the triode gun, the basic 4.46 microperveance gun configuration was scaled to four other microperveances, (8.92, 28.6, 35.2, and 44.6). Figure 2.7 shows the basic configuration of the guns.

Component parts for the 4.46, 8.92, and 28.6 microperveance guns were fabricated, and the guns were in the final stages of assembly when work was stopped on the electrostatically focused tubes. Consequently, there is no test data on these guns.

2.1.3 R-F Match. The r-f matching method was completed for the 100-watt tube. While the 1000-watt tube matching system was to be similar to the 100-watt system, work had just been started on it when the program objectives were changed.

The basic matching device consisted of a pin sealed in the glass envelope which made a direct contact between the center conductor of a coaxial connector and the end of the helix. To reduce stray capacitance and stray inductance, a short taper was inserted in the coaxial line where it approached the tube. Shields were then placed around the glass envelope to modify the helix impedance near each end, and, in addition, the pitch of the last several turns of the helix was altered. Figure 2.8 shows the coaxial line and shields which were the most successful in providing a good match. The pitch of the helix taken along an axially directed line through the junction of the helix and pin was 0.50, 0.35, 0.33, and 0.30 inch between succeeding turns. The 0.30 inch pitch is that of the original helix design. Figure 2.9 shows a plot of the VSWR of a single transition, and Fig. 2.10 shows the VSWR of a two transition system.

2.2 Mechanical Design. The 1000-watt and 100-watt tubes were to employ similar mechanical designs.

The helix was supported on three ceramic rods which were fitted inside a precision glass envelope. The helix for the 100-watt tube was fabricated from 0.100-inch diameter molybdenum wire, while the helix for the 1000-watt tube was fabricated from 0.150-inch diameter molybdenum wire. These wires made very stiff helices and no special mechanism was used to hold each turn of the helix in its proper pitch position, such as the common practice of putting notches in the ceramic support rods to hold each turn of less rigid helices.

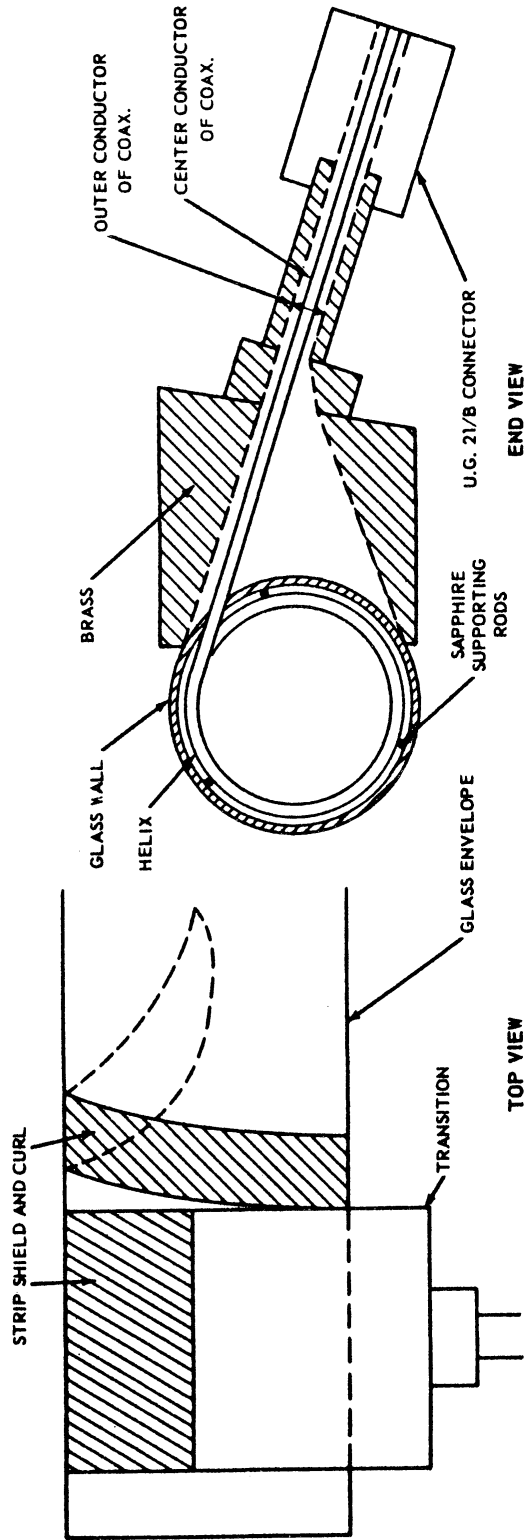


FIG. 2.8 TANGENTIAL TRANSITION

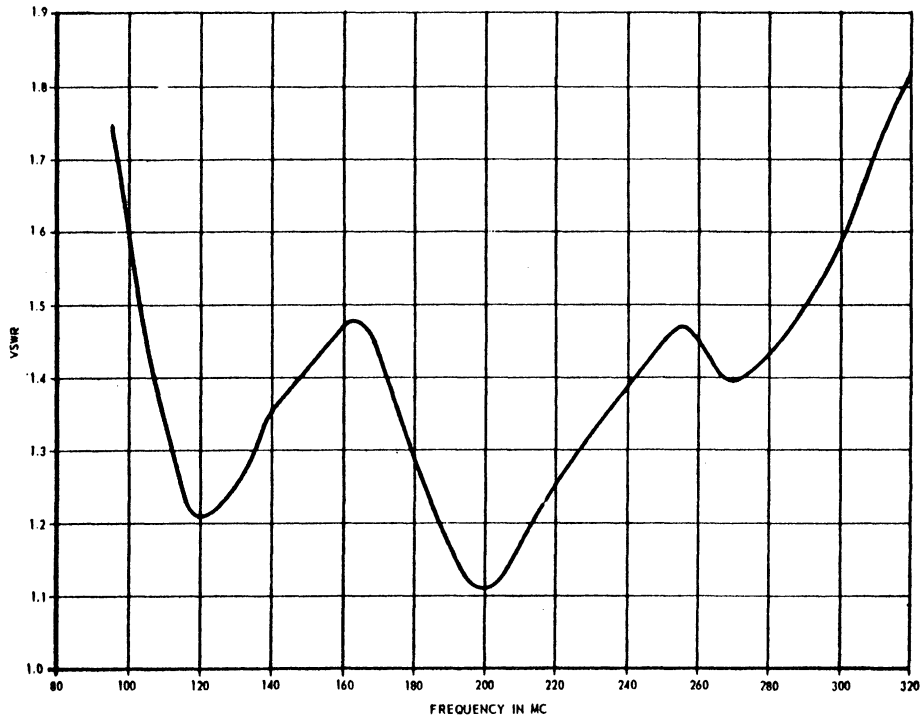


FIG. 2.9 VSWR OF SINGLE TRANSITION.

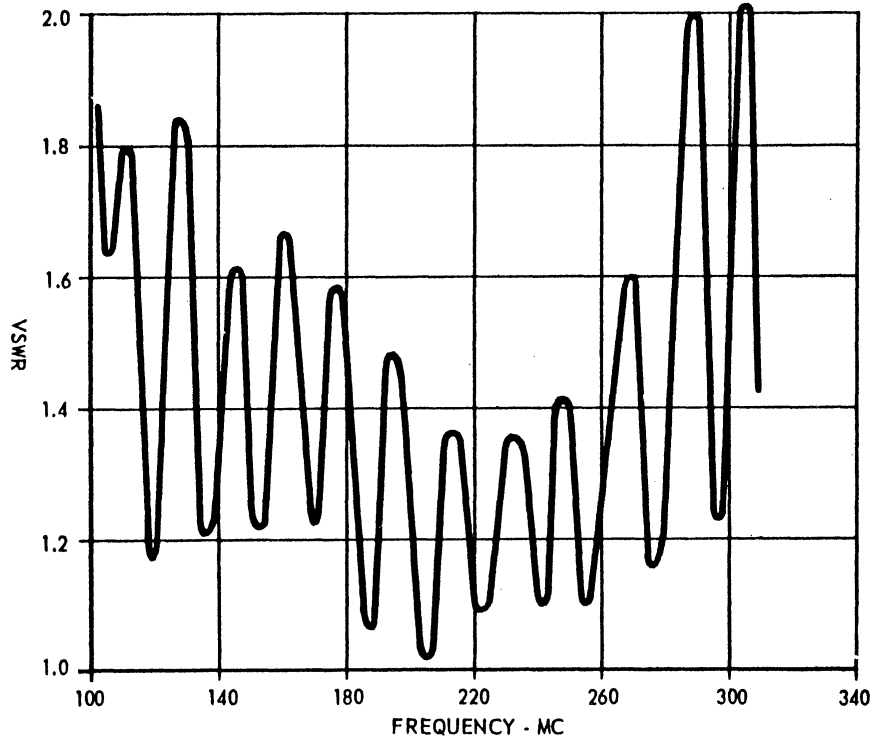


FIG. 2.10 VSWR OF TWO-TRANSITION SYSTEM.

Early models of the 100-watt tube used 7052 glass envelopes and glass to kovar seals at the helix connection pins, d-c feedthrough pins, and collector to envelope junction. In addition, techniques were being developed to use high melting temperature alumino-silicate glass for the tube envelopes, since alumino-silicate glass would permit higher bake-out temperatures and result in a much cleaner (less gassy) tube.

The electron gun electrodes were supported on concentric cylinders, which were held in place by three radial ceramic rods passing through tight fitting holes in the cylinders and a central support rod, which was concentric with the cylinders. The central support rod was held by a centering disk behind the gun which fit the inside diameter of the glass envelope over the gun region. The central support rod extended in front of the gun and fit rigidly into the electrostatic focusing structure, which was also supported at the collector. Figure 2.1 shows the 100-watt tube subassemblies.

Precision glass envelopes of this large size could be obtained from vendors only on special orders, and then only with a long and doubtful delivery schedule. The envelope had a nominal inside diameter of 1.774 inches over the helix and 2.772 inches over the gun. The helix section was 22 inches long, and the gun section 5 inches long.

The process developed by Bendix Research Laboratories Division for producing this precision glass tubing consisted of placing glass tubing over a precision stainless steel mandrel, which was then supported above an open top oven with the axis of the assembly vertical. A mechanical vacuum pump was used to evacuate the space between the mandrel and glass. The assembly was then lowered slowly into the ovens passing through a preheating zone first, which heated the glass to just below

its softening temperature. The glass-mandrel assembly then passed into a narrow hot zone where the glass softened and ambient air pressure forced the glass snugly around the steel mandrel. The assembly then passed into an annealing oven which maintained a temperature just below the softening temperature of the glass until the forming process in the hot zone had passed over the full length of the mandrel. The annealing furnace temperature was then reduced slowly to room temperature. Since the coefficient of expansion of the stainless steel mandrel is greater than that of the glass, the mandrel becomes smaller than the glass by several thousandths of an inch when the assembly is cooled. This allows relatively easy removal of the steel mandrel from the glass envelope. Figure 2.11 shows a picture of the apparatus used in forming the glass envelopes.

Envelopes of 7052 glass were successfully formed using this process with typical out-of-roundnesses of less than 0.0005 inch and total diameters within 0.003 inch of the nominal diameter. These envelopes were used both by The University of Michigan and the Research Laboratories Division.

Work was progressing in forming 1723 alumino-silicate glass by the same process. A complete tube envelope had not been formed, but substantial progress had been accomplished. Sections of tubing several inches long had been formed during initial tests.

Critical conditions in this process include the polished finish on the steel mandrel; the avoidance of sharp corners anywhere on the mandrel; the maintenance of a good vacuum during the forming process; preheat zone, hot zone, and annealing temperatures and time durations; and the uniformity of heating around the circumference of the assembly.

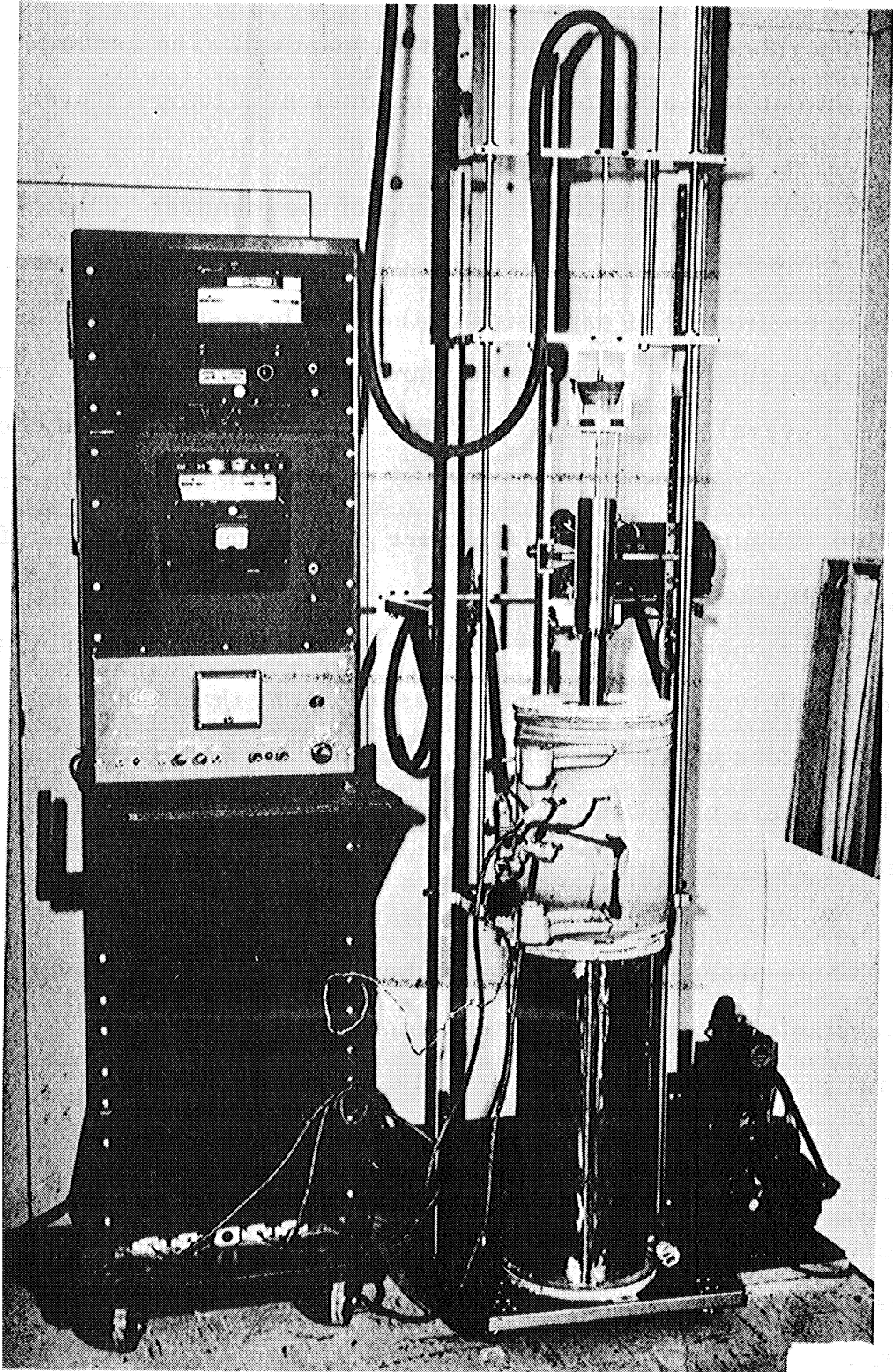


FIG. 2.11 ENVELOPE FORMING FURNACE

3 Phase I---100-Watt Magnetically Focused Crestatron
Feasibility Studies

3.1 TW-143. The development of this tube (TW-143) was undertaken to fulfill the redirected program objectives; viz., develop a broadband 100-watt power output tube capable of being used in present equipment. This tube was to employ magnetic focusing in order to take advantage of the smaller size possible with such a tube as compared to an electrostatically focused tube. Laboratory models of the tube were to be tested in solenoids with the objective of using permanent magnets for the focusing structure.

The design of the helical r-f circuit was of prime importance in developing a 100-watt tube capable of operating over the 100- to 300-megacycle range and still be within the eighteen-inch length limit. It is well known that when the operating voltage of a microwave tube is raised above the maximum small-signal gain voltage the gain decreases. Small-signal theory predicts that this gain reduction is frequency dependent in that the gain at high frequencies reduces faster than the gain at low frequencies. This suggests a method of electrically tuning the small-signal gain to cover a lower frequency band than would otherwise be expected. At some expense of small signal gain per stream wavelength, a tube could be of smaller design with more wavelengths per unit length. The TW-143 tube design was such a design. Several designs were analyzed at The University of Michigan by a computer programmed with small-signal theory, then the final design was evaluated and was confirmed with a small-signal computer program at Bendix Research Laboratories Division.

This design was not evaluated from a large-signal point of view, and subsequently, a large-signal phase-focusing problem was discovered after several tubes had exhibited an inverse saturation characteristic. (An explanation of this phenomenon is given in Section 3.1.1.) The design parameters for TW-143 are as follows:

| <u>Frequency</u> <u>(Mc)</u> | <u>ka</u> | <u>ya</u> | <u>C</u> | <u>QC</u> | <u>Measured</u> <u>DLF</u> | <u>Impedance</u> <u>K</u> |
|---------------------------------|-----------|-----------|----------|-----------|-------------------------------|------------------------------|
| 100 | 0.02 | 0.69 | 0.332 | 0.115 | 0.871 | 387 |
| 200 | 0.04 | 1.256 | 0.308 | 0.130 | 0.873 | 210 |
| 300 | 0.06 | 1.830 | 0.261 | 0.176 | 0.874 | 75 |

- a = 0.376 inch (mean helix radius)
- TPI = 11.5 (helix turns per inch)
- R/a = 1.5 (shield to helix radii ratio)
- d = 0.030 inch (helix wire diameter)
- r₁ = 0.238 inch (hollow electron beam inner radius)
- r₂ = 0.294 inch (hollow electron beam outer radius)
- L = 9.6 inch (length of helix)
- V_o = 870 volts (electron beam voltage)
- I_o = 452 milliamps (electron beam current)

Eighteen tubes were built, tested, and the results evaluated during this portion of the program.

It was concluded that:

A. For large-signal operation the r-f circuit would not operate as intended because of phase-focusing effects.

B. Triode, hollow beam, immersed flow, electron guns will provide a good, though not optimum, electron beam.

C. Many mechanical design features and methods of tube parts fabrication were perfected.

D. Phase-focusing considerations are complicated by the effects of the shields used to taper the impedance of the helix for r-f matching purposes.

E. A phase-focusing phenomenon resulting in inverse saturation characteristics was discovered.

3.1.1 Electrical Design. The TW-143-A tubes were designed for the minimum possible size for a helical tube operating over the 100- to 300-megacycle frequency range. To achieve the small size, it was considered advantageous to exploit the effects of operating an O-type traveling-wave tube at voltages higher than the voltage at which the small-signal gain is a maximum. It can be shown, for a dispersionless helix, that this overvoltage operation will reduce the small-signal gain and, further, that the reduction in gain is more pronounced at the higher operating frequencies. In addition, the dispersion of a helix without shields, or with moderate shielding, will have higher phase velocities at the lower frequencies; therefore, operating in an overvoltage condition will tend to favor the lower frequencies. Thus, it would be expected that the combined effects of overvoltage operation would result in a lowering of the operating band. Small-signal computer programs, one at The University of Michigan and one at the Research Laboratories Division, verified this; i.e., both computer programs predicted a lower frequency band of operation than would be predicted by the same or similar small-signal theories where the voltage is adjusted for maximum small-signal gain.

The experimental results taken at low voltages confirm the band center frequency as would be predicted by Dunn's method.² In this method the beam velocity parameter is always optimized for any given set of parameters. Thus, the beam velocity parameter is effectively eliminated from consideration, and the response is predicted on the basis of the helix and beam geometries.

The experimental results taken at high voltage and small-signal levels also confirm the expected downward shift of the frequency band due to high voltage operation. Figure 3.16 shows the gain and power output versus frequency for tube number 9 obtained under these conditions; i.e., tube was operated at high voltage, one-watt input, and about 5 to 10 watts of output. Tube number 9 used tapered matching sections which are essentially frequency insensitive, and the characteristic shown in Fig. 3.16 is due to the helix-beam interaction only. This operation confirms the computer predictions based on small-signal theory.

In O-type traveling-wave tubes energy is transferred to the circuit wave at the expense of the kinetic energy contained in the electron beam. As long as the tube operates at a small-signal level, the energy transferred is only a small percentage of the total kinetic energy, and the beam velocity is approximately constant throughout the tube. If, however, the tube is driven into saturation, the energy transferred can range from 10 to 35 percent or more of the total beam kinetic energy. For example, some of the TW-143-A tubes gave an electronic efficiency of 20 percent. Since the kinetic energy varies as

2. Dunn, D. A., "Traveling-Wave Amplifiers and Backward-Wave Oscillators for VHF," Trans. PGED IRE, Vol. ED-4, No. 3, pp.246-264; July, 1957.

v^2 , where v is the velocity and the velocity corresponds to the square root of voltage V , it is seen that a 1000-volt beam giving up 20 percent of its energy would slow to a velocity corresponding to 800 volts.

It is to be expected that such wide velocity variations would have detrimental effects on the response of the tube. The effect in a typical high gain tube is a loss of synchronism between the electron beam and the circuit wave causing a 3 to 6 db compression of gain at saturation as compared to small-signal inputs.

In a tube, such as TW-143, designed to work at overvoltages and large-signal levels, the beam slows down to synchronous velocities near the output end of the tube. This results in two effects which alter the desired performance characteristics of the tube.

The first effect is that the frequency response reverts back to the usual band; i.e., that band which would be predicted by small-signal theory with synchronous velocities. This results since the synchronous condition near the output end of the circuit represents a substantial portion of the total circuit length in a low gain tube, such as the TW-143. If velocity slowing effects are significant over the last 5 to 6 db of gain in a tube of 12 to 15 db of electronic gain, then 30 to 50 percent of the circuit is affected and the frequency response is substantially shifted back to that of the synchronous tube.

The second effect manifests itself as the inverse saturation characteristics displayed by the TW-143 tubes. Consider a low gain tube (approximately 10 db) operated at overvoltage and small-signal conditions. Under such conditions, the beam passes through the helix at a high velocity resulting in a low gain but maintaining nearly a constant velocity. If the tube is driven into large-signal operation,

the beam experiences a progressive deceleration through the tube. In the last part of the tube the average beam velocity will be near the synchronous velocity of the circuit. Since this is the optimum gain velocity, the gain in the last half of the tube is increased over the small-signal value. The overall tube gain increases by the same amount with the result that the large-signal gain exceeds the small-signal gain. This qualitative description explains the inverse saturation characteristic from a conceptual point of view; but, a quantitatively accurate theoretical evaluation of this operating condition would require a large-signal computer analysis which was not attempted on this program.

The TW-143 electron gun was designed by the same method used to design the electrostatically focused gun: that is, by using a space-charge-limited diode to simulate the potential profile. An electrolytic tank was used for the experimental measurements. A special effort was made to keep the electrode shapes as simple as possible while obtaining good potential profiles. A triode gun (one containing the cathode, focusing electrode, and one anode) was selected. Figure 3.1 shows a detailed assembly drawing of the gun. The grid voltage with respect to the cathode is zero, and the anode voltage for rated current is 870 volts. In the original design shown in Fig. 3.1, the required heater power was greater than that expected, which caused excessively high heater temperatures and aggravated a leakage problem. A combination of heat shields and a better method of mounting the cathode alleviated the heat problem; the leakage problem was reduced by undercutting the ceramic spacers.

The triode gun was tested in a beam tester. The results indicated considerable scalloping of the electron beam. Figure 3.2 shows a series

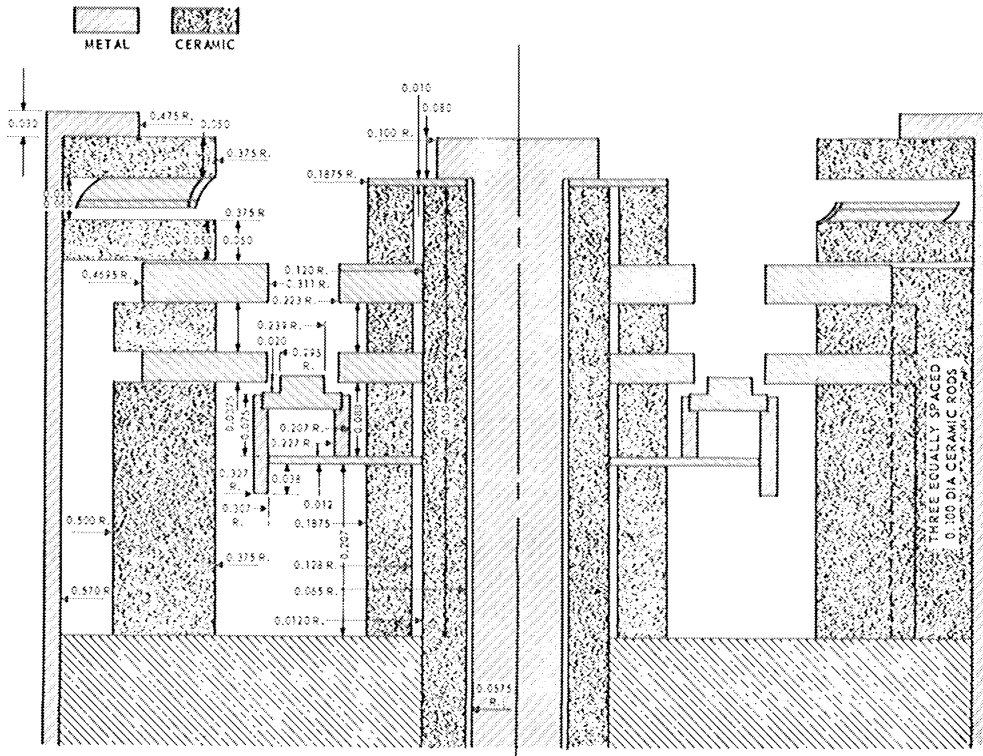
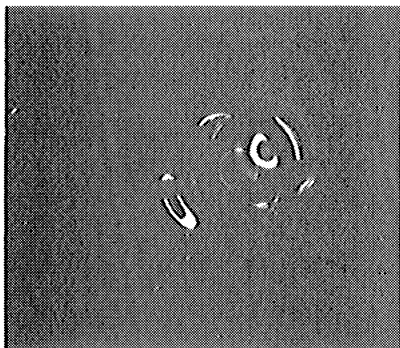
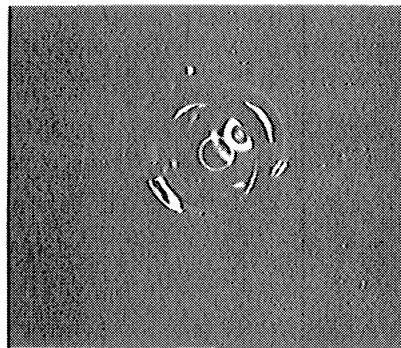


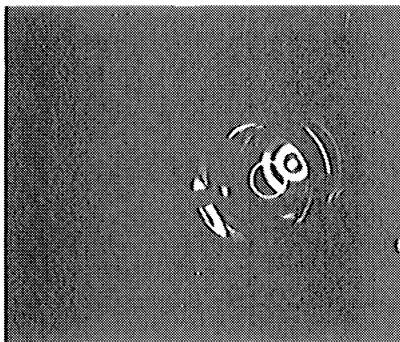
FIG. 3.1 DETAILED ASSEMBLY DRAWING OF GUN



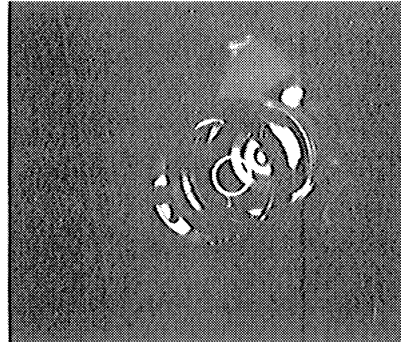
PULSED
 $I_K = 440 \text{ MA}$
 $I_{SC} = 370 \text{ MA}$
 $V_{SC} = 1275 \text{ V}$
 $I_{SOL} = 2.0 \text{ A}$
 $V_{FOC} = 0$



PULSED
 $I_K = 440 \text{ MA}$
 $I_{SC} = 370 \text{ MA}$
 $V_{SC} = 1200 \text{ V}$
 $V_F = 0$
 $I_{SOL} = 3.5 \text{ MA}$



PULSED
 $I_K = 450 \text{ MA}$
 $I_{SC} = 390 \text{ MA}$
 $V_{SC} = 1200 \text{ V}$
 $V_F = 0$
 $I_{SOL} = 6.0 \text{ A}$



PULSED
 $I_K = 480 \text{ MA}$
 $I_{SC} = 410 \text{ MA}$
 $V_{SC} = 1200 \text{ V}$
 $V_F = 0$
 $I_{SOL} = 6.0 \text{ A}$

FIG. 3.2 PHOTOS OF THE ELECTRON BEAM FROM THE GUN TESTER

of photos indicating the beam outline. The thick incandescent ring is the cathode of the gun. The thin ring, which appears to be floating in the foreground, is the beam outline as it strikes a carbonized tungsten screen. The variation in the brightness of the beam outline from picture to picture is caused by intercepting the beam at different points in its cycloidal path which, in effect, varies the current density of collection and therefore, the brightness. A three-anode gun was designed at a later date. This gun was tested and results indicated a decrease in beam scalloping.

The collector for this tube was designed to operate in a uniform magnetic field. Beam collection over a large collector area was accomplished by tapering the sides of the collector to gradually intercept the beam. The original collector was designed to operate at the full beam potential and was water cooled. A depressed potential air-cooled collector was to be designed after the r-f tests had been successfully completed. However, since this tube design was only partially successful, only one depressed potential collector was tested. This collector was incorporated into tube TW-143-A-16. Successful r-f operation was obtained with the collector operating at $3/4 V_0$.

The r-f matching problem consisted of making a transition from a 50-ohm coaxial line to the helical structure, which has an operating impedance of approximately 400 ohms. The requirements of the transition were low insertion loss (less than 1 db) and low VSWR (2 to 1 or less) over the 100- to 300-megacycle frequency range. A shield to gradually taper the impedance is one method of making the r-f match. These matching devices exponentially taper the characteristic transmission line impedance from 50 to 400 ohms. In addition, this type of

taper has a lower cutoff frequency but no upper cutoff frequency. Matches of this type allow the full bandwidth of the helical circuit to be utilized, as evidenced by tube TW-143-A-4 in which useful gain was exhibited over the 200- to 1000-megacycle frequency band (higher frequencies were not tested because of equipment limitations). Insertion losses of 1 to 2 db were obtained for complete tubes. With such low loss, the suppression of forward-wave oscillations depends almost completely upon the VSWR relationship of the matching sections and loads. In operating tubes, VSWR's of near 1.5 to 1 were achieved. Oscillations in these tubes would start at gains corresponding to the expected maximum stable gain as calculated from the VSWR's of the input and output matching sections.

Mechanically the gradual transition consists of a shield which surrounds the helix. At the end of the helix the shield is very close to the helix. This spacing between the helix and shield is chosen so that the helix operates as a 50-ohm line above ground. The coaxial line connects directly to the helix at the end. The shield gradually flairs away from the helix as the wave progresses along the helix. The helix is supported by ceramic rods which, because of the close helix to shield spacing, fit in grooves in the shield. These grooves represent electrical discontinuities, and therefore, only a less than perfect correlation between experiment and theory is possible.

The contour of the shield was chosen so that the impedance varies exponentially with distance. In this case it can be shown that

$$|\Gamma| = \left| \frac{\sin \theta}{2\theta} \right| \ln \frac{Z_h}{Z_1} \quad (\theta > 2),$$

where

Γ = voltage reflection coefficient,

θ = length of transition in radians = $2\pi L/\lambda$,

Z_h = high impedance at one end of the transition,

Z_l = low impedance at the other end, and

L = length of transition.

In TW-143, the helix impedance, Z_h , is approximately 400 ohms; and the coaxial line impedance, Z_l , is 50 ohms. The solid line shown in Fig. 3.3 is a plot of the theoretical VSWR for $Z_h/Z_l = 8$ and the transition length from $0 \leq L/\lambda \leq 4$. The dotted line shows the experimental results obtained with an actual transition operating in the 100-300-megacycle frequency range. Another transition was fabricated which operated in the $0.9 < L/\lambda < 2.7$ range. Figure 3.4 shows a plot of the VSWR of tube TW-143-A-2 which utilized the longer matching taper.

The literature³ shows that as a shield is moved close to a helix, the phase velocity and interaction impedance are reduced. Both of these effects affect the beam wave interaction in the especially important output or large-signal region of the helix. For this reason it was decided to investigate other r-f matching sections which would have less effect on the interaction process.

It appeared that helical matching sections would eliminate the velocity taper and have less effect on the interaction impedance. Consequently, helical matching sections were designed, cold tested, and used in several tubes. The VSWR's obtained with the helical matching

3. Mathers, G. W. C., and Kino, G. S., "Some Properties of a Sheath Helix with a Center Conductor or External Shield," Technical Report No. 65, Electronics Research Laboratory, Stanford University, Naval Research Contract N60NR 251, Task No. 7, NRO 73 360; June, 1953.

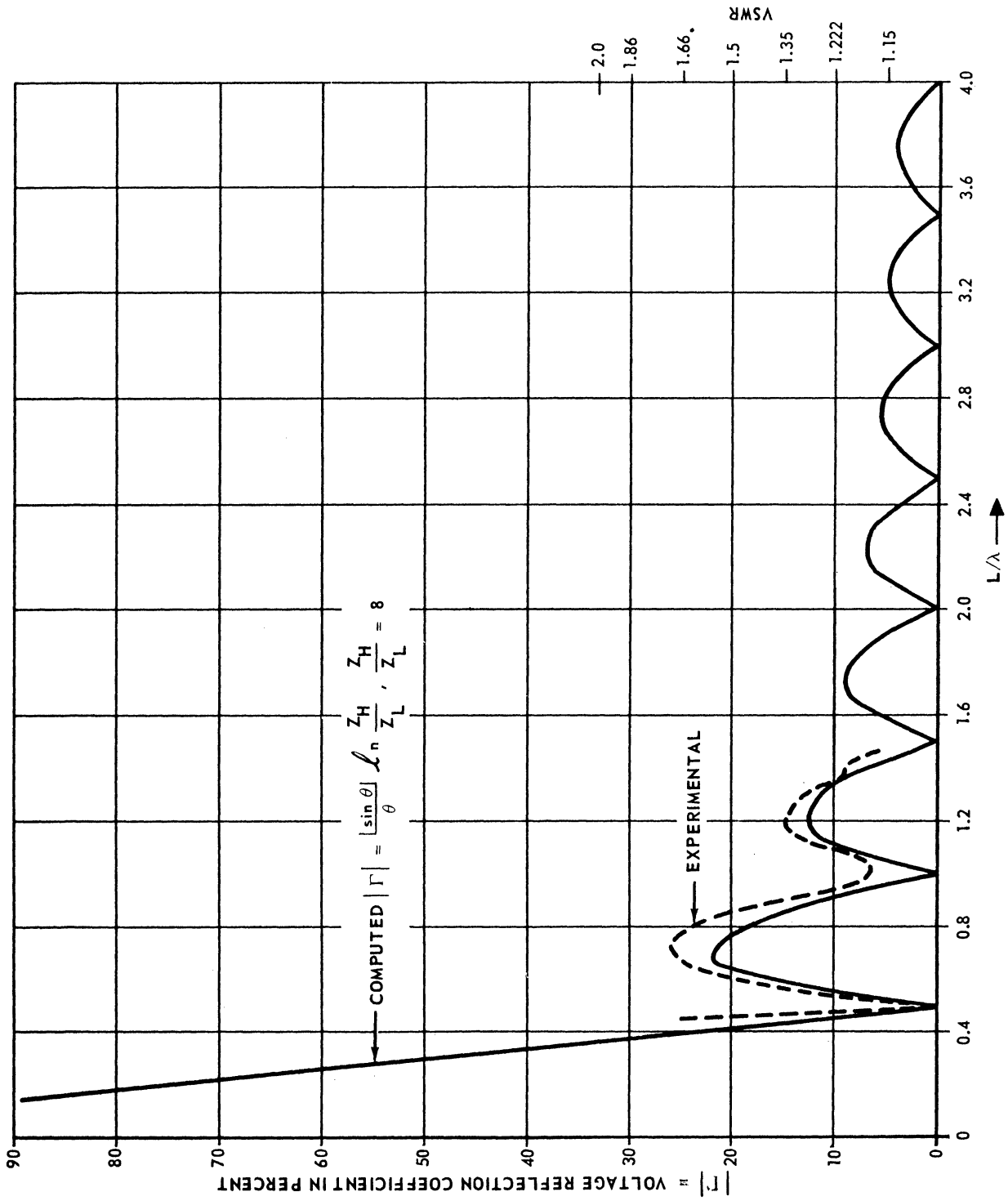


FIG. 3.3 VOLTAGE REFLECTION (VSWR VS. L/λ).

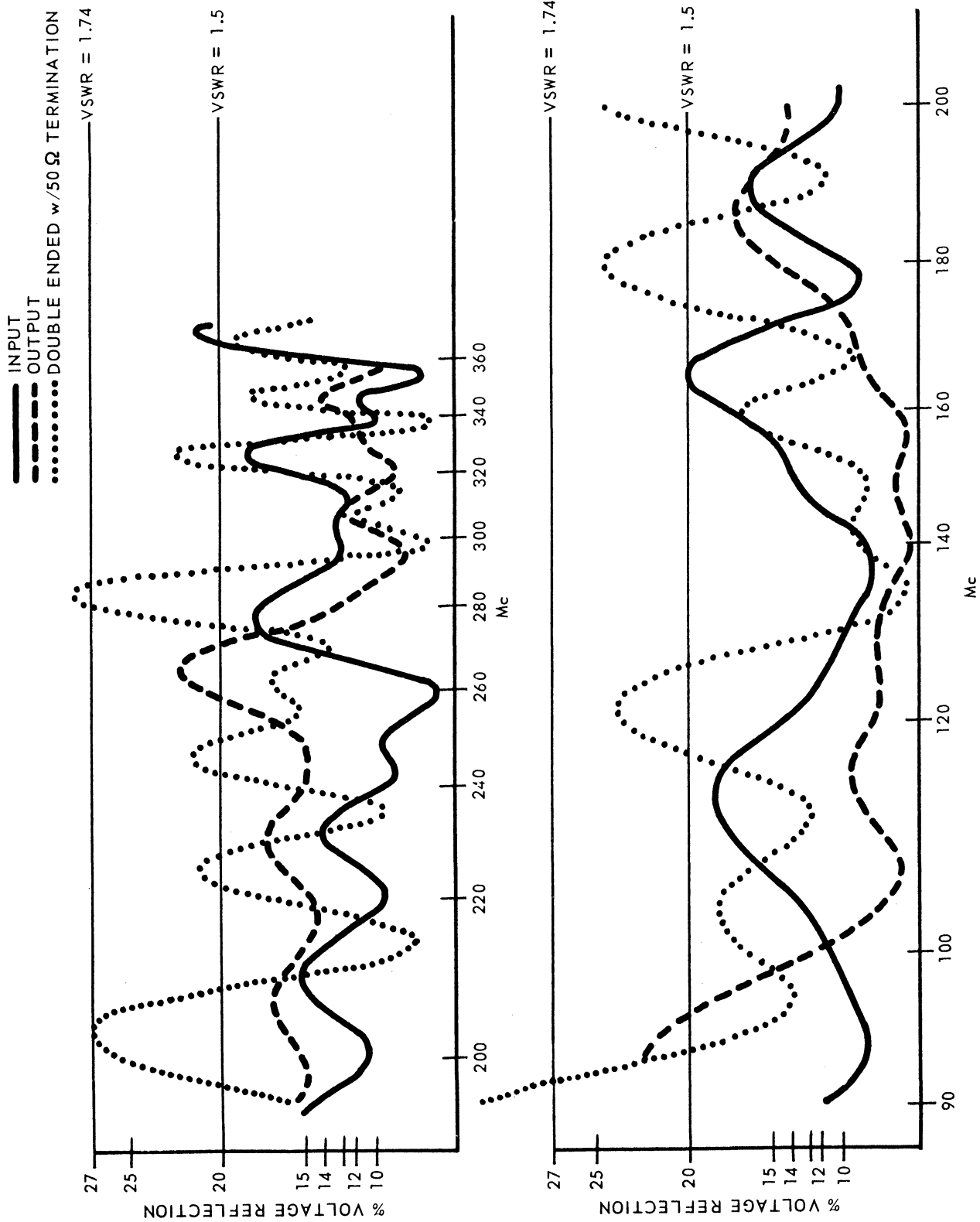


FIG. 3.4 VSWR VERSUS FREQUENCY FOR TUBE NO. 3.

sections were marginal, because of the extreme bandwidths required. In general, it was very difficult to obtain good matches over bandwidths of greater than 2 to 1. Figure 3.5 shows a plot of the VSWR of a helical matching section over a 3 to 1 frequency band. In addition to marginal VSWR's, the helical matching section, when adjusted to give broad bandwidth, introduced excessive insertion loss. Figure 3.6 compares the insertion loss of two tubes of the same length. One tube contained two tapered matching sections, while the other contained one tapered matching section and one coupled helix matching section. Coupled helix matching sections were tested in operating tubes with less than satisfactory results and, therefore, were discontinued.

Folded helix matching sections were also investigated. Figure 3.7 shows a cross-sectional view of the folded helix configuration. The helices in this case are parallel wound, rather than contrawound as in the helical case. This type of winding minimizes the inductive coupling between the helices. The advantages of the folded helix configuration are that the phase velocity of the circuit helix can be adjusted anywhere in the interaction region with very little effect on the coupling and no effects on the interaction impedance.

Cold tests were first conducted on a scaled model because of the availability of tapered matching sections. Figure 3.8 shows the VSWR obtained from the scaled model.

A high impedance window through the tube shell with a matching transition outside the tube was also considered. Again, this method would permit complete freedom for phase velocity tapering and cause no deterioration of the interaction impedance. The fundamental problem in this method arises due to the difference in the mode of transmission

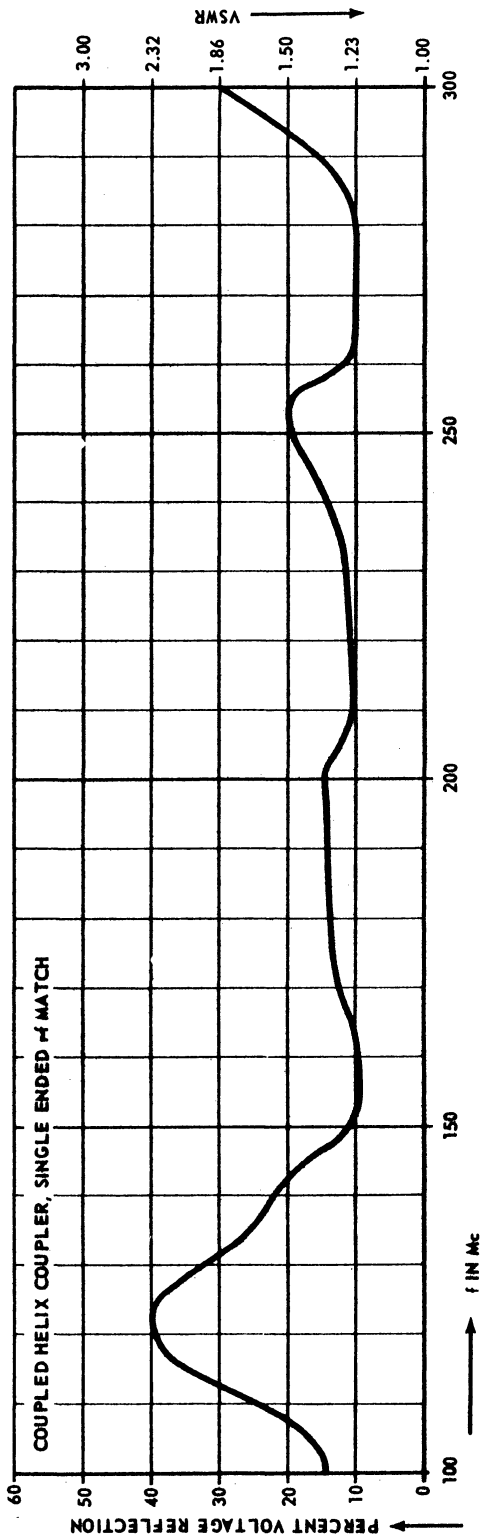


FIG. 3.5 R-F MATCH OF THE COUPLED HELIX.

- A. INSERTION LOSS OF TUBE #13 CONTAINING TWO TAPERED MATCHING SECTIONS AND 5.6 INCH LENGTH BETWEEN INPUT AND OUTPUT.
- B. INSERTION LOSS OF TUBE #14 CONTAINING ONE TAPERED MATCHING SECTION AND ONE COUPLED HELIX MATCHING SECTION WITH 5.6 INCH LENGTH BETWEEN INPUT AND OUTPUT.

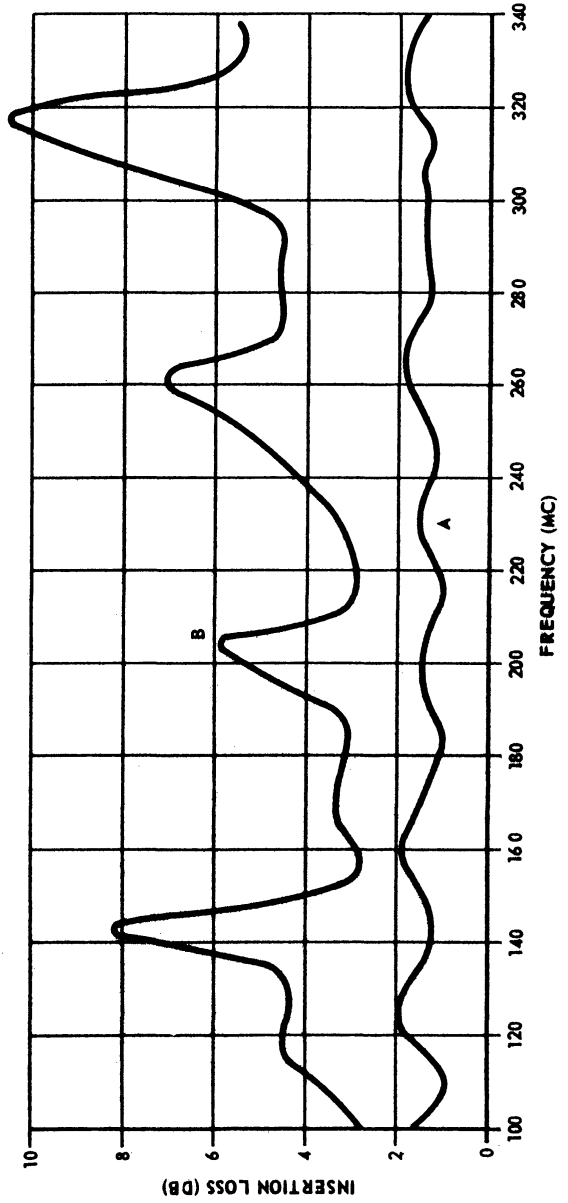


FIG. 3.6 COMPARISON OF INSERTION LOSSES.

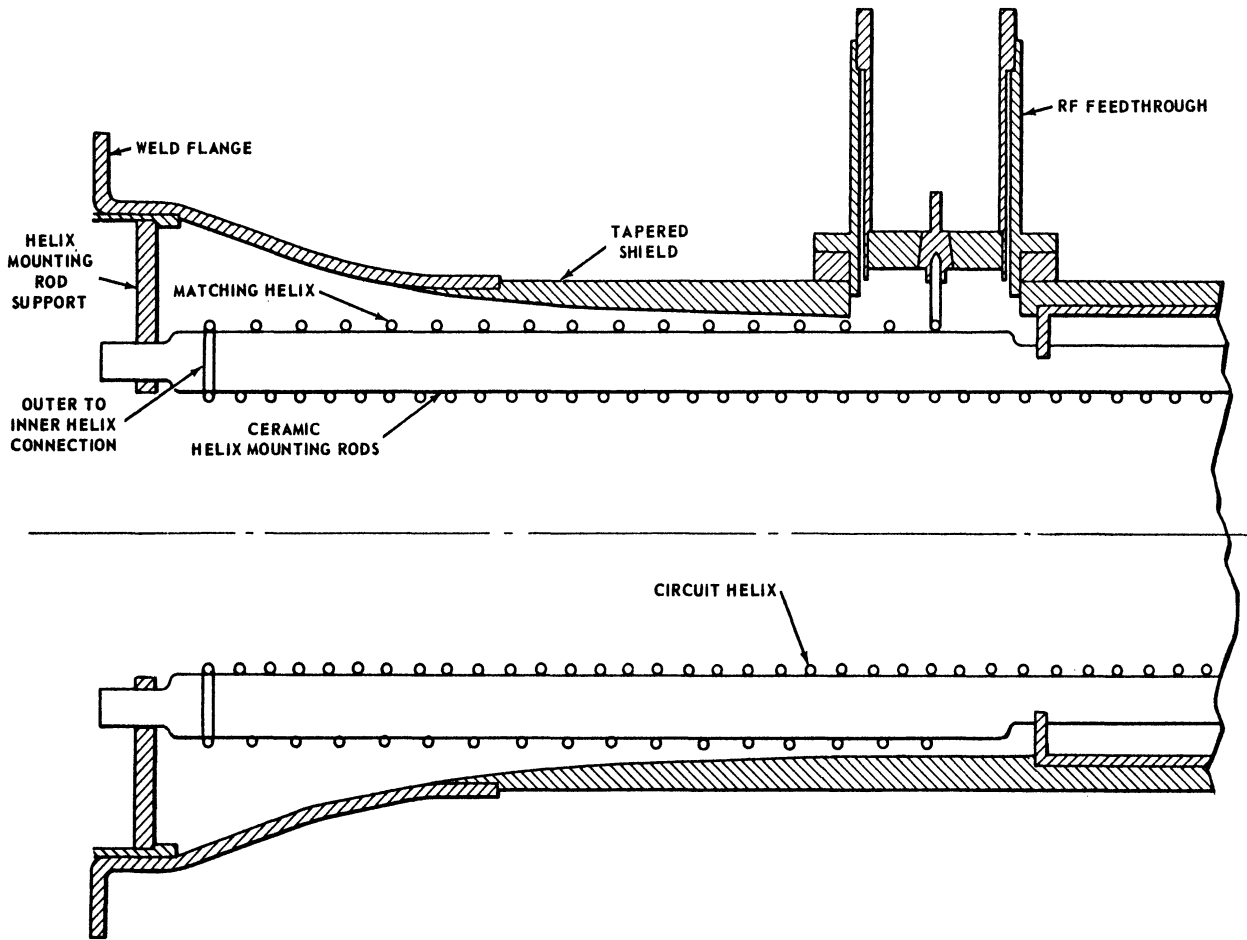


FIG. 3.7 CONFIGURATION OF FOLDED HELIX MATCHING SECTION.

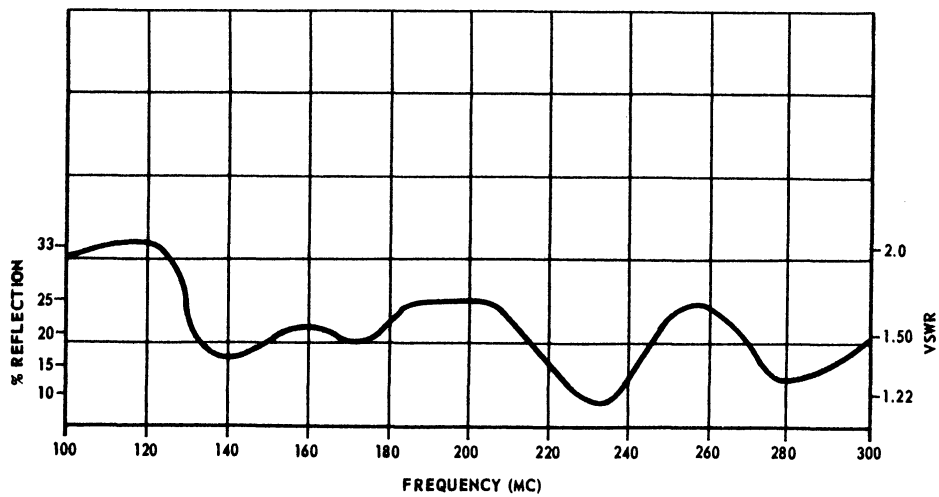


FIG. 3.8 VSWR OF FOLDED HELIX MATCH.

on a helix as compared to a coaxial line or a line above ground. In a two-conductor line the dominant mode normally used is the TEM mode, where the electric field is between the two conductors. In a helix with no shield, or with a shield relatively far away, the electric field from turn-to-turn of the helix becomes predominant. As a result, no satisfactory method was devised to make a high impedance feedthrough.

It is believed that both this method and the folded helix method merit further consideration in appropriate applications.

3.1.2 Mechanical Design. TW-143 employed all metal and ceramic construction. Figure 3.9 shows an assembly drawing of the tube utilizing one tapered matching section and one helical coupler. The electron gun details are shown in Fig. 3.1. The collector and gun were attached to the tube body with demountable weld flanges, although this was not the case for the first several tubes. The tapered matching sections fit inside the tube shell and were locked in place by a cylinder extending through the shell into the wall of the matching section. This was brazed into the tube shell and used as the r-f feedthrough shell. The helical coupler was wound on a ceramic spool which fit the inside diameter of the tube shell. The helical coupler wire was held very close to the tube shell to form a 50-ohm line above ground. This provided a direct connection to an incoming 50-ohm coaxial line. A lossy ceramic material was employed in the tube, as shown in Fig. 3.9, to attenuate the r-f power which the helix coupler radiated in the reverse direction.

3.1.3 Experimental Results. Table 3.1 gives a brief summary of the TW-143 and the TW-147 tubes constructed and tested. It should be noted that the rated current and voltage for these tubes were 452 milliamperes and 870 volts. Many of the tubes were tested

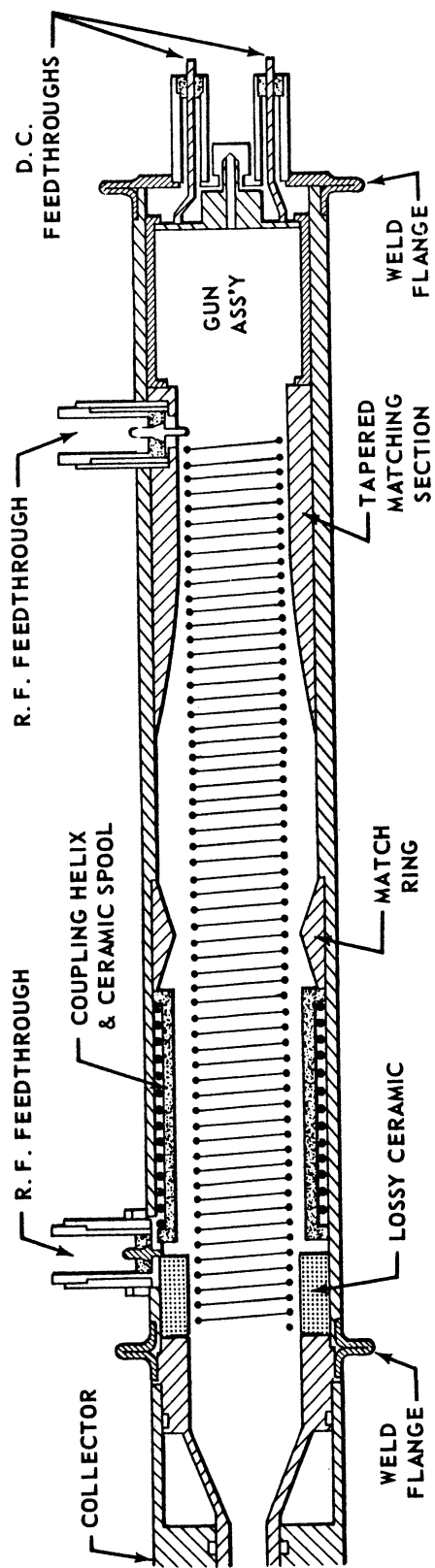


FIG. 3.9 CROSS SECTION OF COUPLED-HELIX TUBE.

TABLE 3.1 ELECTRICAL AND PHYSICAL DATA OF TUBES CONSTRUCTED.

| Tube No. TW-143-A | Date Completed | Helix Length Inches | TPI Helix | Input Conn. and Length | Output Conn. and Length | Gun Type | Operating Conditions I_o V_o | Nominal Gain Obtained | Power Output Obtained | Notes |
|----------------------|-------------------|---------------------------|--------------------------------------|---------------------------------|----------------------------------|-------------|--|-----------------------------|-----------------------------|---|
| 1 | 3-1-63 | 9.6 | 11.5 | Tapered Shield 4" | Tapered Shield 4" | Triode | 105 680 | 15 to 18 | 15 | Glass to kovar r-f feedthrus and stem header. Filter not used so low freqs. appear better than they should. |
| 2 | | 9.6 | 11.5 | Tapered Shield 4" | Tapered Shield 4" | Triode | --- --- | --- | --- | Tube not completed due to data on No. 1 indicating change of plans. |
| 3 | 3-20-63 | 9.6 | 10 | Tapered Shield 4" | Tapered Shield 4" | Triode | 143 700 | 16 | 15 | This tube developed an open inner anode and arc breakdown. Filters not used so low freqs. appear better than they should. |
| 4 | 4-2-63 | 5.6 | 10 | Tapered Shield 2" | Tapered Shield 2" | Triode | 350 830 | 16 to 23 | 40 to 60 | Ultimate failure due to leakage in gun. |
| 5 | 5-8-63 | 5.6 | 10 | Tapered Shield 2" | Tapered Shield 2" | Triode | --- --- | --- | --- | Heater failure before data could be obtained. |
| 6 | 5-24-63 | 5.6 | 10 Tapered to 20 | Tapered Shield 2" | Tapered Shield 2" | Triode | --- --- | --- | --- | Helix connection to r-f feed-through failed during bake out. |
| 7 | 5-30-63 | 5.6 | 10 Tapered to 20 | Tapered Shield 2.8" | Tapered Shield 2.8" | Triode | 200 to 490 560 | 12 | 20 | Helix tapered to much r-f performance poor. |
| 8 | 6-20-63 | 5.6 | 10 Tapered to 15 | Tapered Shield 2" | Tapered Shield 2" | Triode | 280 770 | 15 | 30 to 40 | Helix tapered too much. |
| 9 | 6-22-63 | 5.6 | 11.5 | Tapered Shield 2" | Tapered Shield 2" | Triode | 400 1180 | 10 | 50 to 100 | First tube to give 100 watts. |
| 10 | 6-26-63 | 5.6 | 11.5 Stretched Output Match | Tapered Shield 2" | Tapered Shield 2" | Triode | 250 to 680 940 | 10 | 30 to 60 | Obtained momentary I_k of 600 ma and P_o of 140 watts but sufficient examination of P_o not made, osc. possible. |
| 11 | 6-28-63 | 5.6 | 13 | Tapered Shield 2" | Tapered Shield 2" | Triode | --- --- | --- | --- | R-F feedthrough failure during bake out. |

TABLE 3.1 ELECTRICAL AND PHYSICAL DATA OF TUBES CONSTRUCTED (CONT')

| Tube No. TW-143-A | Date Completed | Helix Length Inches | TPI Helix | Input Conn. and Length | Output Conn. and Length | Gun Type | Operating Conditions I _o V _o | Nominal Gain Obtained | Power Output Obtained | Notes |
|----------------------|-------------------|---------------------------|--------------|---------------------------------|----------------------------------|--------------------------------|---|-----------------------------|---|--|
| 12 | 7-3-63 | 5.6 | 13 | Tapered Shield 2" | Tapered Shield 2" | Triode | 150 to 700 | 10 to 13 | 15 | Poor activation of cathode 150 ma, maximum cathode current. |
| 13 | 8-8-63 | 5.6 | 13 | Tapered Shield 2" | Tapered Shield 2" | Triode | 200 to 840 | 10 | 15 to 20 | 200 ma maximum cathode current. |
| 14 | 9-19-63 | 5.6 | 11.5 | Tapered Shield 2" | Coupled Helix 2" | Triode | 400 to 990 | 5 to 10 | 20 to 30 | High loss in output coupler degraded performance. |
| 15 | 10-16-63 | 7.7 | 11.5 | Tapered Shield 2" | Coupled Helix 2" | 3 Anode | 600 to 1240 | 10 to 12 | 40 to 85 | Severe inverse overload and high loss in output coupler degraded performance. |
| 16 | 10-28-63 | 6.6 | 11.5 | Coupled Helix 2" | Coupled Helix 2" | 3 Anode | 400 to 910 | 4 to 6 | 10 | High loss in both input and output couplers degraded performance. Depressed potential collector. |
| 17 | 12-16-63 | 7.7 | 11.5 | Tapered Shield 2" | Coupled Helix 2" | 3 Anode | 460 to 540 | 12 | 10 | Low temperature bake out limited cathode activation severely to 75 ma. low temperature due to leak. |
| 18 | 1-7-64 | 6.6 | 11.5 | Coupled Helix 2" | Coupled Helix 2" | 3 Anode | 400 to 850 | 14 | 40 to 50 | Best operation of coupled helix tubes but excessive trouble with oscillations due to matches |
| Tube No. TW-147- | | | | | | | | | | |
| 1 | 1-24-64 | 7 | 8 | Coupled Helix 3" | Coupled Helix 3" | 3 Anode Spokes Coated | 200 to 1070 | 5 | 15 to 30 | R-F matches not very good oscil- lations limited testing to excessively high voltages. Depressed potential collector. |
| 2 | 2-13-64 | 7 | 8 | Coupled Helix 3" | Coupled Helix 3" | 3 Anode Spoke Coated | 250 to 1300 | 6 | 13 to 22 | R-F matches changed during bake out same problem as with tube 1. Results to this time not conclusive. |
| 3 | 3-26-64 | 9 | 8 | Tapered Shield 2½" | Tapered Shield 2½" | 2 Anode | 500 to 1500 | 15 | 60 to 167 99 to 149 @ 1450 volts | R-F matches changed some during bake out. Tube much more stable than previous. Power outputs 99 to 149 over 100 to 300 mc at 1450 volts. Optimum : oltages caused oscillation due to high gain so gain must be reduced. Most successful tube to date. |

at reduced currents due to leakage problems. The following paragraphs discuss only those tubes and test findings particularly important to the direction and conclusions of the program.

TW-143-A-1 and 3. These tubes had excessively high gain at low beam currents; therefore, the following tubes were constructed with shorter helical circuits.

TW-143-A-4. With the reduction of helix length it was necessary to reduce the length of the matching sections from four inches to two inches. This resulted in a somewhat poorer r-f match than was obtained with the first two tubes. The initial tests on this tube indicated that the tube would work well at higher frequencies, so r-f tests were performed up to a frequency of 1000 megacycles. Figures 3.10 and 3.11 show the results of the r-f tests on tube number 4. A test was also conducted at 1500 megacycles; although good electronic gain was indicated, the test equipment was not calibrated for this frequency, and therefore, the power level could not be determined.

As can be seen, the tube operated over an extremely wide bandwidth with a much higher center frequency than anticipated. It was believed that the tapered matching sections affected the low frequencies detrimentally; consequently, a program of r-f match re-evaluation was started.

TW-143-A-7, 8, and 10. These tubes were constructed with circuit phase velocity tapering. Tubes numbered 7 and 8 were tapered in an attempt to keep the beam and circuit wave in phase with each other, and tube number 10 had a greatly increased phase velocity at the output to effectively decouple the beam and circuit under the tapered matching

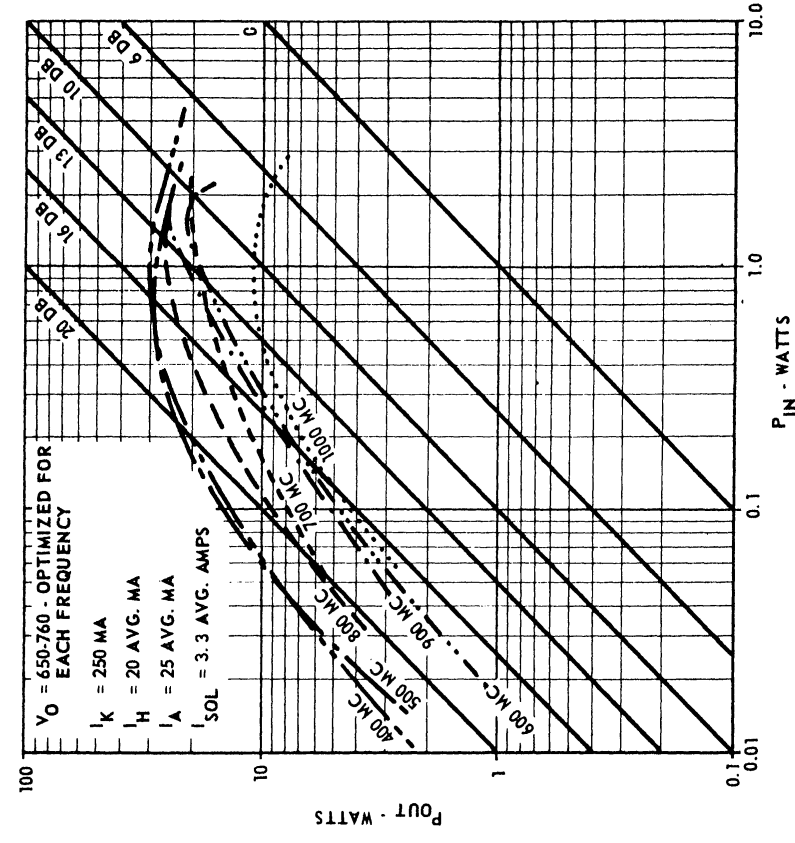


FIG. 3.11 PERFORMANCE CHARACTERISTICS OF TUBE NO. 4 (400-1000 MC).

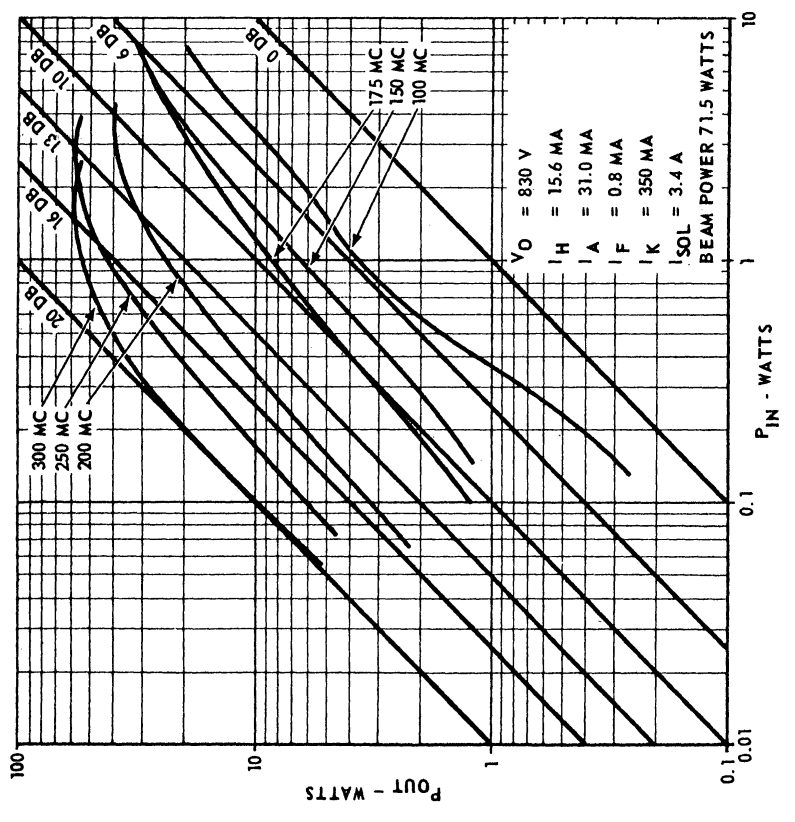


FIG. 3.10 POWER OUT OF TUBE NO. 4 (100-300 MC).

section (Figs. 3.12, 3.13, and 3.14, respectively). It was apparent from the test results of these tubes that the tapered matching sections were introducing phase velocity tapering in addition to that added by helix pitch variation.

TW-143-A-9. This was the first tube which produced a 100-watt output and also the first tube in which the phenomenon of inverse saturation was apparent. Figures 3.15 and 3.16 show the data obtained on this tube.

TW-143-A-14. This was the first tube to use a helical coupler. The coupler was used in the output section of the tube. Figures 3.17 and 3.18 show the data obtained from this tube. As shown in Fig. 3.6, this output coupler introduced high insertion loss with the result that gain, power output, and efficiency of this tube was substantially less than the average values obtained from previous tubes. The efficiency of this tube ranged from 10 to 14 percent as compared to a range of 18 to 21 percent in previous tubes.

TW-143-A-18. This tube operated the best of all tubes employing helical couplers. As shown in Fig. 3.19, the operation of this tube was not as good as that obtained from those tubes employing tapered matching sections. The efficiency of this tube was 15 to 19 percent.

3.2 TW-147. At a conference held with University of Michigan personnel during the latter part of the TW-143-A program, it was agreed that the tube would utilize a new helical circuit to minimize the effects of overvoltage operation at large-signal levels. Consequently, a basic design was selected which would allow using the TW-143-A electron gun. This new design was designated TW-147.

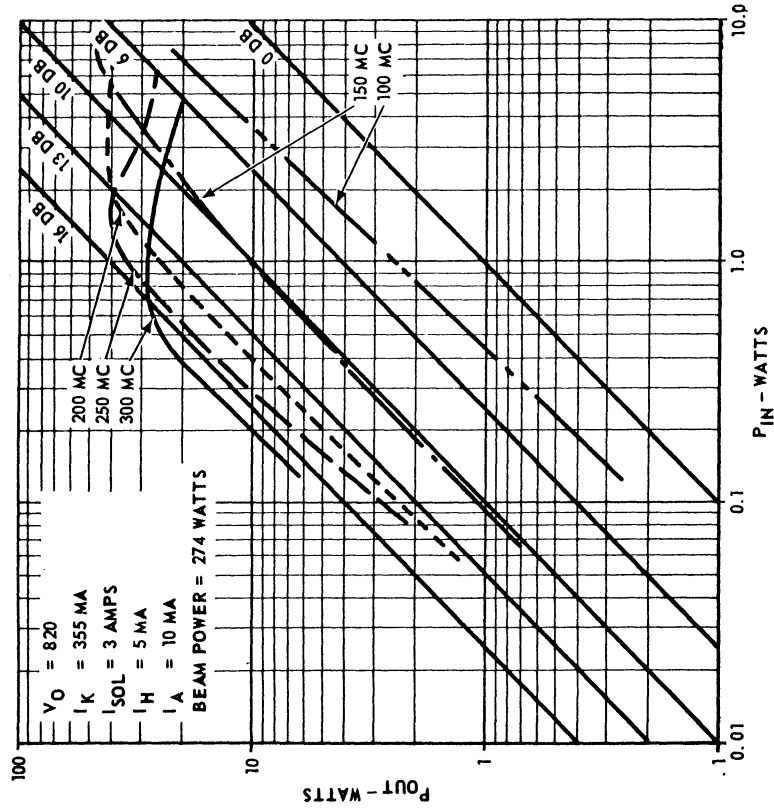


FIG. 3.13 POWER OUT OF TUBE NO. 8.

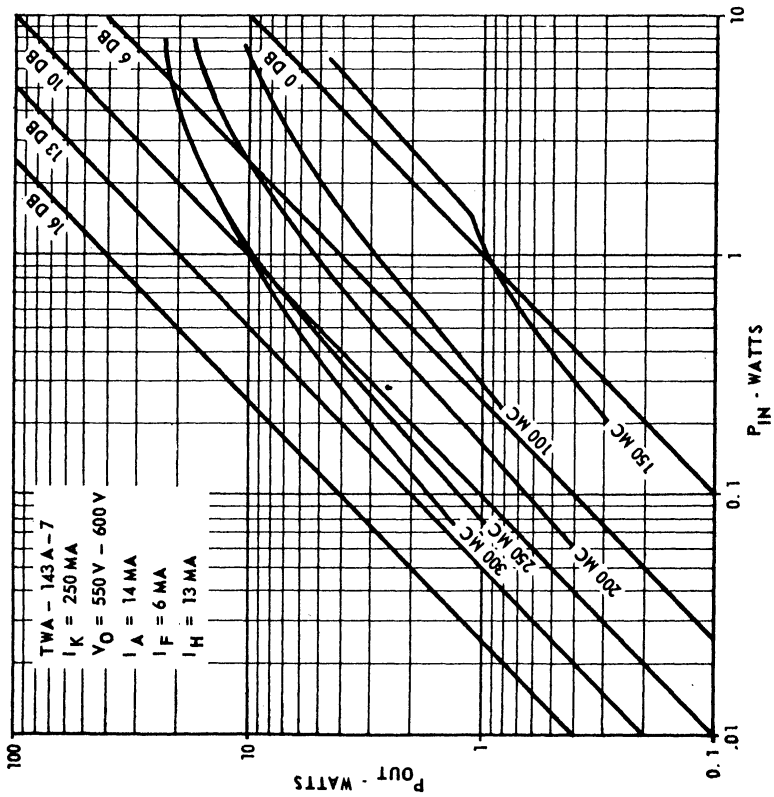


FIG. 3.12 POWER OUT OF TUBE NO. 7.

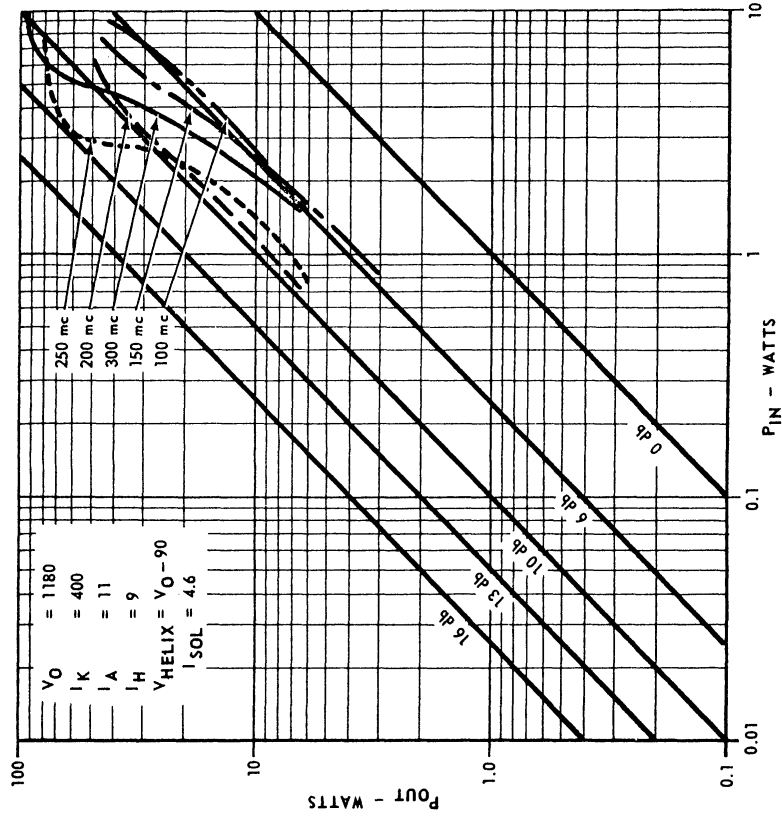


FIG. 3.15 POWER OUTPUT OF TWT-143-A-9. (I_K) = 400 MA.

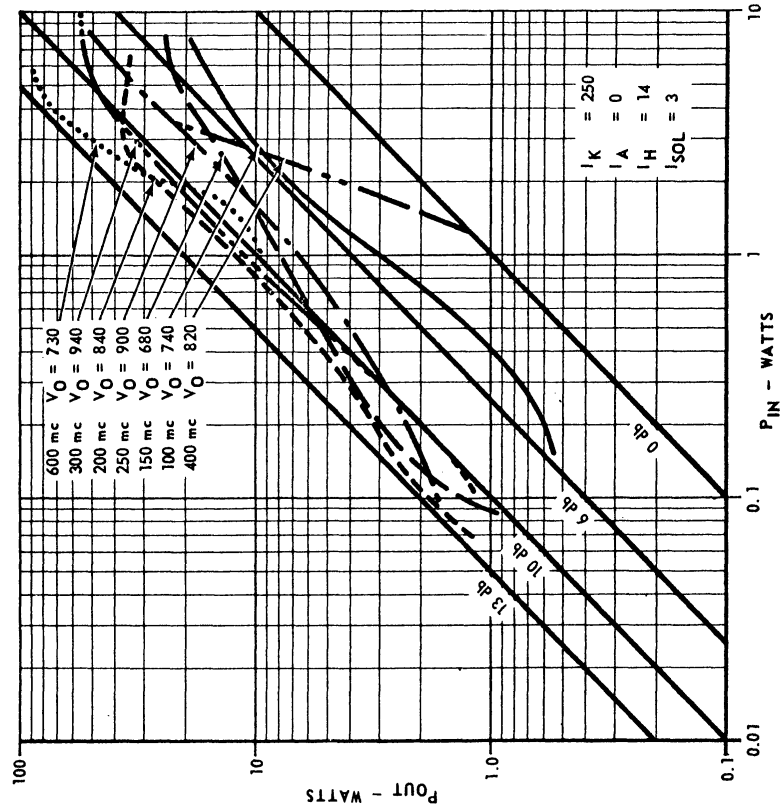


FIG. 3.14 POWER OUTPUT OF TWT-143-A-10.

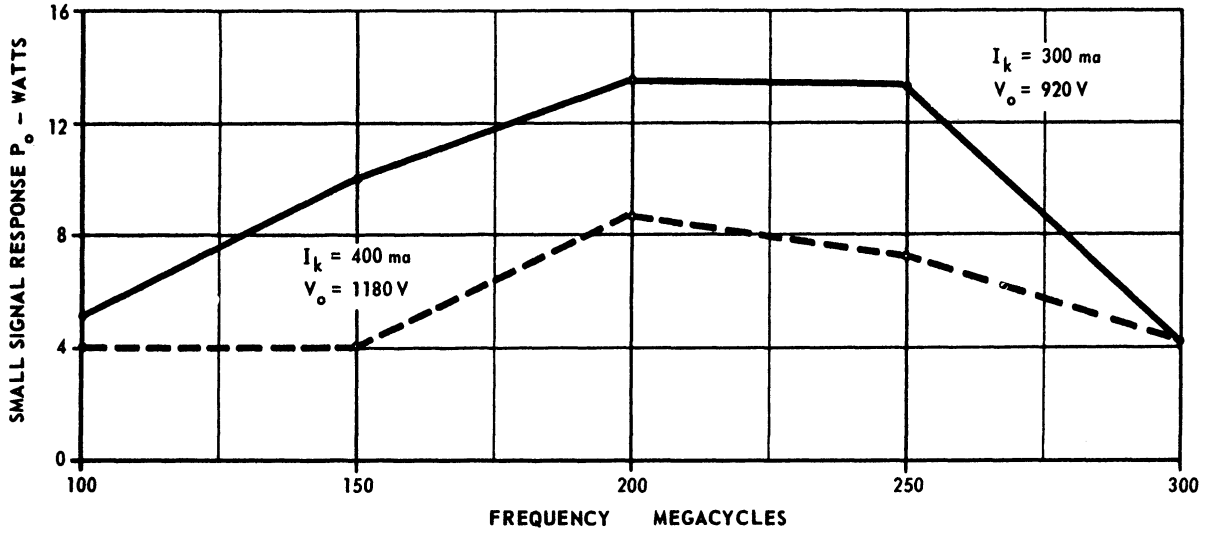


FIG. 3.16 SMALL SIG. RESPONSE VS. FREQUENCY, TWT-143-A-9
POWER OUTPUT VS. FREQUENCY AT 1 WATT DRIVE WHICH
IS 3 TO 6 DB BELOW SATURATING DRIVE LEVEL.

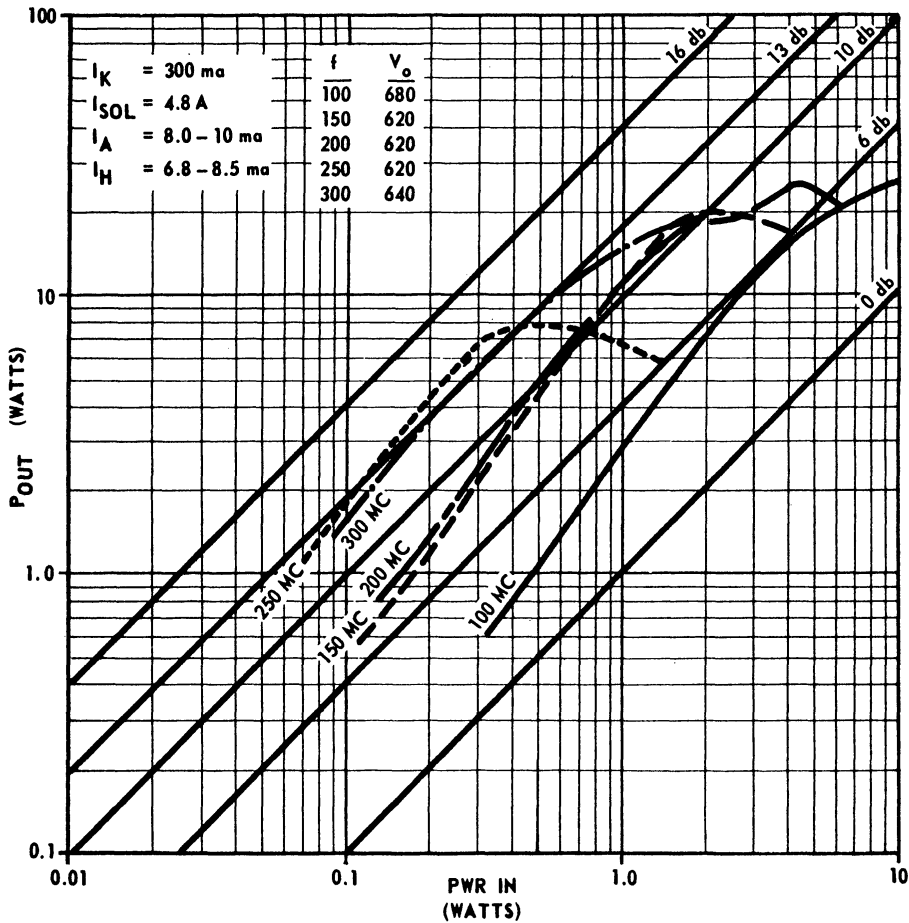


FIG. 3.17 POWER OUTPUT CHARACTERISTICS OF TWT-143-A-14
($I_K = 300 \text{ MA}$).

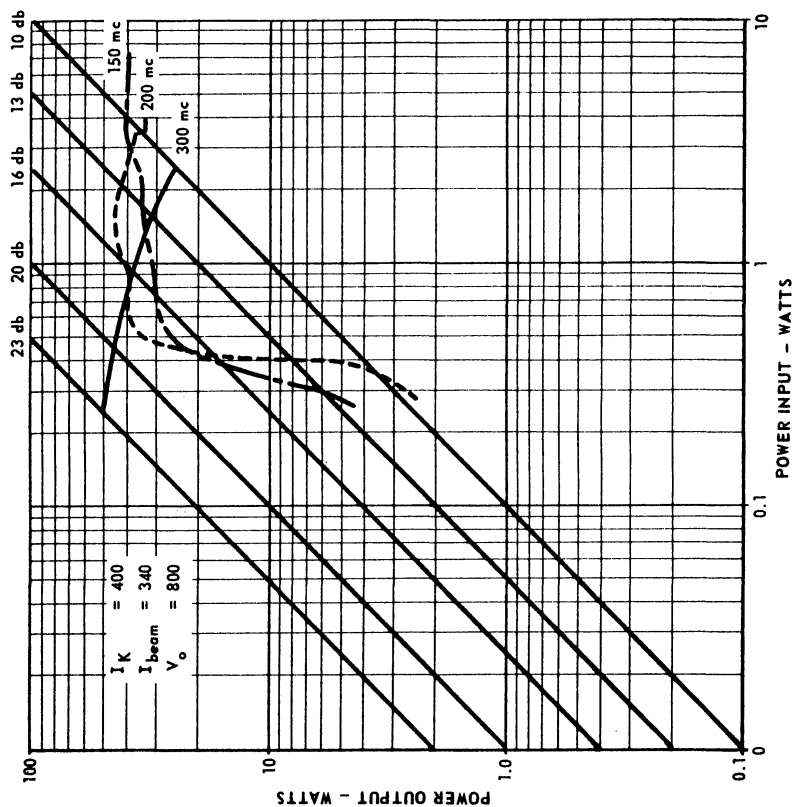


FIG. 3.19 POWER OUTPUT VS. POWER INPUT TWT-143-A-18.

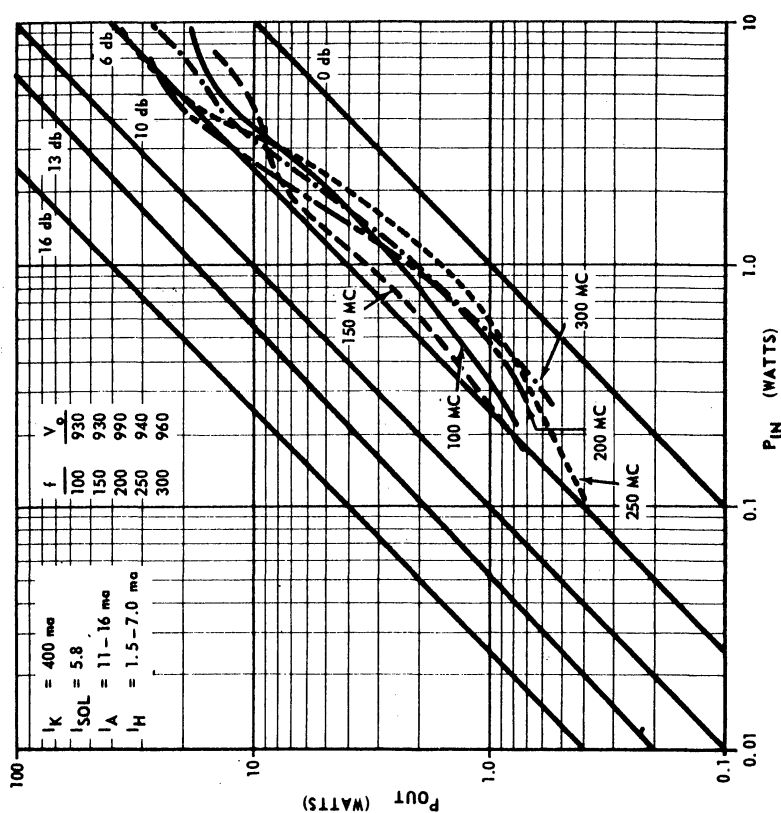


FIG. 3.18 POWER OUTPUT CHARACTERISTICS OF TWT-143-A-14. ($I_K = 400 \text{ MA}$).

The larger size of the TW-147 tube permitted more freedom in designing the r-f couplers; therefore, helical couplers were employed in the first two TW-147 tubes to further evaluate their performance. The third tube used tapered matching sections which proved superior to coupled helices for wide-band application.

Three tubes were constructed and tested. The third tube, which employed tapered matching sections achieved the required power and large-signal gain over the specified frequency band, but some inverse saturation characteristics were observed.

3.2.1 Electrical Design. The TW-147 design was based on a power output of 125 watts at midband to allow for a 1 db fall-off of power at the band edges, thus providing the required 100-watt output over the 100- to 300-megacycle band. A maximum electronic conversion efficiency of 22.5 percent at midband was assumed. Since the beam required 550 watts of d-c power, a 0.5 ampere, 1100-volt electron beam was chosen, and the small-signal response was computed at a voltage of 1000 volts. The following list gives the various electrical and physical parameters of the TW-147 tube design:

| <u>Frequency</u> <u>(Mc)</u> | <u>ka</u> | <u>γa</u> | <u>C</u> | <u>QC</u> | <u>Assumed</u> <u>DLF</u> | <u>$\gamma(a-r_o)$</u> |
|---------------------------------|-----------|------------------------------|----------|-----------|------------------------------|-----------------------------------|
| 100 | 0.025 | 0.58 | 0.38 | 0.117 | 0.800 | 0.252 |
| 200 | 0.050 | 1.29 | 0.30 | 0.176 | 0.800 | 0.560 |
| 300 | 0.075 | 2.09 | 0.21 | 0.341 | 0.800 | 0.910 |

$V_o = 1000$ V (small-signal optimum), 1100 V (large-signal optimum)

$I_o = 0.500$ ampere

$a = 0.472$ inch (helix mean radius)

$b = 0.950$ inch (shield radius)
TPI = 8
 $J_o = 0.84$ amp/cm²
 $B_b = 182$ gauss (Brillouin magnetic field)
 $B = 350$ gauss (expected operating magnetic field)
 $a = 0.55$ (beam thickness to beam to helix spacing)
R-f Match - helix couplers
Collector - one stage depressed potential
Gun - TW-143-A gun with (4) electrode lens cancellation

3.2.2 Mechanical Design. Figure 3.20 shows a cross section of the TW-147 design. The electron gun for TW-147 was the same gun used in TW-143-A. Except for the addition of two electrodes, the construction details of this gun are the same as in Fig. 3.1. This tube employed all metal and ceramic construction as did TW-143. TW-147-3 contained tapered matching sections which were assembled with the tube shell by the same method used in TW-143-A.

3.2.3 Experimental Results. Three tubes employing this design were built and tested, tube numbers 1 and 2 used helical couplers while tube number 3 used tapered matching sections.

The helical couplers exhibited insufficient performance. Their VSWR was marginal and they had an excessive loss. In addition, these tubes had a strong tendency to oscillate; the maximum beam currents achieved for tube numbers 1 and 2 were 200 and 250 milliamperes, respectively. Figures 3.21 and 3.22 show plots of the double-ended VSWR and insertion loss for tube numbers 1 and 2, respectively, and Figs. 3.23 and 3.24 show the power outputs versus power inputs for tube numbers 1 and 2, respectively.

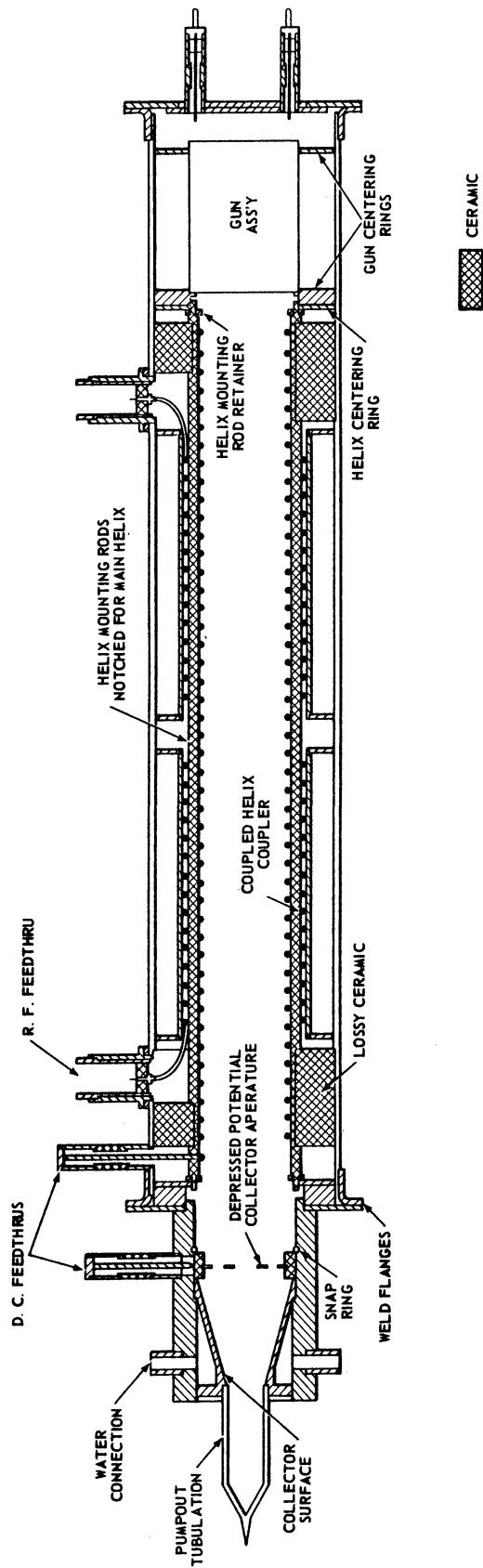


FIG. 3.20 TW-147 CROSS-SECTION VIEW.

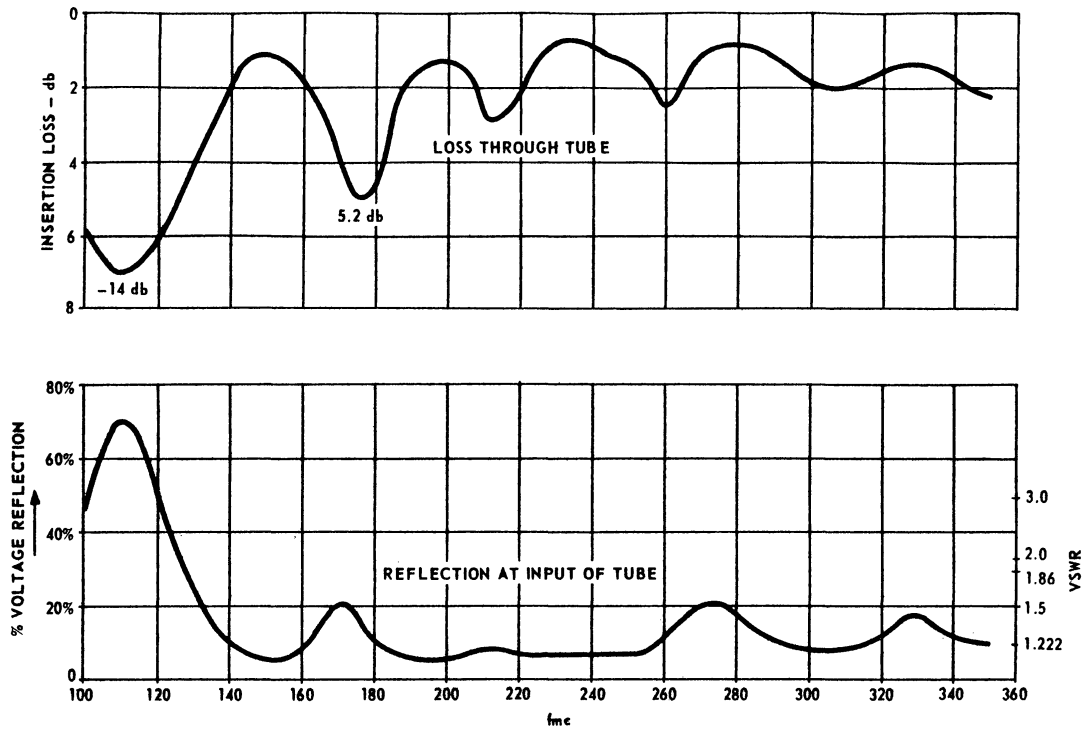


FIG. 3.21 VSWR AND INSERTION LOSS VS. FREQUENCY TW-147-1.

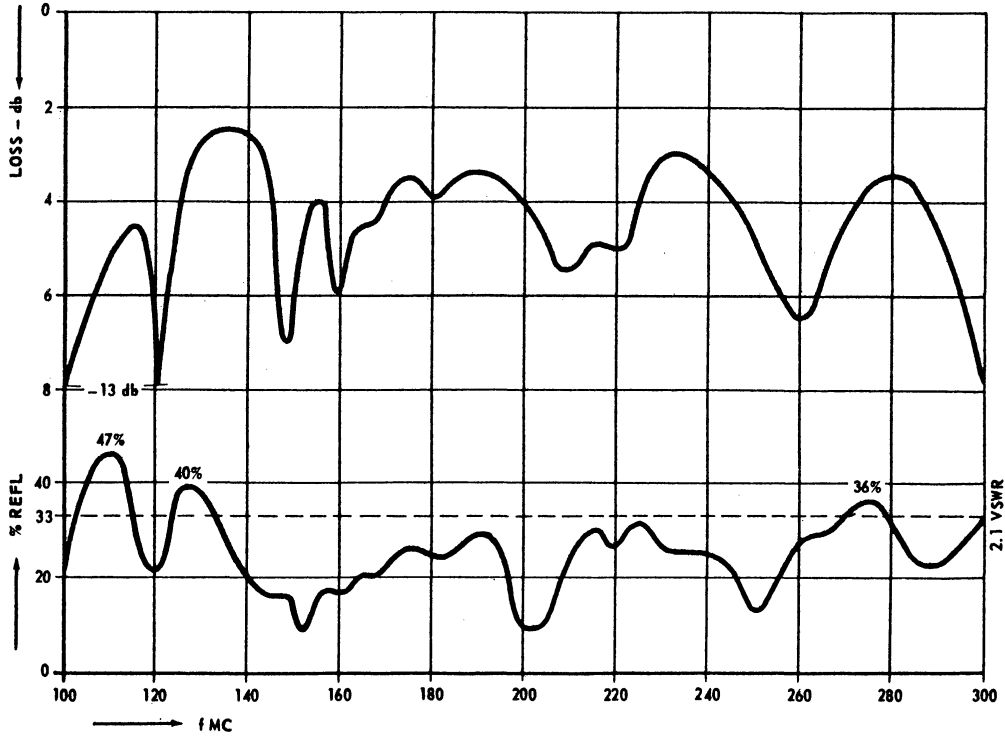


FIG. 3.22 VSWR AND INSERTION LOSS VS. FREQUENCY TW-147-2.

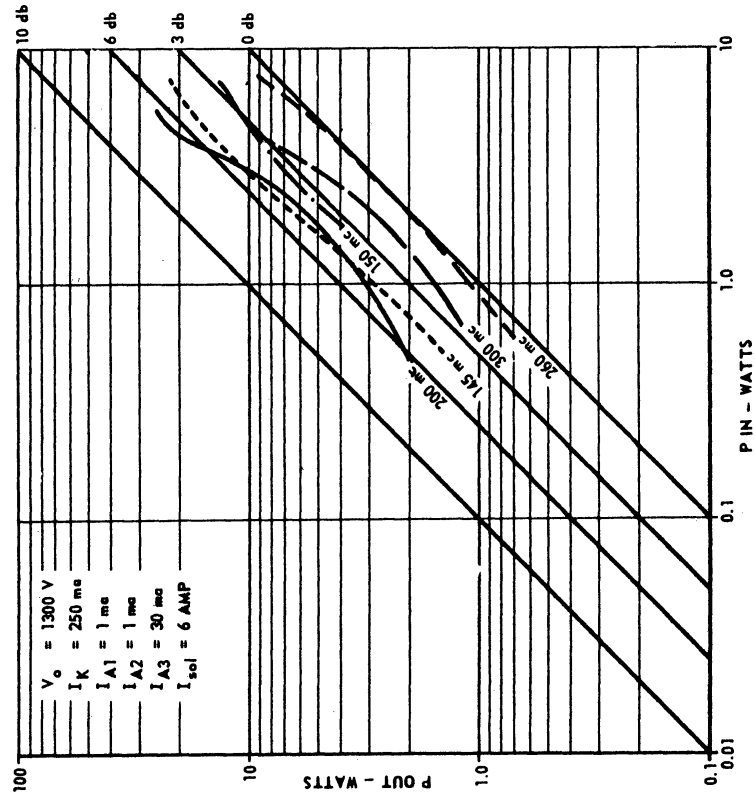


FIG. 3.24 POWER OUTPUT VS. POWER INPUT TW-147-2.

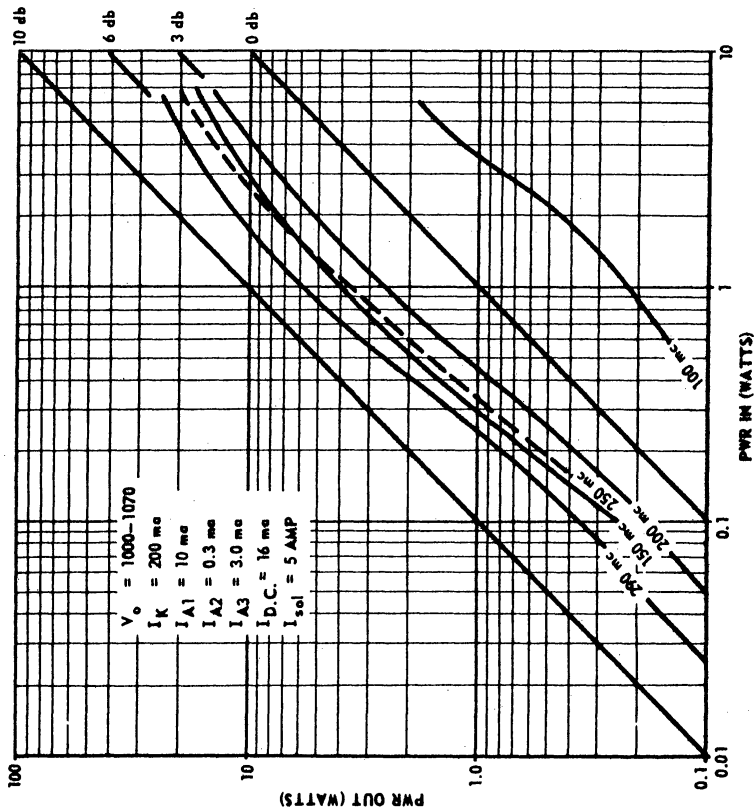


FIG. 3.23 POWER OUTPUT VS. POWER INPUT TW-147-1.

Tube TW-147-3 was constructed using tapered matching sections and was the first tube to utilize a new two-anode spokeless electron gun. This tube was operated at a beam current of 500 milliamperes and at voltages above and below the optimum voltage. The 9-inch helix resulted in a higher gain than expected; and, as a result, the tube oscillated when operated at voltages between 1100 and 1400 volts. Small-signal gains of 20 to 24 db were recorded at full beam currents and 1100 volts. Figure 3.25 shows a plot of the maximum power output versus frequency with beam voltage as a parameter. Figure 3.25 also shows the saturated gains associated with the power outputs, while Fig. 3.26 shows a plot of synchronous voltage versus frequency as obtained experimentally by adjusting the voltage for maximum small-signal gain with a very low (10 ma) beam current. This velocity is synchronous with the phase velocity on the helix. For large currents the optimum small-signal velocity is much higher. Figure 3.27 shows a plot of power and gains at 250 milliamperes of beam current with the voltage adjusted for both maximum small-signal gain and maximum power output.

It can be seen from the test data that 99-watts or more of r-f output power was obtained at 100, 150, 200, 250, and 290 megacycles. R-f data was not taken at 300 megacycles because of test equipment limitations which has since been rectified. This power output was obtained at beam currents of 500 milliamperes and a voltage of 1450 volts. This voltage was higher than optimum to reduce the gain and, as a result, the power output versus power input had some inverse saturation overload characteristics. At 1100 volts, which was below optimum voltage, 100 watts was obtained across the frequency range except at 100 megacycles. At this lower voltage, the power output

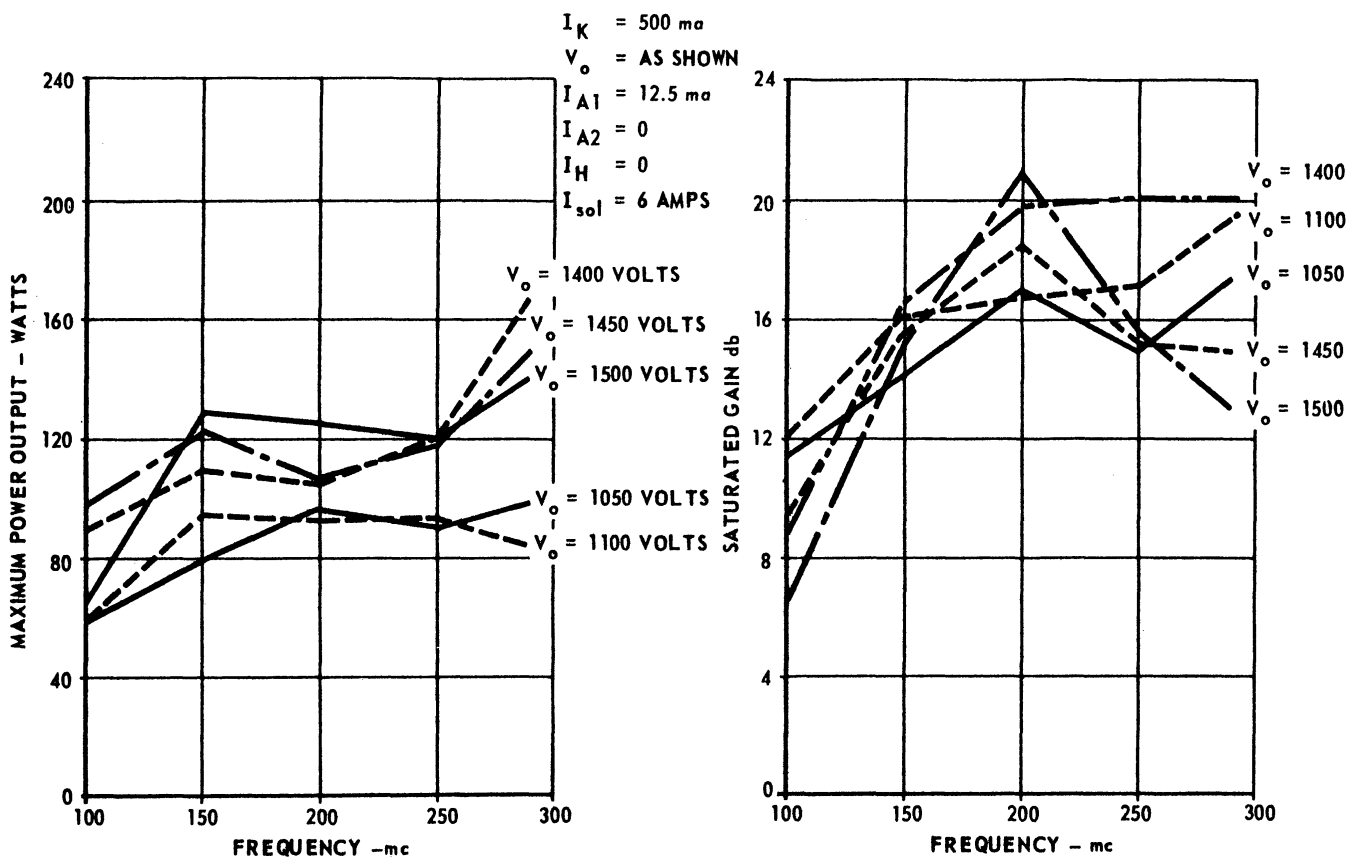


FIG. 3.25 MAXIMUM POWER OUTPUT AND SATURATED GAIN VS. FREQUENCY TW-147-3.

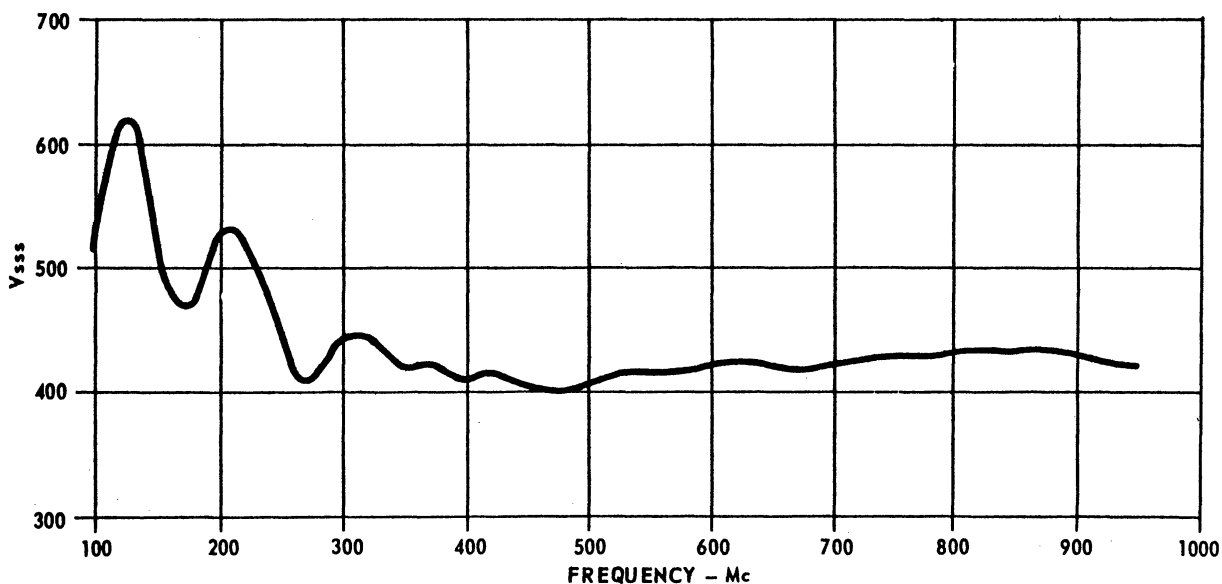


FIG. 3.26 SMALL-SIGNAL SYNCHRONOUS VOLTAGE -- LOW BEAM CURRENT TW-147-3.

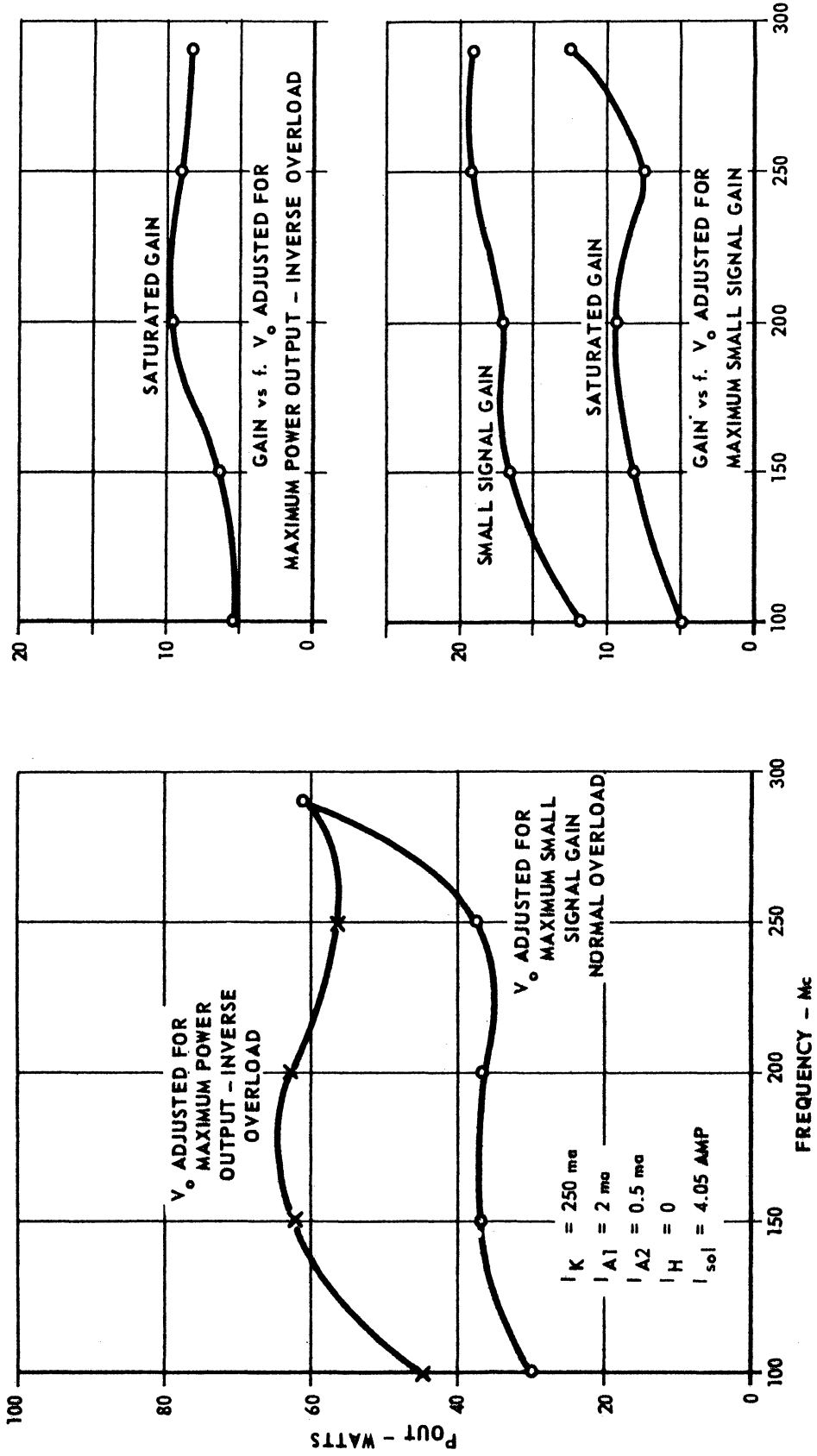


FIG. 3.27 POWER OUTPUT AND GAIN VS. FREQUENCY
 MEDIUM BEAM CURRENT TW-147-3.

versus power input curves exhibited the normal saturation overload characteristics. All of the output power measurements were made at the r-f output terminal of the tube. Filters are used in the r-f line so that all harmonic power is eliminated from the power output measurement.

Thus tube number 3 met the electrical requirement; i.e., 100-watts power output over the 100- to 300-megacycle frequency range -- justifying the initiation of Phase II. However, an adjustment of the design was discussed with the Bureau of Ships personnel to improve the band centering, and improve the power output at 100 megacycles.

4. Phase II - Development of Deliverable 100-Watt Magnetically Focused Crestatron

Phase II effort was directed toward constructing three tubes which would meet all the contractual requirements. Essentially, a new mechanical design was required to adequately meet the environmental requirement as well as an electrical design adjustment to further improve the low frequency performance and result in a better centered frequency range. This tube design was designated TW-148 and constitutes the type of tubes delivered.

These tubes have operated very satisfactorily, and have demonstrated power output, gain, and environmental characteristics which have equaled or exceeded the required specifications. Three of these tubes (Fig. 4.1) have been delivered along with solenoid focusing structures. In addition, ion appendage pumps and magnets have been included with each tube, since the tubes might have extended periods of off or nonoperating time. Appendix A presents typical and maximum operating voltages and currents.

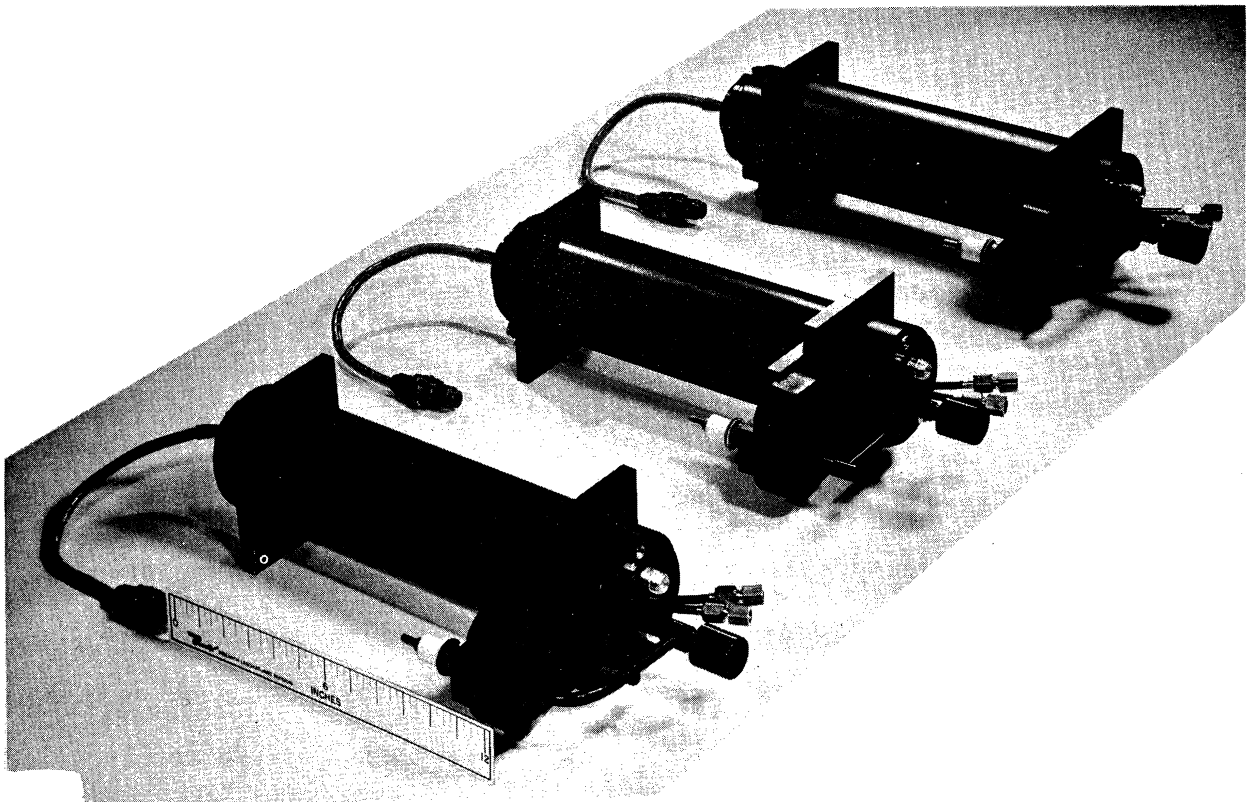


FIG. 4.1 TW-148 100-WATT MAGNETICALLY FOCUSED CRESTATRON

4.1 Electrical Design of TW-148

4.1.1 R-f Circuit. The test results of TW-143-A and TW-147 indicated that electronic lowering of the frequency response, exhibited by an O-type traveling-wave tube operating in an overvoltage condition, was not feasible when the tube was required to operate under large-signal conditions and high efficiencies. The adjusted design, designated TW-148, was based on small-signal theory where the beam velocity was considered optimized for maximum small-signal gain. The information presented by Dunn² was used as a guide in defining this design; then the Bendix small digital computer program was used to select an optimum design. The design parameters for TW-148 are as follows:

| <u>Frequency</u> <u>(Mc)</u> | <u>ka</u> | <u>γa</u> | <u>C</u> | <u>QC</u> | <u>b</u> | <u>K</u> |
|---------------------------------|-----------|-----------|----------|-----------|----------|----------|
| 100 | 0.036 | 0.908 | 0.33 | 0.134 | 1.18 | 230 |
| 200 | 0.073 | 1.92 | 0.248 | 0.214 | 1.91 | 98 |
| 300 | 0.109 | 2.97 | 0.176 | 0.368 | 2.94 | 35 |

$$a = 0.688 \text{ inch (helix radius)}$$

$$r_o = 0.472 \text{ inch (beam mean radius)}$$

$$\Delta = 0.162 \text{ inch (beam thickness)}$$

$$a - r_o = 0.216 \text{ inch (beam to helix spacing)}$$

$$\left[\frac{a - \Delta}{a - r_o} \right] = 0.75 \text{ (beam thickness to beam spacing ratio)}$$

$$\left[\gamma (a - r_o) \right] = 0.65 \text{ (normalized beam to helix spacing)}$$

$$\text{TPI} = 5.5 \text{ (turns per inch of helix)}$$

$$b/a = 1.38 \text{ (shield to helix radii ratio)}$$

$$\text{DLF} = 0.85 \text{ all frequencies (dielectric loading factor)}$$

- V sync = 327 (synchronous voltage)
- V_o^1 = 800 (beam drift voltage)
- V_o = 1000 (beam applied voltage)
- I_o = 0.500 amp (beam current)
- J_o = 0.161 amp/cm² (beam current density)
- P_k = 15.8 (gun microperveance)
- P_k/sq = 0.862 (gun microperveance per square)
- P_b/sq = 1.21 (beam microperveance per square)
- $P_b - sq/a$ = 1.61 (beam P_b/a to a ratio)
- B_b = 90.6 gauss (Brillouin magnetic field)
- B = 400 gauss (magnetic field to be used)
- L = 8.5 inch (helix length)

4.1.2 Electron Gun. The electron gun designed for the TW-148 employs a single anode gun with focusing grid, utilizes a double helical coil noninductive type heater, and has a microperveance of 15.8. Special emphasis has been placed on the cathode mount to minimize thermal leakage, and emphasis was placed on the overall mechanical design to produce a very rugged structure. The inner and outer electrodes are supported independently of each other from behind the cathode to eliminate any obstruction in the annular beam. R-f tests performed on tube numbers 3, 4, and 5 which incorporated this electron gun indicated that under certain operating conditions ion current to the cathode was excessive, thus resulting in cathode poisoning and current slumping. This condition was not prevalent in prior tubes which utilized two-anode type electron guns. Since the resulting beam from the one-anode gun performed satisfactorily as indicated by the tube performance characteristics, the incorporation of the second anode for the purpose

of providing cancellation of lens effect was not required. However, the outer electrode was added to the one-anode electrode gun to provide an ion trap to protect the cathode. Initial tests on TW-148-5 confirmed the effectiveness of this electrode in protecting the cathode from ion bombardment, and no noticeable effect was experienced in r-f performance. Figure 4.2 shows a cross-sectional view of the final gun configuration. This simplified one-anode gun design greatly aids the fabrication and assembly of the electron gun.

4.1.3 R-f Match. It was concluded from the TW-147 results that tapered matching sections provide the best impedance transformation between the coaxial lines and the helical interaction circuit of this tube.

The helix in TW-148 is formed from 0.020 by 0.080 inch molybdenum tape. The wide side of the tape faces the ground shield and allows a much larger clearance between the helix and the ground shield, as compared with the previous tube types which used round wire. The grooves in the matching sections still represent electrical discontinuities; however, their effect is small and can be neglected in this particular tube.

A shield type input matching section is located near the outside diameter of the helix. It tapers away from the helix to provide an exponential impedance taper. This is essentially the same type as that used in the TW-143 tubes.

The output matching section, however, is a "bullet-shaped" plug which fits inside the helix and serves as the collector as well as the matching section. Two advantages result from using this type of interior matching section for the output match. First, the helix

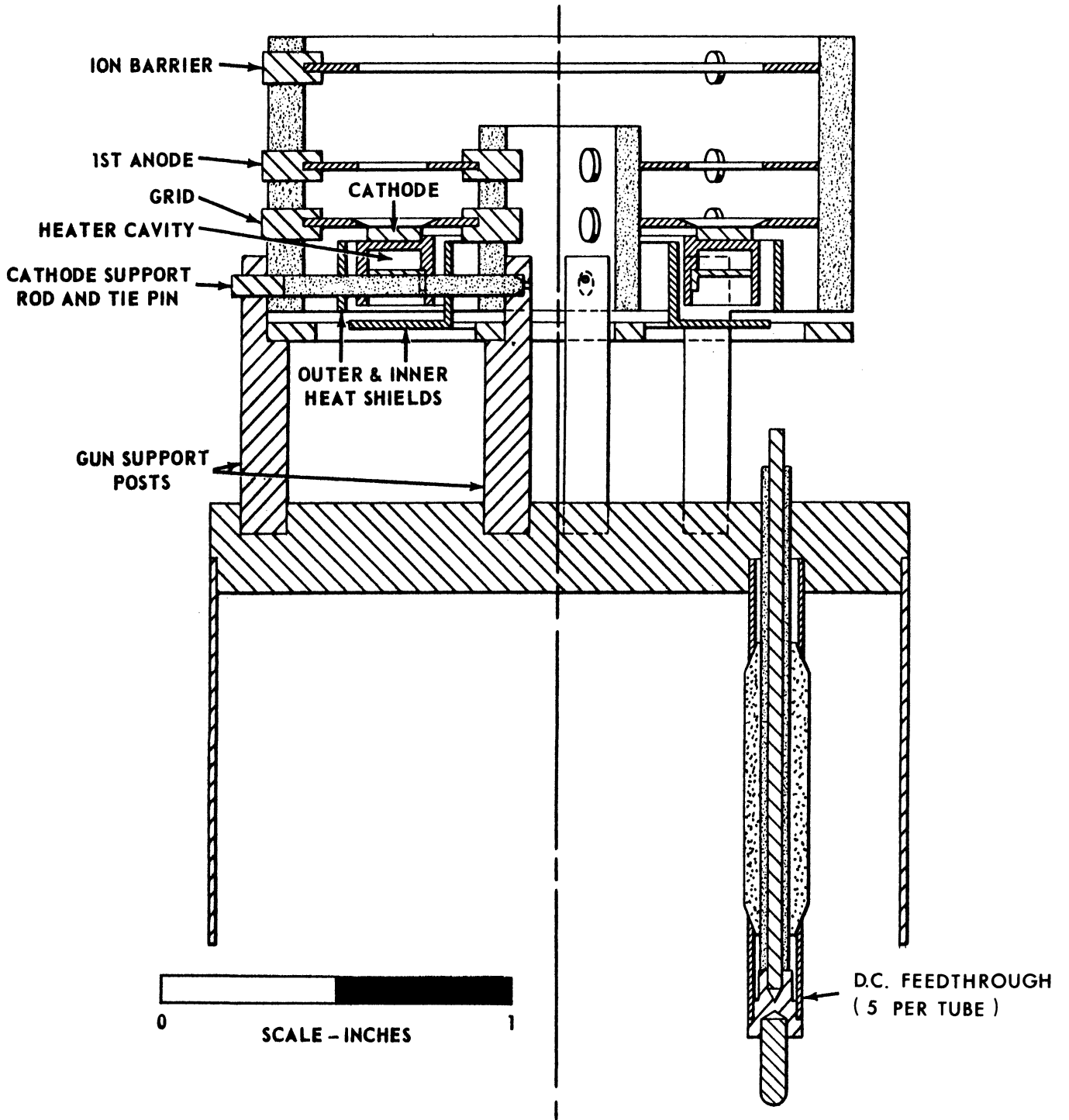


FIG. 4.2 TW-148 ELECTRON GUN CROSS SECTION.

mounting is simplified because no grooves are needed in the matching shield for the helix mounting rods which are on the outside of the helix. Second, the electron beam is collected while the shield is still some distance from the helix; thus, high interaction impedance is available up to the point of beam collection. This high interaction impedance is necessary in obtaining high efficiency.

One disadvantage of the internal matching section, however, is that secondary electrons and ions are produced in the interaction region. However, in TW-148 an ion barrier electrode, described in Section 4.1.2, was included to protect the cathode from ion bombardment. The suppression of secondary electrons was accomplished by supporting the matching section shield from the inside by a soft magnetic material. This produces a strong radial magnetic field in the collector region. Thus, any secondary electrons generated experience $V \times B$ forces which forces them to return to the collector.

The output matching section uses a Dolph-Tchebycheff taper⁴ in place of the exponential tapers used in the other matching section. An exponential taper exhibits periodic VSWR peaks which decrease with increasing frequency. Although the Dolph-Tchebycheff taper also exhibits periodic peaks, the peaks do not vary with frequency. Consequently, the Dolph-Tchebycheff taper results in an improved VSWR across the frequency band of interest.

4.2 Mechanical Design. These tubes employ all metal-ceramic construction, and are rugged enough to meet the shipboard environmental

4. Kloppenstein, R. W., "A Transmission Line Taper of Improved Design," Proc. I.R.E., Vol. 44, No. 1, pp.31-35; January, 1956.

specifications required by the contract. The r-f structure, a self-contained assembly, fits into and is sealed in the shell by an inert gas weld. The electron gun is also a separate self-contained assembly which is sealed into the shell with an inert gas weld, but is easily removable if repairs should be necessary.

The mechanical details of the gun are shown in Fig. 4.2, and those of the tube, except gun details, are shown in Fig. 4.3.

The N-type r-f connectors are rigidly attached to the tube at the collector end. A coaxial input line extends along the length of the r-f circuit to transmit the input signal from the collector end of the tube to the input matching section. Flying leads are supplied for the d-c electron gun connections.

The collector is liquid cooled; 1/8 inch pipe thread connections are provided. The tube clamps inside the solenoid focusing structure, and an O-ring at each end provides the seal. The liquid cooling fluid is routed through the space between the tube shell and solenoid inside diameter so that it cools both the tube body and the solenoid. Cooling the tube in this manner will reduce the peripheral temperatures in the gun region and promote longer tube life.

4.3 Focusing Methods

4.3.1 Periodic Permanent Magnets. Periodic permanent magnet focusing balances the inward force, produced by the periodic magnetic field, against the outward forces produced by space-charge repulsion in the electron beam. In a hollow electron beam, the electrons which form the inside edge do not experience an outward force. Periodic magnetic focusing of a hollow beam tends to collapse the center of the beam and cause many electron crossings with intolerable results. If,

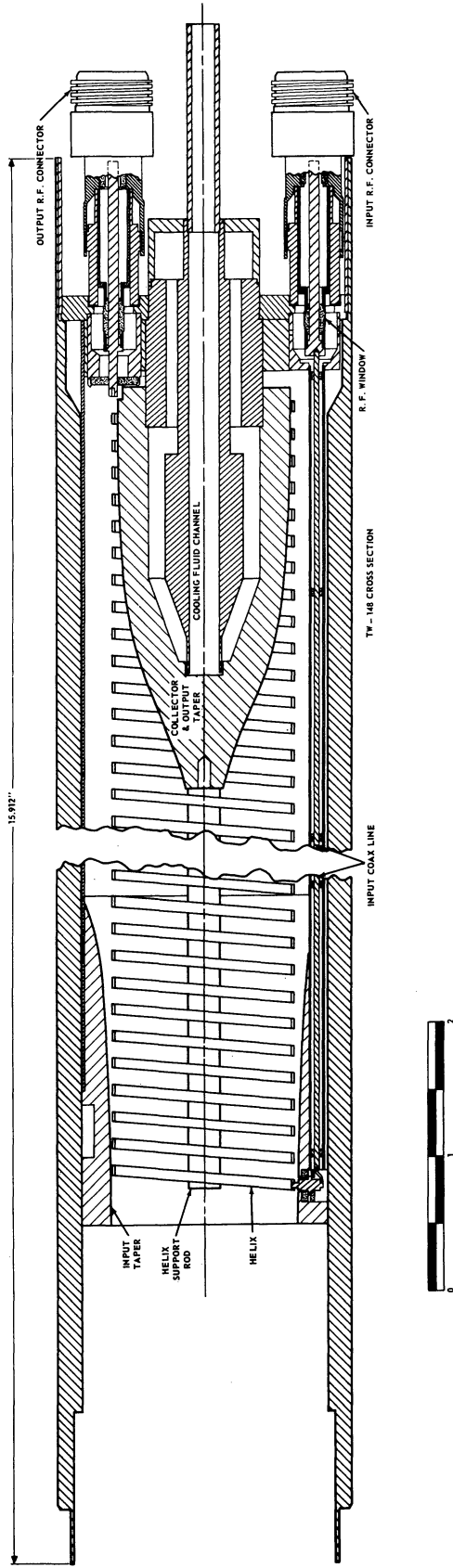


FIG. 4.3 TW-148 CROSS SECTION

however, a charged rod is placed in the center of the hollow beam, the electrons can be made to experience an outward electric force just balancing the periodic magnetic focusing force. The practicality of periodic magnetic focusing for a hollow-beam tube depends upon the electrical effects and mechanical complication caused by the rod in the center of the beam and circuit.

As shown by Mathers and Kino,³ the electric field strength must go to zero at the surface of a conducting shield inside a helical circuit. This is a major change in the field configuration as compared to a helical conductor without a shield in the center. In this case the electric field follows the J_0 Bessel function with the radius as the independent variable. The greatly reduced electric field strength affecting the electron beam causes a reduced interaction impedance with an attendant loss in gain per unit length and a decrease in efficiency. Since this tube required a very short length and relatively high interaction efficiency, periodic magnetic focusing is not compatible with the goals of the contract.

4.3.2 Straight Permanent Magnets. A permanent magnet capable of producing a uniform axial magnetic field avoids the problems of the periodic type. Figure 4.4 shows an outline drawing of a typical permanent magnet which would focus the TW-148 type tubes. The estimated weight for such a magnet is 15 pounds.

For laboratory and experimental development, however, permanent magnets are not as versatile as solenoids, since the magnetic field cannot be varied. Consequently, permanent magnets were not used in the developmental program. However, permanent magnets could be used in further production or production refinement programs.

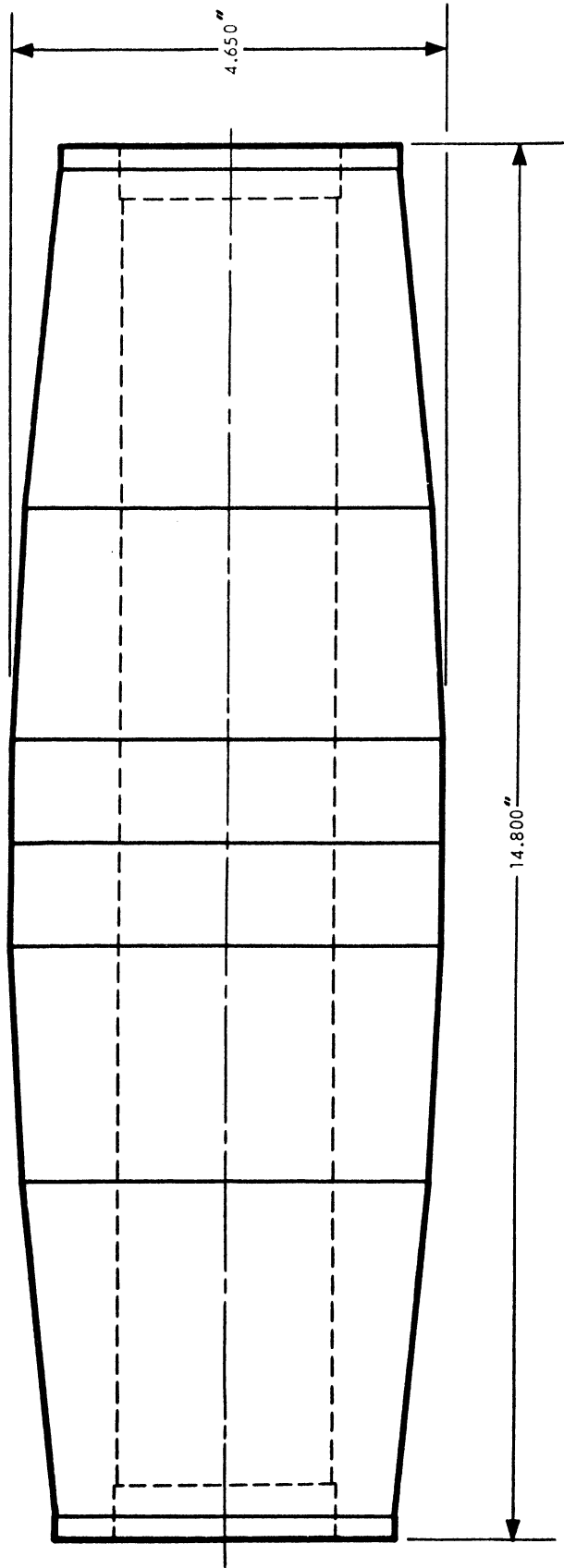


FIG. 4.4 OUTLINE OF ESTIMATED PERMANENT MAGNET REQUIRED TO FOCUS TW-148.

4.3.3 Solenoids. The versatility of solenoids makes their use important in experimental work. Figure 4.5 shows an outline drawing of the focusing solenoid. The solenoid weighs 28 pounds and requires 110 volts at 3.7 amperes to produce a 715 gauss focusing field for the tube. As mentioned in Section 4.2, the tube is sealed in the solenoid by an O-ring at each end.

4.4 Test Results. Six TW-148 tubes were built, the first three were primarily test vehicles, while the last three were for delivery. The design of TW-148 was started in April 1964 and completed on May 1, 1964. The first tube was processed on July 7, 1964. Tube number 6 was processed on January 4, 1965, and the testing was completed on January 8, 1965.

Tube TW-148-1. The helix shorted to the input matching section during bakeout; consequently, only electron gun tests were performed.

The gun operated at design perveance and at full rated beam current. Anode number one, however, intercepted excessive beam current when the gun was operated at the rated parameter values; and, although the interception beam current could be held within acceptable limits by increasing the solenoid magnetic field, the tube was disassembled and an inspection of the gun revealed that the outer electrode stack was not properly aligned. The misalignment produced a skewed electric field in the critical anode-to-cathode space causing the high interception.

Tube TW-148-2. Tube number 2 was assembled with 2 to 8 db of loss added to the helix circuit. The gun from tube number one

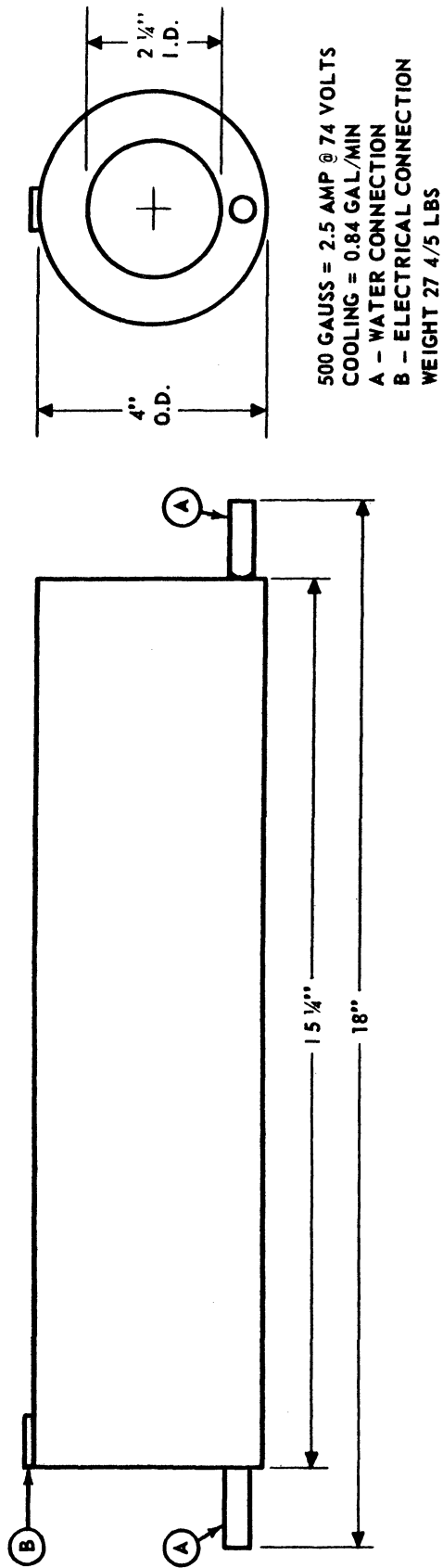


FIG. 4.5 TW-148 SOLENOID, TYPE 9.

was used in this tube. The small-signal band center occurred at about 250 megacycles, and the electronic gain was 8 db at 100 megacycles, 13 db at 200 megacycles, 13 db at 300 megacycles, and 12 db at 400 megacycles. The net gain ranged from 4.5 to 7 db across the band. A constant 7-watt input level was used in determining this gain. Figure 4.6 shows the power output and gain versus frequency for a 7-watt input signal.

Tube number 2 was then rebuilt and designated 2R. The same electron gun was used, but the 2 to 8 db of helix loss was removed. The gain increased 1 to 2 db over the same circuit with added loss. Net gains ranged from 6 to 9 db with saturated outputs exceeding 100 watts. Figure 4.7 shows the power output versus frequency for both a 7-watt and 30-watt input signal. Tube number 2 was rebuilt a second time with a new gun which had the electrodes in the proper position. This gun operated as predicted, but little difference was noted in either gain or power output, as compared to tube 2R. After extensive testing, this gun developed leakage and became inoperable.

Gun number one was then put back into the tube and the tube designated 2RRR. This tube was then used as a driver in the testing of subsequent tubes.

Tube TW-148-3. As a result of the extensive tests performed on TW-148-2, the r-f structure was lengthened to provide more gain, and the output r-f matching section was redesigned for a lower cutoff frequency to improve the tube performance at 100 megacycles.

Tube TW-148-3 was assembled and processed. Partial gun failure required immediate replacement of the gun. The tube was then designated 3R. This longer circuit had no added loss and utilized a

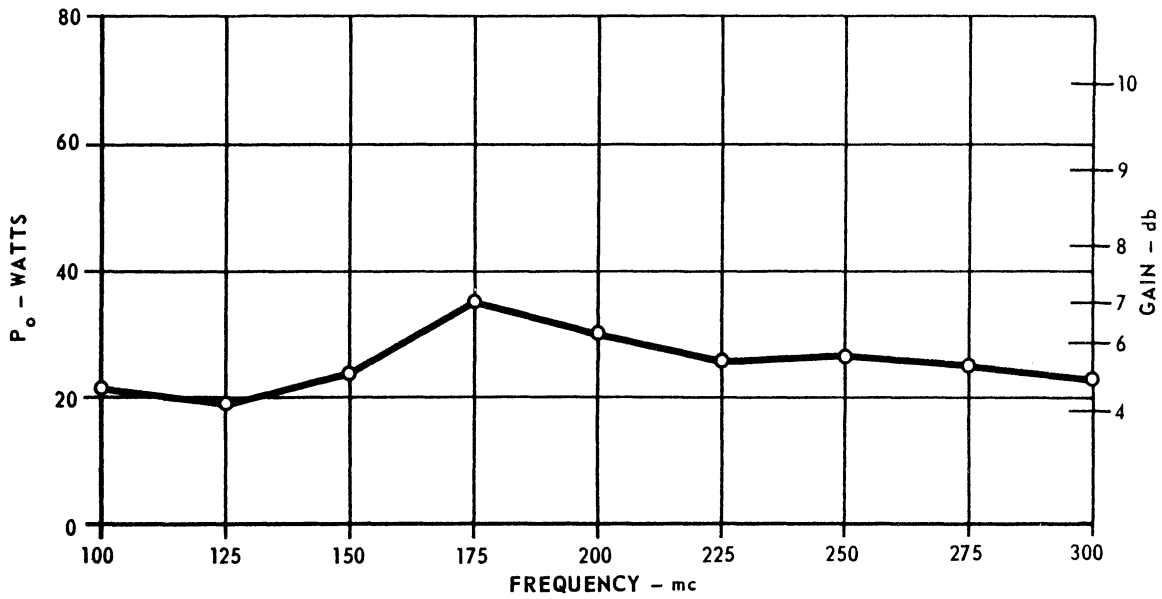


FIG. 4.6 POWER OUTPUT VS. FREQUENCY WITH 7 WATTS INPUT DRIVE; TW-148-2.

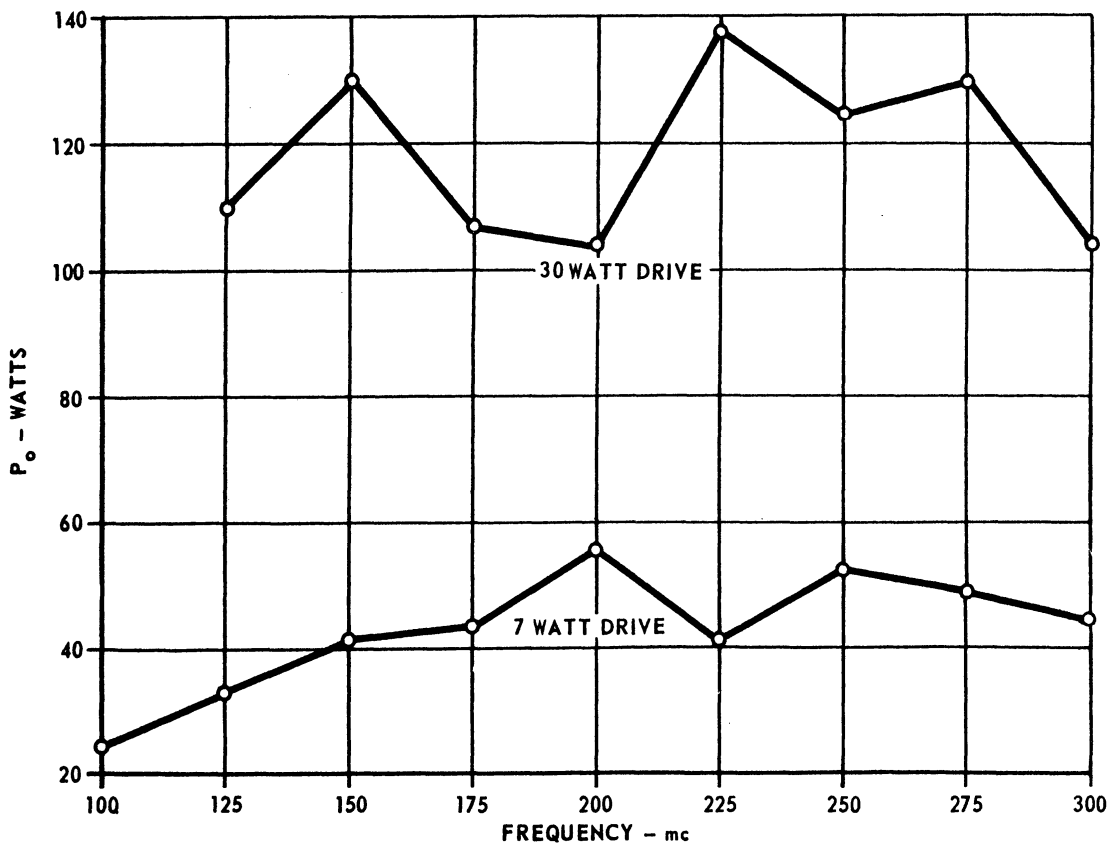


FIG. 4.7 POWER OUTPUT VS. FREQUENCY FOR TW-148-2R; 7-WATT AND 30-WATT DRIVES.

longer output r-f matching section. The gain of tube 3R, both small and large signal, was within acceptable limits. Figure 4.8 shows a plot of the power output versus power input at several frequencies.

Environmental tests were performed at Bendix Systems Division. After the data shown in Fig. 4.8 was taken, the tube was subjected to nonoperating vibration tests. The tube was vibrated parallel to the axis of the tube with a frequency of 5 C.P.S. to 500 C.P.S. and at an amplitude of 0.12 inch or 5 g, whichever was the limiting value. The rate of frequency change was such that 5 C.P.S. to 500 C.P.S. and back to 5 C.P.S. took about 15 minutes. The test continued for 60 minutes. Appendix B is Bendix Systems Division's report on the vibration test.

Tube 3R was then thoroughly retested. Figure 4.9 shows the power output versus power input data obtained. As can be seen, no significant changes occurred as a result of the vibration tests.

The tube was then subjected to shock tests and again no adverse effects were detected. The test consisted of a 15 g shock for a 11 ± 1 millisecond duration with six shocks in each of three mutually perpendicular directions. Appendix C is Bendix Systems Division's report on the shock test. Figure 4.10 shows the power output versus power input characteristics of the tube after shock.

Figure 4.11 shows a plot of the power output versus frequency with a 10-watt input drive signal for the three measurements discussed above. Figure 4.12 shows a plot of the maximum power output versus frequency as obtained by using optimum input signals for each frequency.

In the interest of simplifying the two-anode gun and possibly providing improved performance, a one-anode gun was assembled and

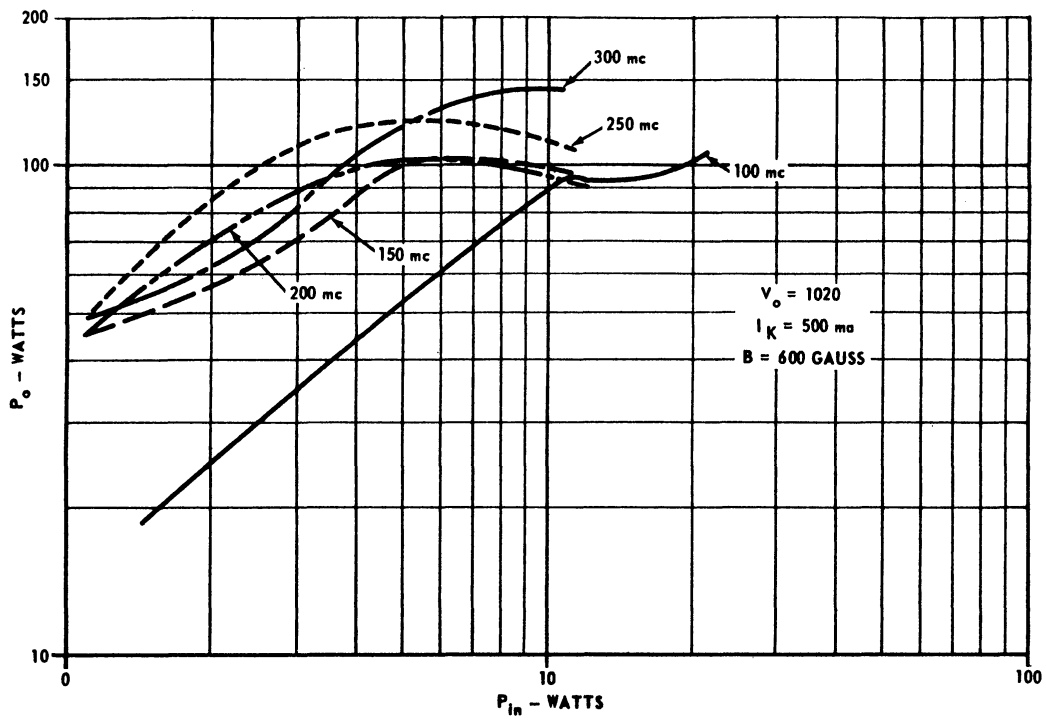


FIG. 4.8 POWER OUTPUT VS. POWER INPUT BEFORE ENVIRONMENTAL TESTS; TW-148-3R.

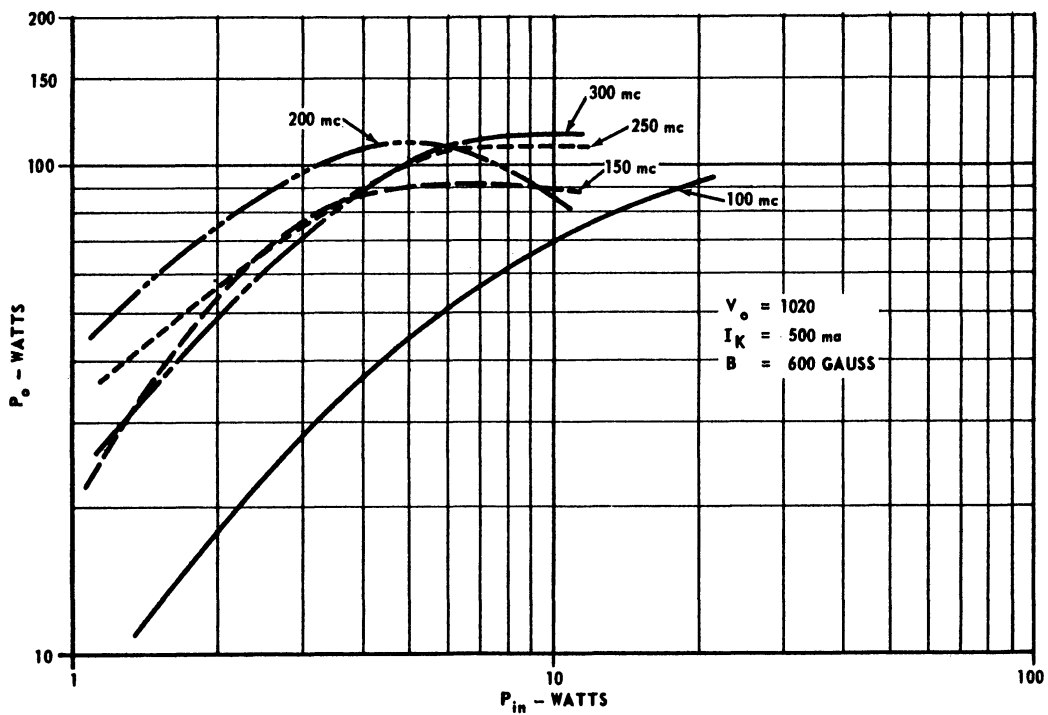


FIG. 4.9 POWER OUTPUT VS. POWER INPUT AFTER VIBRATION; TW-148-3R.

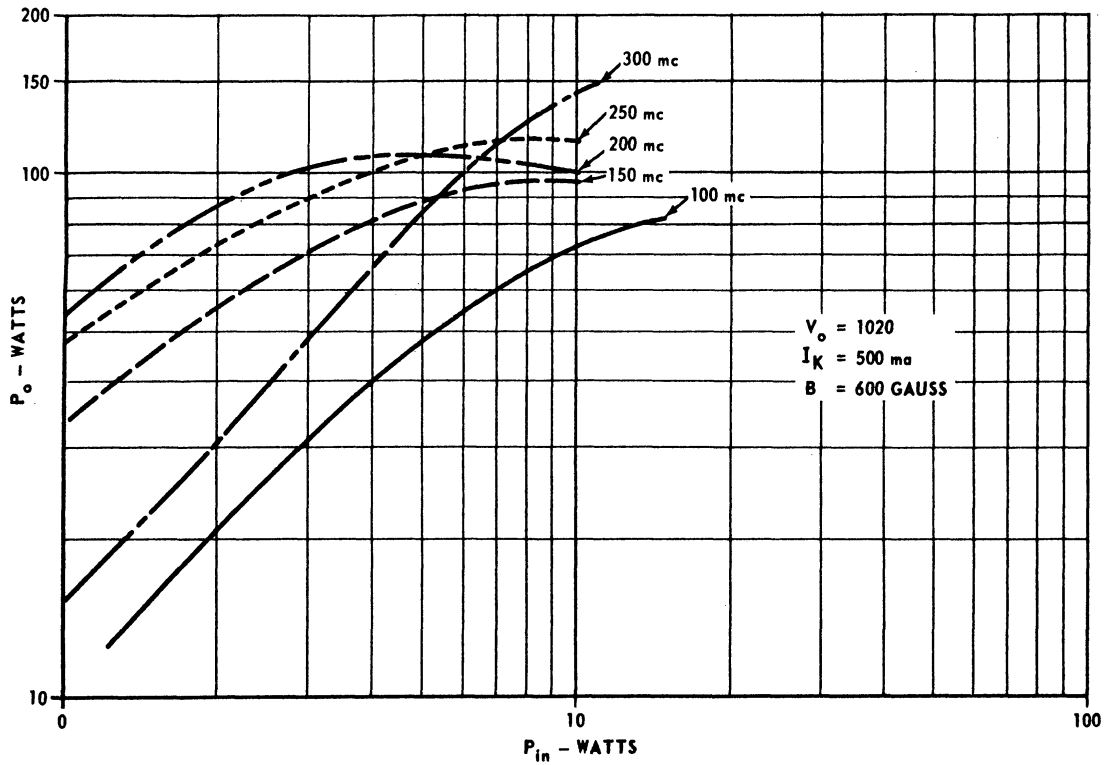


FIG. 4.10 POWER OUTPUT VS. POWER INPUT AFTER VIBRATION AND SHOCK TESTS; TW-148-3R.

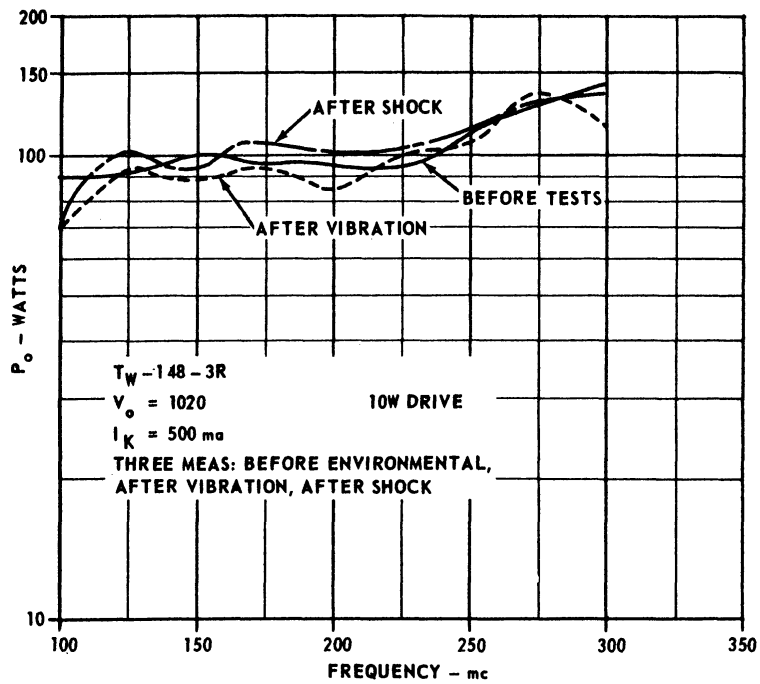


FIG. 4.11 POWER OUTPUT VS. FREQUENCY AT 10-WATTS DRIVE; TW-148-3R.

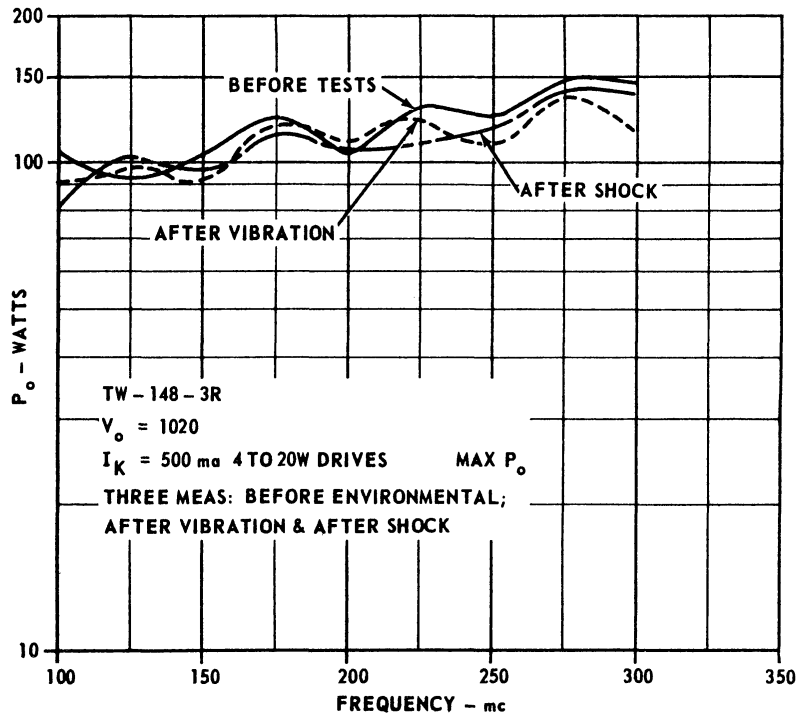


FIG. 4.12 MAXIMUM POWER OUTPUT VS. FREQUENCY --OPTIMUM DRIVE POWER; TW-148-3R.

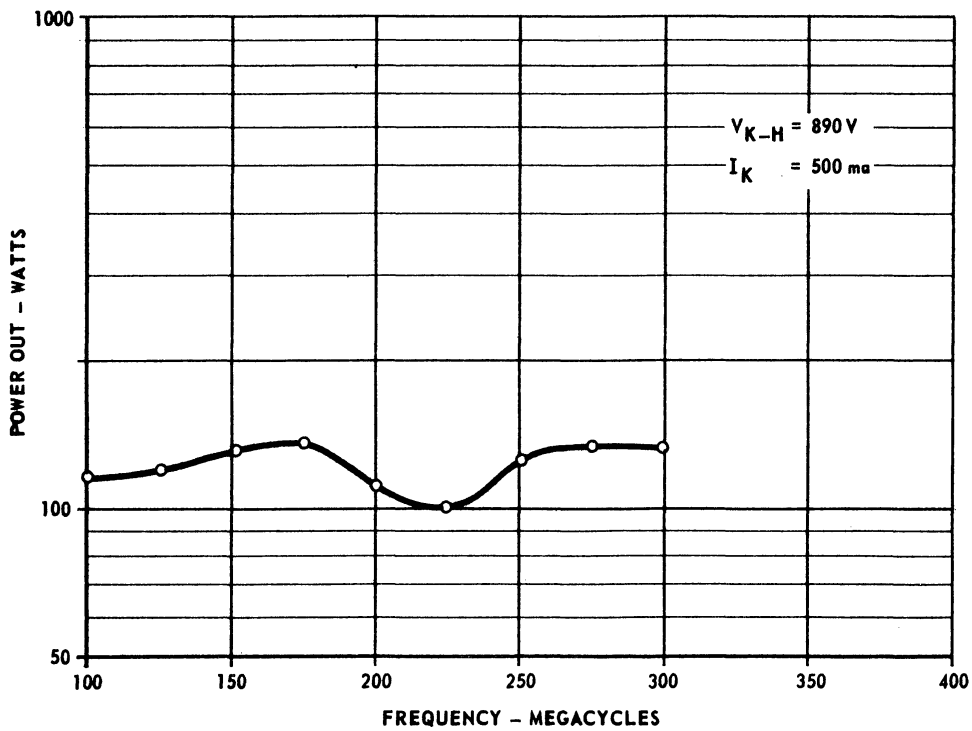


FIG. 4.13 P_o max VS. f TW-148-4.

tested in tube number 3. This combination was designated TW-148-3RR. The r-f performance of TW-148-3 was essentially unchanged, but later tubes suffered from cathode ion poisoning.

Tube TW-148-4. This tube was assembled with a one-anode gun and tested. This tube produced over 100 watts of r-f power, across the 100- to 300-megacycle frequency band at gains of 10 db or more. Figure 4.13 shows the r-f test data. During these tests a condition of cathode ion poisoning was observed.

During the r-f tests conducted on tube number 5, an intermittent connection between the input coaxial line and the input section was discovered. Although tube number 4 did not display the sudden changes in gain and r-f power output observed in tube number 5, the construction of the two tubes were identical insofar as the parts which caused trouble were concerned. In addition, the mild cathode poisoning observed in tube number 4 was severe in tube number 5. Therefore, tube number 4 was disassembled and modified to correct the cathode poisoning problem and preclude the possibility of intermittent connections in the input line. The test results are shown in Figs.4.14 through 4.18. As shown, this tube meets all the r-f performance requirements. The r-f test setup is fully described in Appendix D.

Tube TW-148-5. This tube was assembled with a one-anode electron gun and a magnetic collector. The magnetic collector reduced the electron beam interception on the helix to zero under most conditions and to about 1 milliamperere with 100 volts depression on the collector. From the standpoint of suppressing secondary electrons, the magnetic collector was very successful. However, the magnetic collector greatly intensified the cathode poisoning by ion bombardment. It was

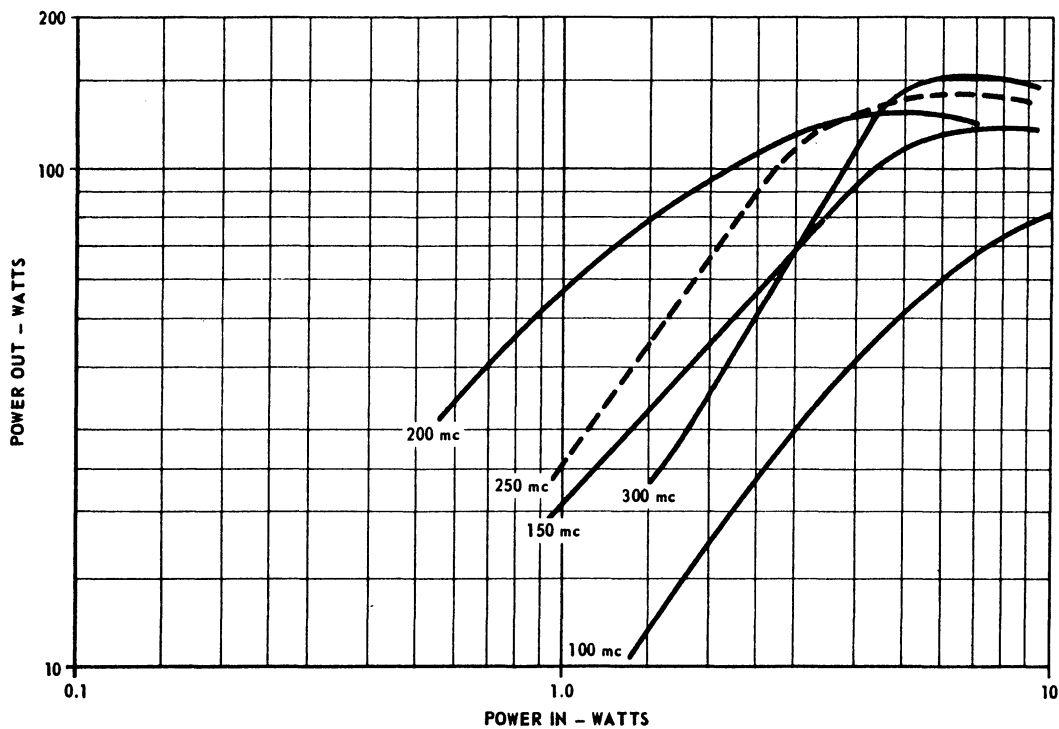


FIG. 4.14 P_o VS. P_{in} , FILTERED, TW-148-4R.

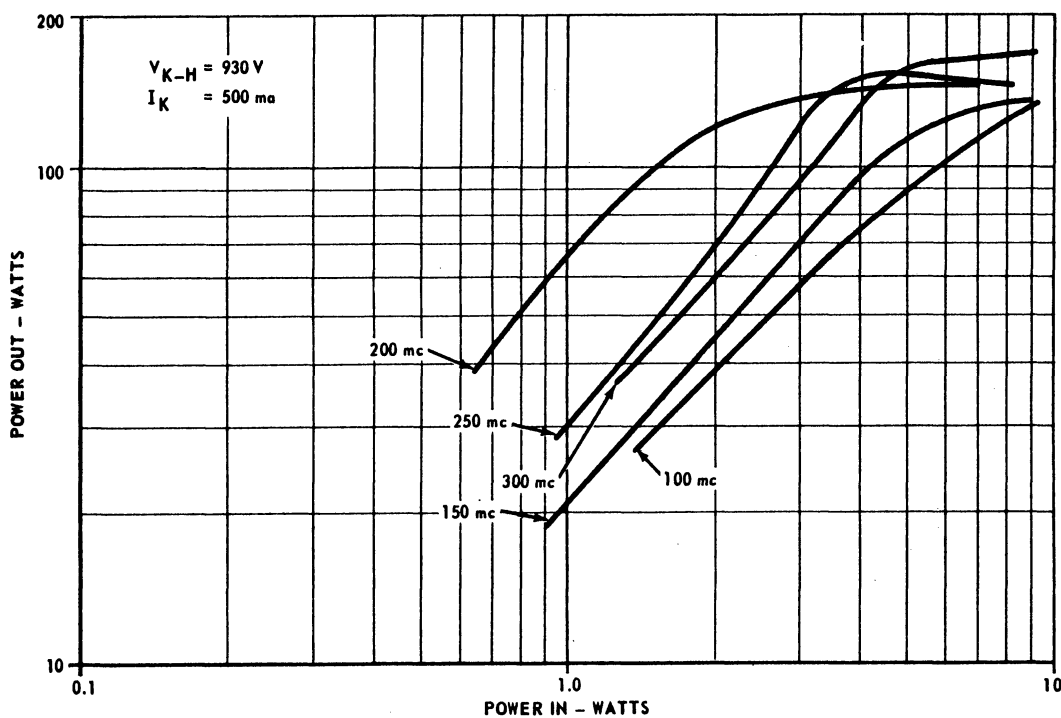


FIG. 4.15 P_o VS. P_{in} , UNFILTERED, TW-148-4R.

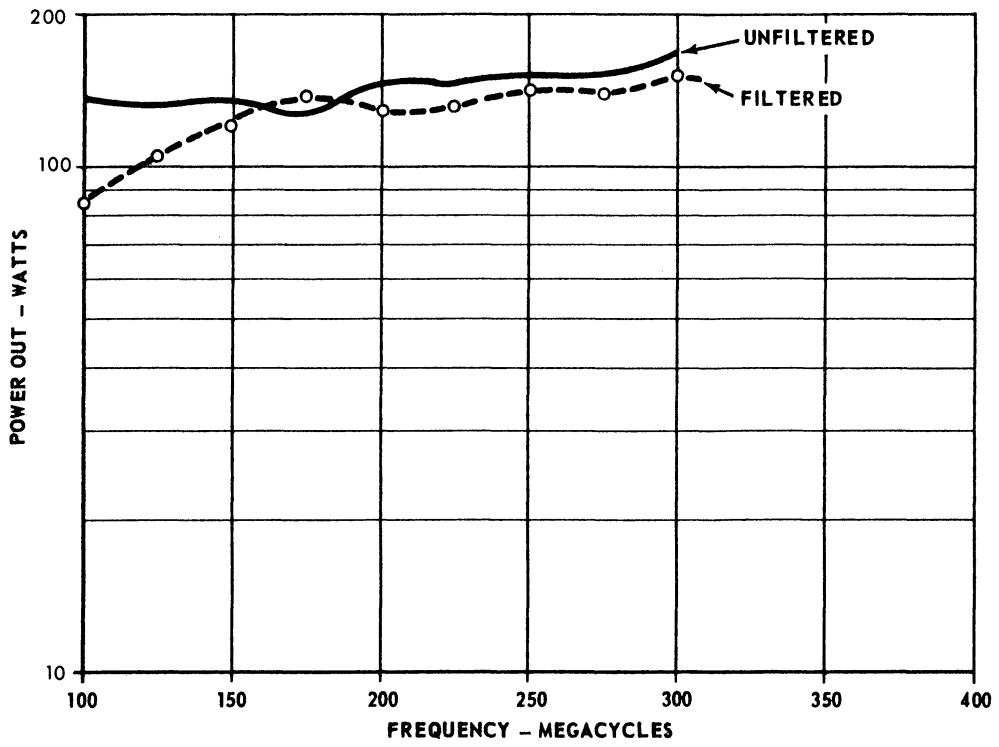


FIG. 4.16 $P_{o\max}$ VS. f - TW-148-4R.

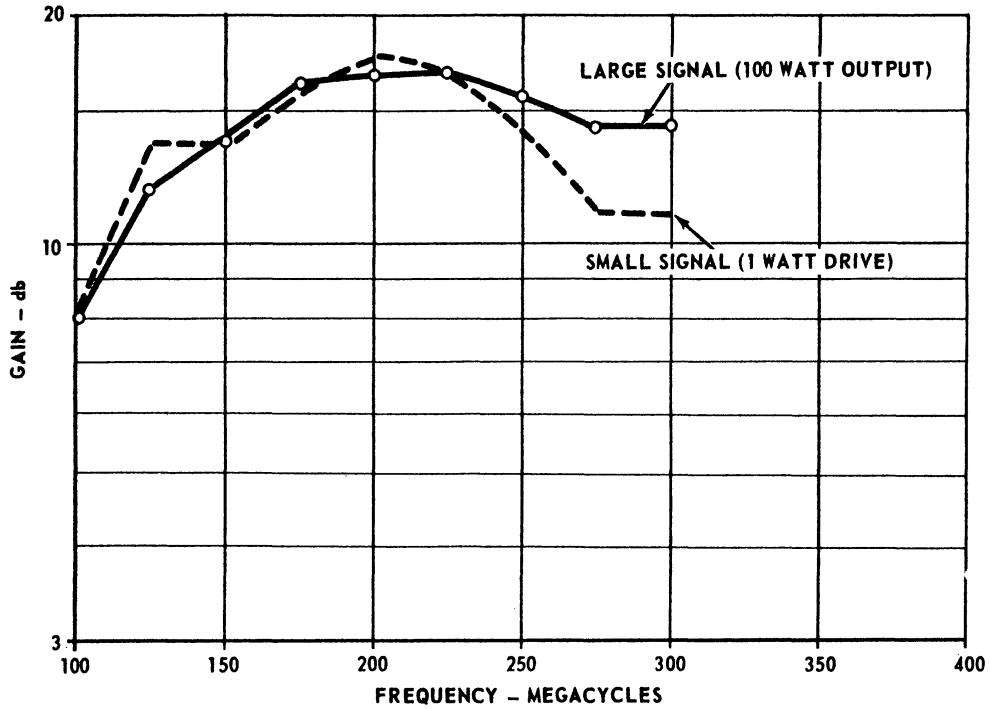


FIG. 4.17 GAIN VS. f ., FILTERED, TW-148-4R.

not possible to obtain meaningful r-f data on this tube with the magnetic collector and one-anode gun.

Consequently, the tube was disassembled and an ion barrier electrode mounted on the gun. The reassembled tube was designated TW-148-5R. The test results showed that the ion barrier electrode effectively protected the cathode from ion bombardment poisoning. However, the cathode heater failed before the r-f tests were completed.

The heater was replaced and the reassembled tube designated TW-148-5RR. R-f tests were conducted but large sudden changes were noted in the gain and power output primarily at a frequency of 150 megacycles, but appeared to degrade the performance anywhere in the 100 to 200 megacycle frequency band. The problem was traced to an intermittent connection between the input coaxial line and the input matching section. Figure 4.19 shows the maximum power output versus frequency, while Fig. 4.20 shows the gain versus frequency. Both filtered and unfiltered power measurements were made.

Tube number 5 was again disassembled and a positive r-f electrical connection made between the input coaxial line and the input matching section. This connection, a flexible strip of wire, was placed in parallel with the intermittently connecting slip joint between the two input parts. The reassembled tube was designated TW-148-5RRR.

Figure 4.21 shows the maximum power output, both filtered and unfiltered, for drive levels up to 10 watts. In some cases this was not the saturated power output. Figure 4.22 shows a plot of filtered power output versus power input at different frequencies, and Fig. 4.23 shows the same information for the unfiltered case. Figures 4.24 and 4.25 show the gain versus frequency (filtered and unfiltered, respectively) for

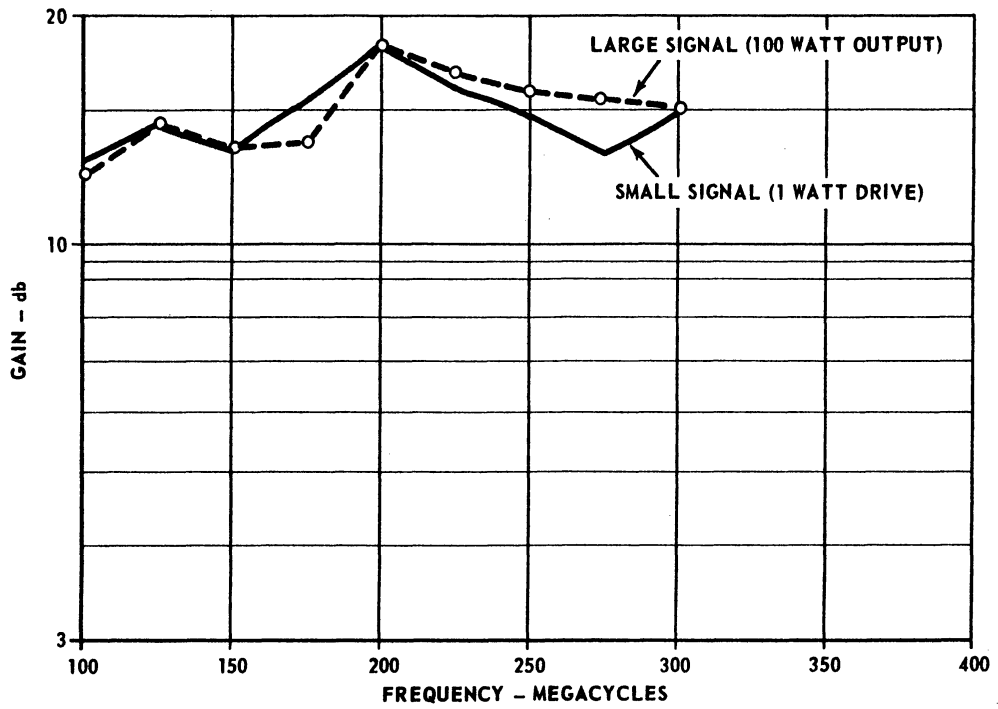


FIG. 4.18 GAIN VS. f , UNFILTERED, TW-148-4R.

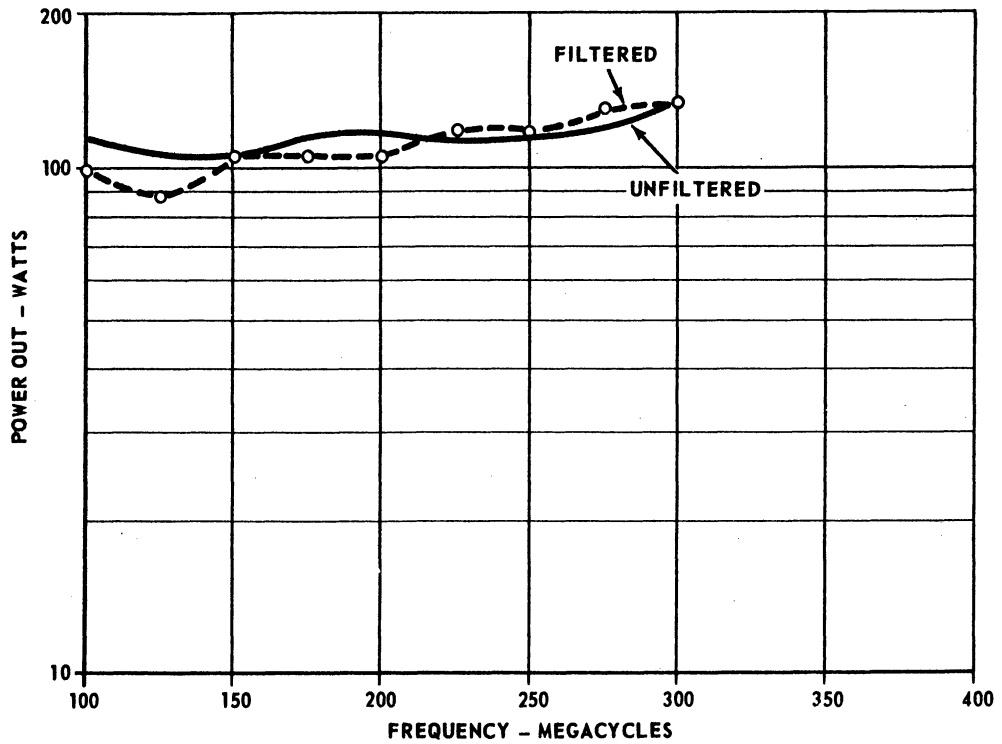


FIG. 4.19 $P_{o\max}$ VS. f TW-148-5RR.

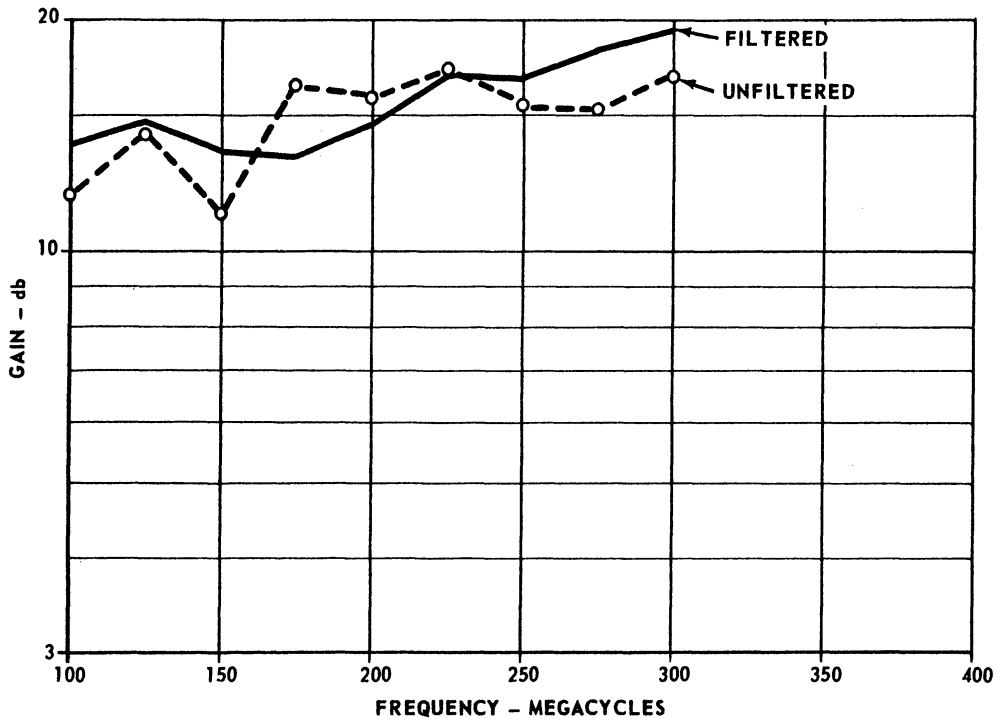


FIG. 4.20 GAIN VS. f TW-148-5RR.

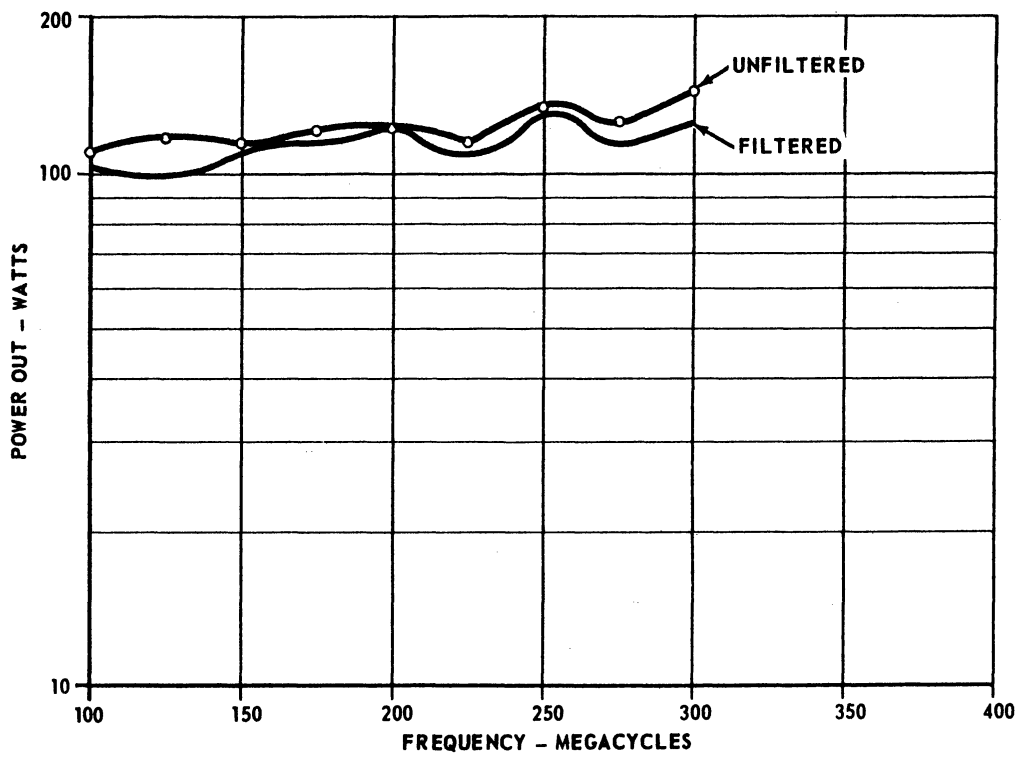


FIG. 4.21 $P_{o\max}$ VS. f TW-148-5RRR.

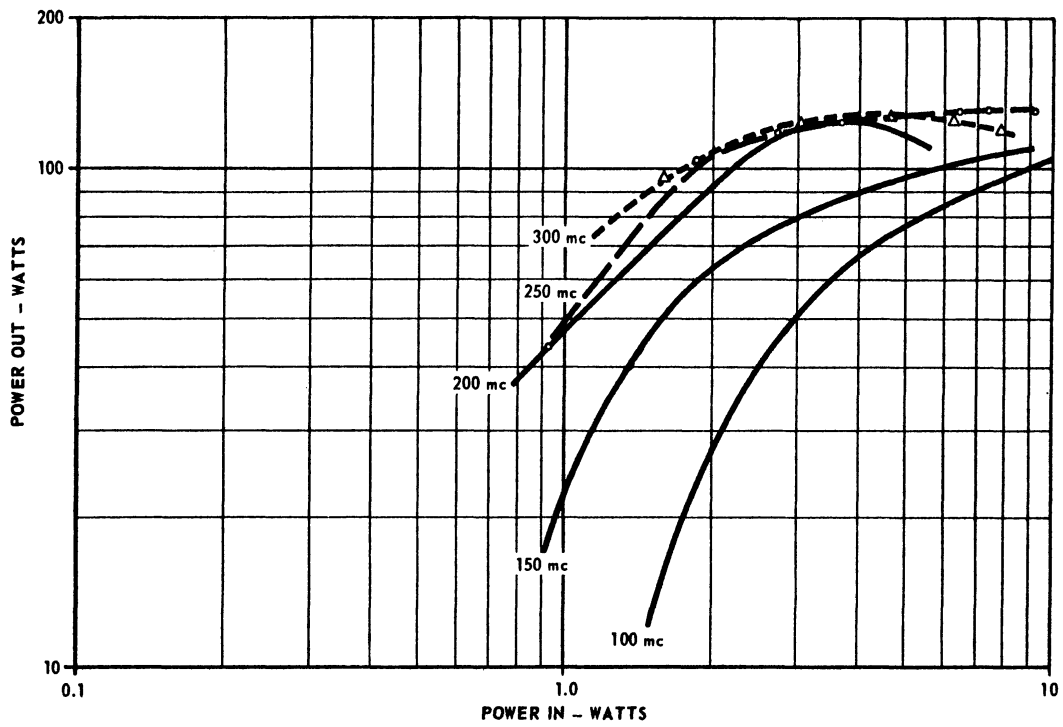


FIG. 4.22 P_o VS. P_{in} , FILTERED, TW-148-5RRR.

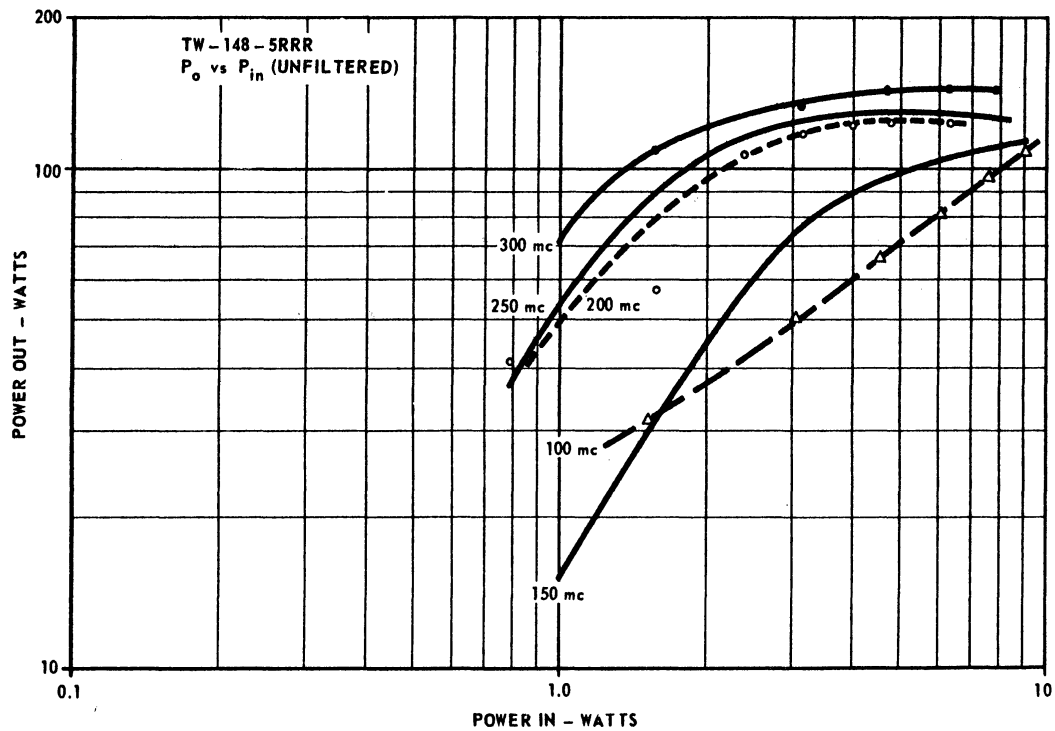


FIG. 4.23 P_o VS. P_{in} , UNFILTERED, TW-148-5RRR.

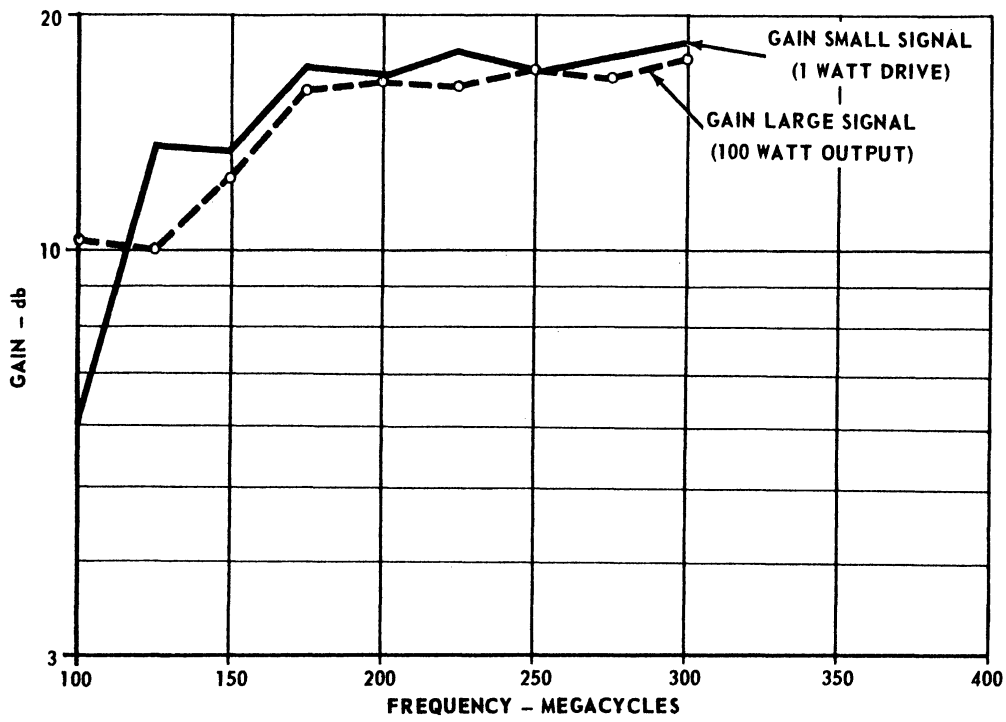


FIG. 4.24 GAIN VS. f , FILTERED, TW-148-5RRR.

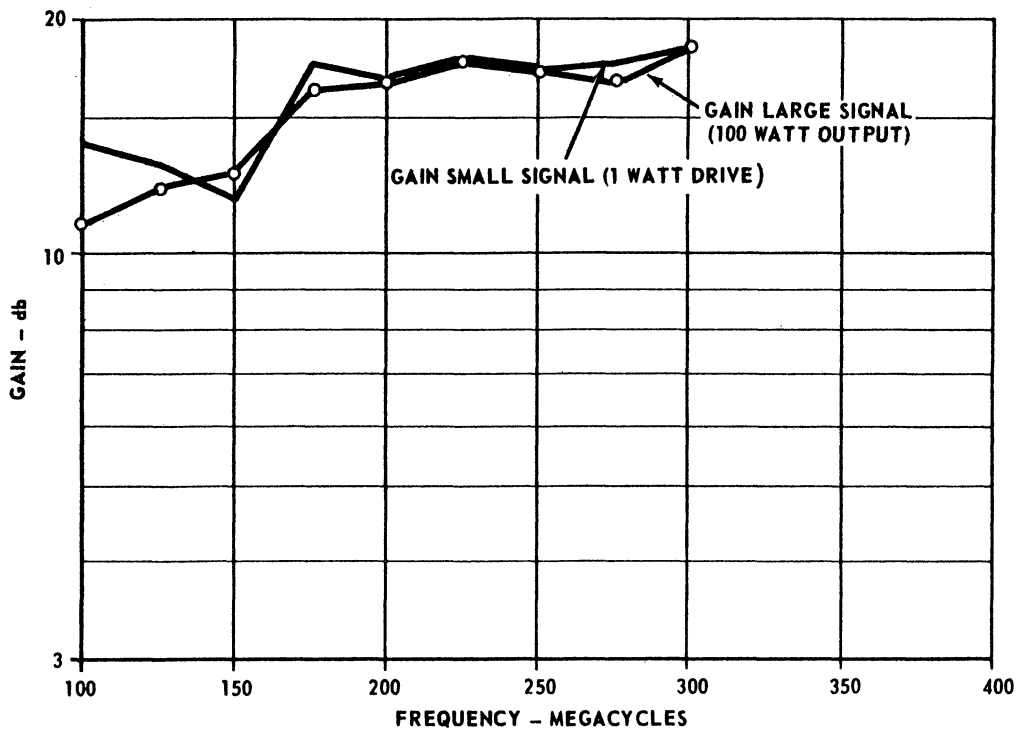


FIG. 4.25 GAIN VS. f , UNFILTERED, TW-148-5RRR.

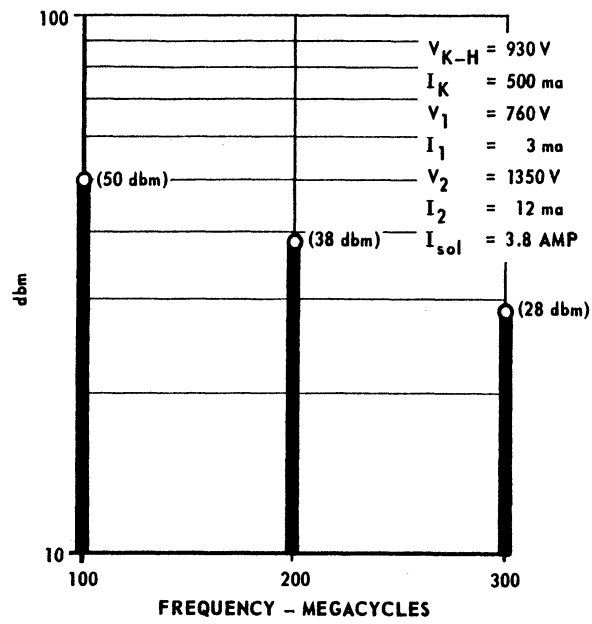
small signal and at 100 watts output. By comparing this data with the data for tubes number 4 and 6, the detrimental affects of the magnetic collector can be seen. Upon comparing the data of tubes number 4 and 5, it was decided to construct tube number 6 with a nonmagnetic collector. Consequently, the construction of tube number 6 was delayed until the comparison of tubes number 4 and 5 could be made.

Figures 4.26 through 4.28 show the spurious signals, primary signals, harmonics, and sum and difference signals in the output for various combinations of signal inputs. All signals in the 100- to 300-megacycle frequency band which were 22 db or less below the saturated power output of 100 watts were recorded. The figures show that no spurious outputs were observed. Moderate harmonic generation was present and strong mixing action occurred when both signals were saturating.

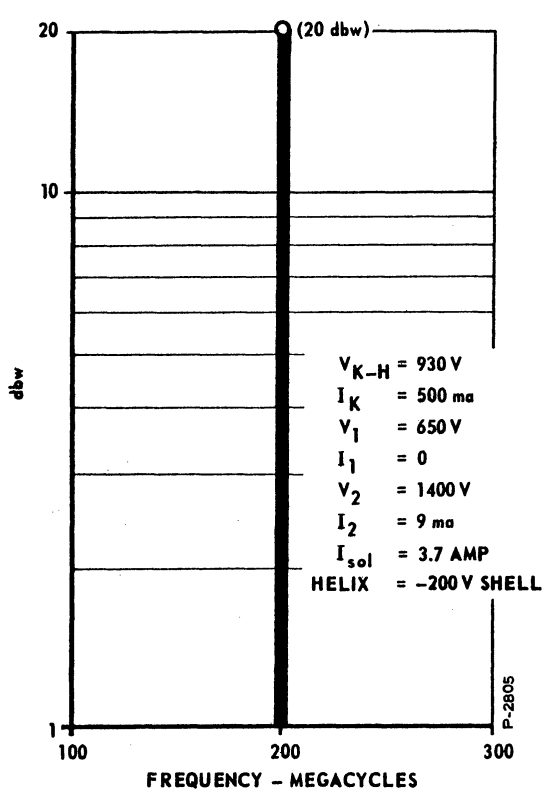
Tube TW-148-6. This tube incorporated all the best features of previous tubes. The tests showed very good results. Figure 4.29 shows the maximum power output versus frequency for both the filtered and the unfiltered cases. Power output versus power input is shown in Figs. 4.30 and 4.31 for the filtered and the unfiltered cases, respectively; while Figs. 4.32 and 4.33 indicate the gain versus frequency operation at small signal and at 100 watts output for the filtered and unfiltered cases, respectively.

5. Summary and Conclusions

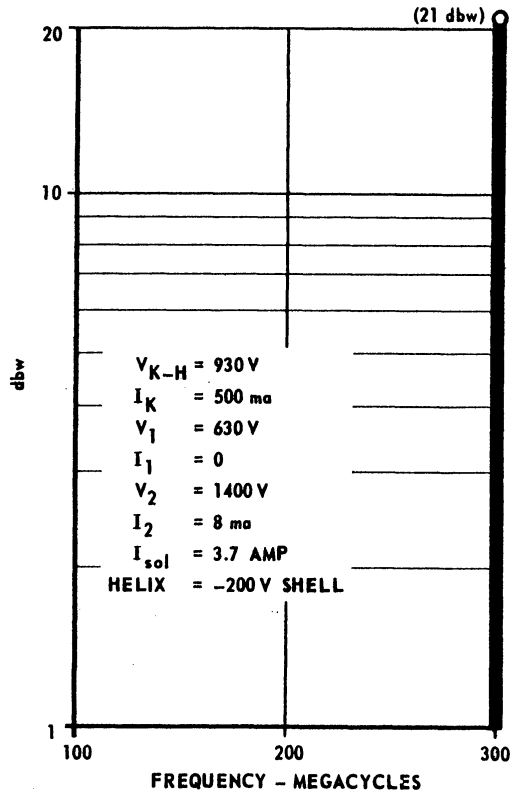
This program began as a research activity to develop two Crestatron-type traveling-wave tubes. These tubes were to operate in the 100- to 300-megacycle frequency band and employ electrostatic



(A) 100 mc INPUT



(B) 200 mc INPUT



(C) 300 mc INPUT

FIG. 4.26 OUTPUT SIGNALS WITH ONE FREQUENCY INPUT, SATURATING.

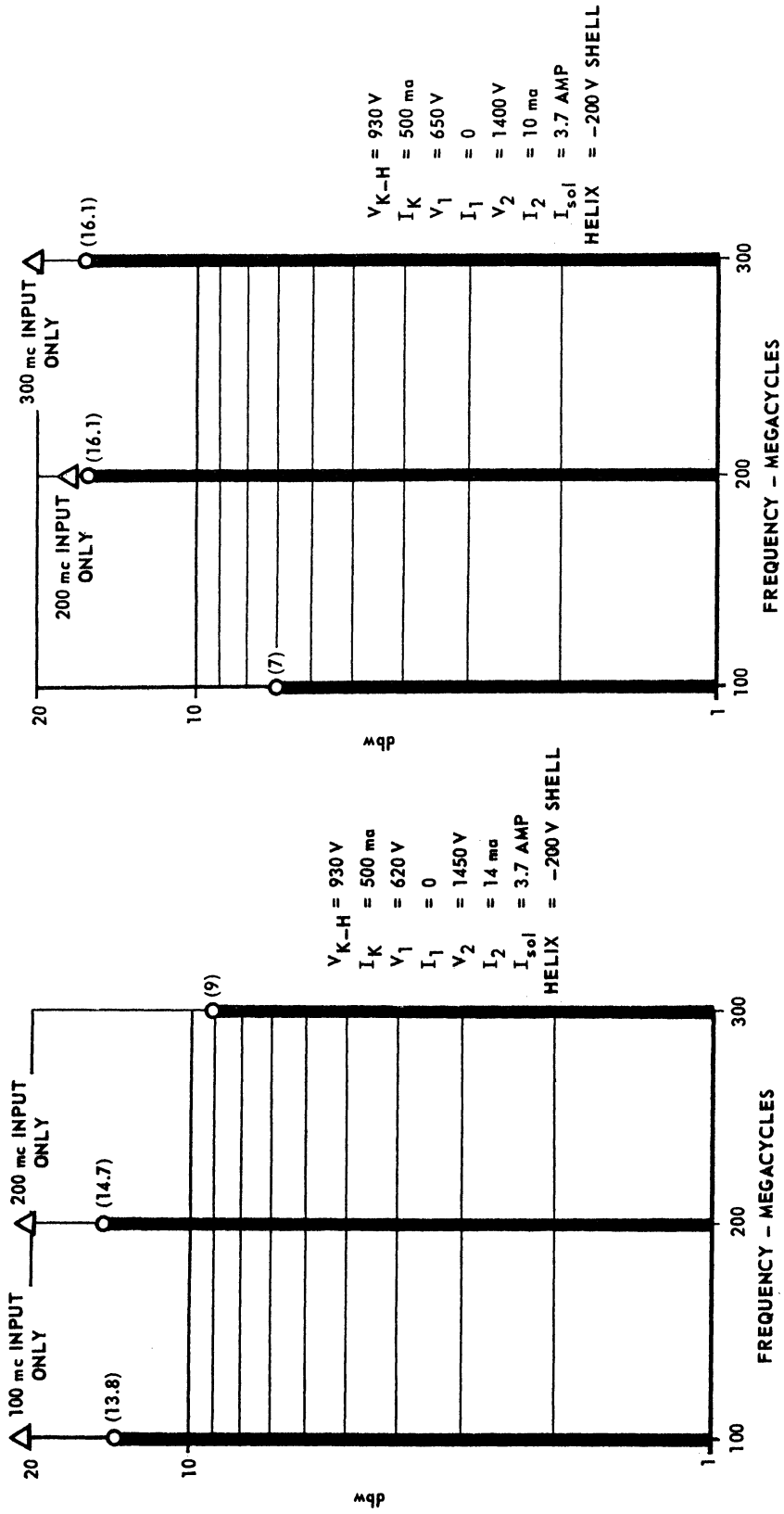


FIG. 4.27 OUTPUT SIGNALS WITH TWO FREQUENCY INPUTS, BOTH FREQUENCIES SATURATING.

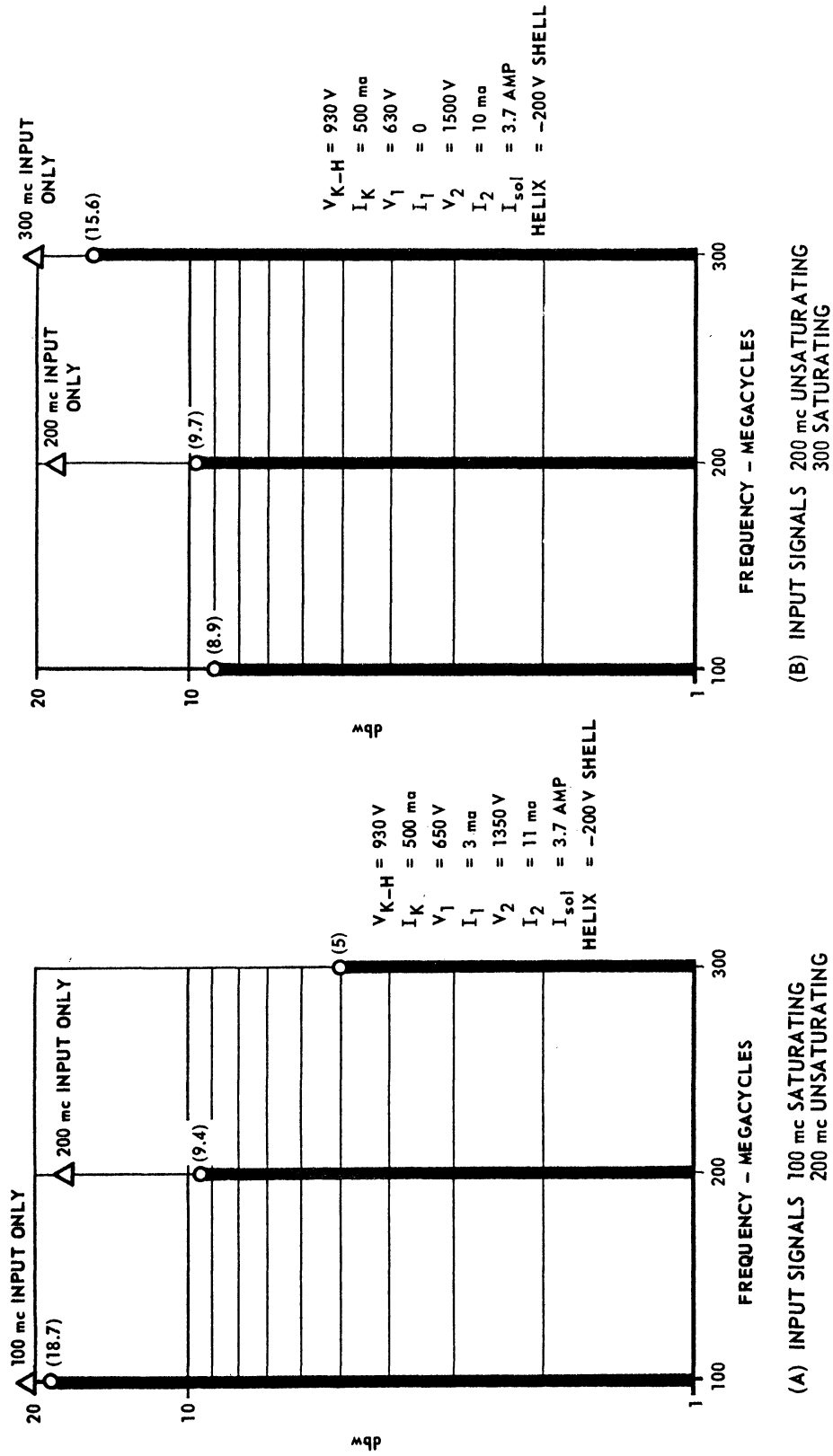


FIG. 4.28 OUTPUT SIGNALS WITH TWO FREQUENCY INPUTS,
 ONLY ONE FREQUENCY SATURATING.

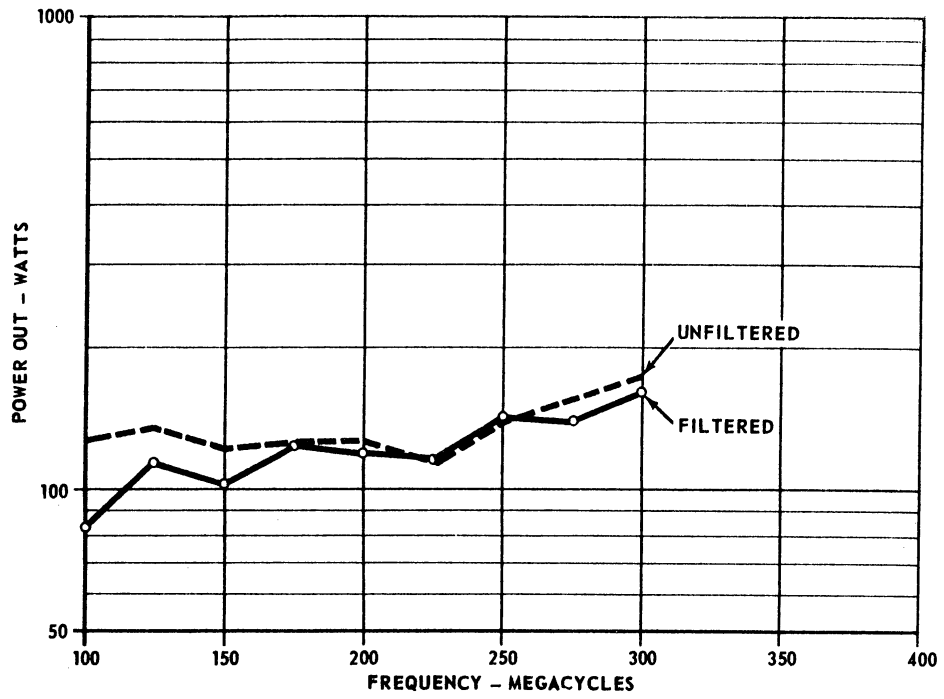


FIG. 4.29 $P_{o \max}$ VS. f TW-148-6.

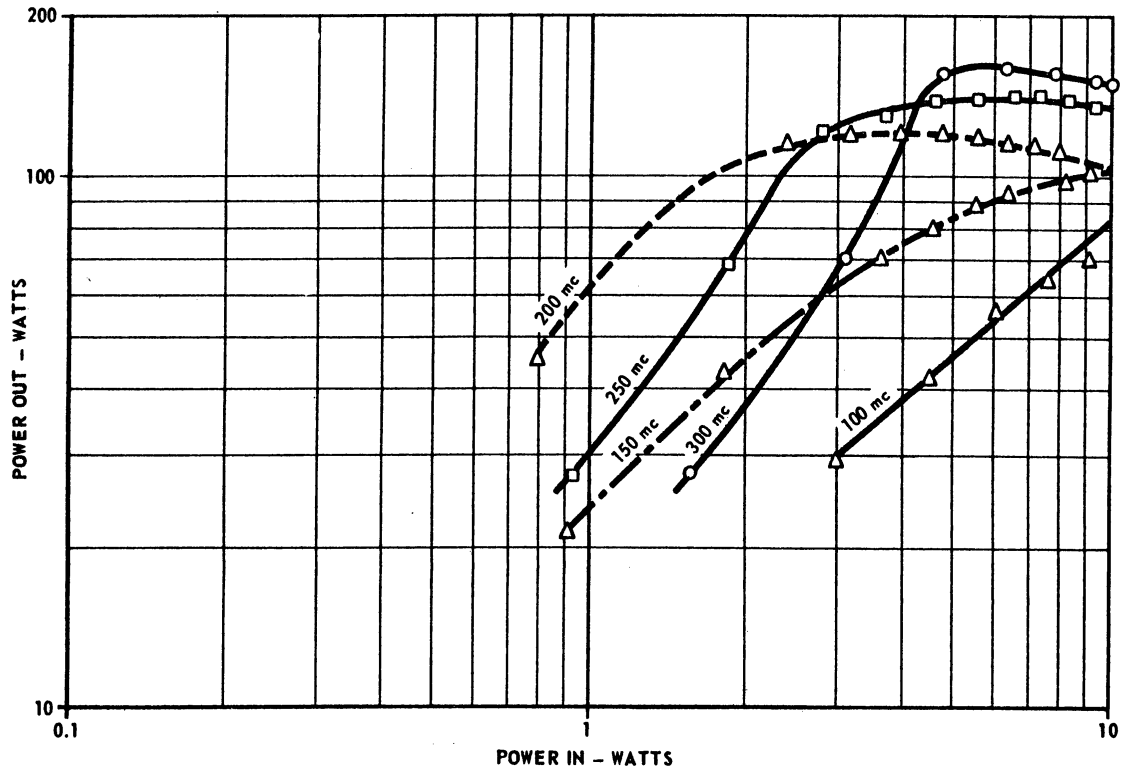


FIG 4.30 P_o VS. P_{in} , FILTERED, TW-148-6.

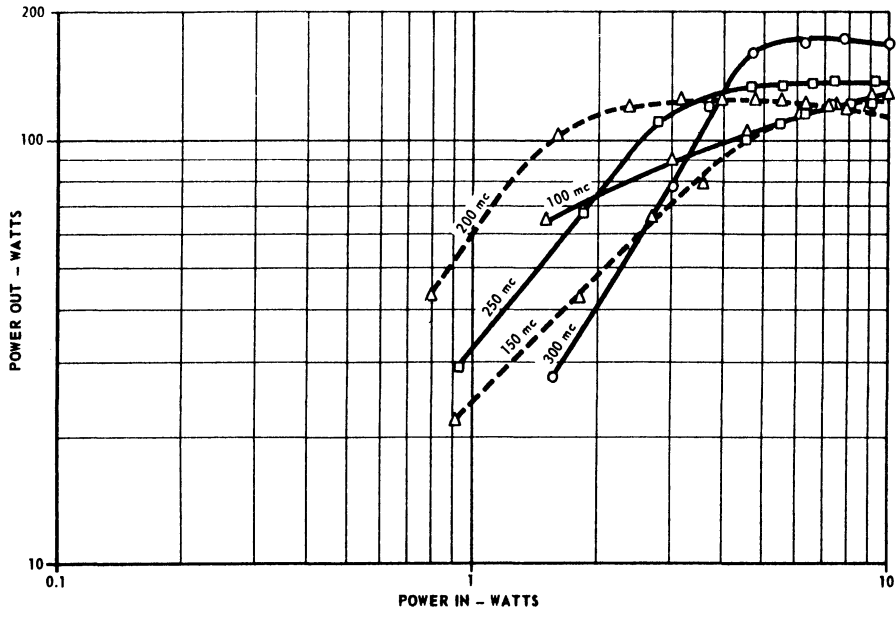


FIG. 4.31 P_o VS. P_{in} , UNFILTERED, TW-148-6.

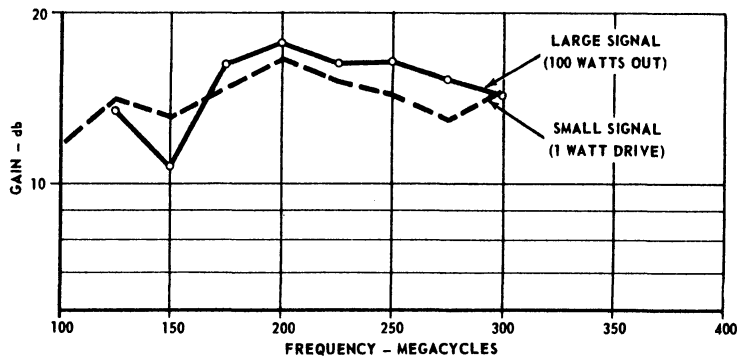


FIG. 4.32 GAIN VS. f , FILTERED, TW-148-6.

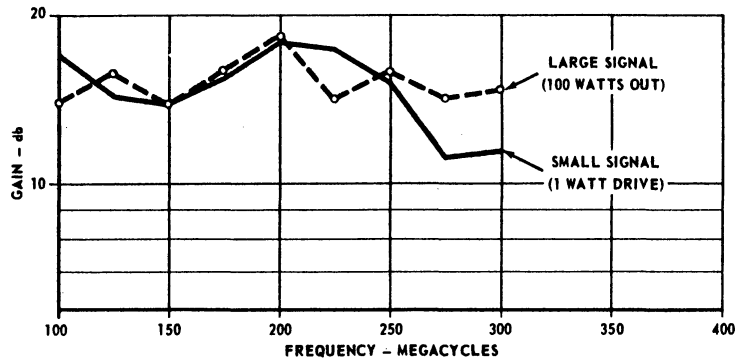


FIG. 4.33 GAIN VS. f , UNFILTERED, TW-148-6.

focusing. One tube was to provide 100 watts and the other tube was to provide 1000 watts of output power. The mechanical aspects of the tubes were successfully completed, coaxial to helical transmission line transitions with low VSWR's were developed, and means of producing large precision envelopes from 7052 glass were devised. Good progress was also made on producing the precision envelopes from 1723 alumino-silicate glass. The first tube had progressed to the point of final assembly before discussion with Navy personnel revealed that these electrostatically focused tubes would be too large to be used in existing equipment. Consequently, work on the electrostatically focused tubes was discontinued and a new program proposed to the Navy. This proposal outlined a development program for a 100-watt magnetically focused tube. Work on the 1000-watt tube was deferred for the duration of the 100-watt tube development program.

The 100-watt tube was designed as the smallest possible tube which would operate over the 100- to 300-megacycle frequency. The design employed a technique for shifting the response of the tube to lower than normal frequencies by operating the tube at higher than usual voltages. Tests performed on this tube, designated TW-143-A, proved that the shift to lower frequencies occurred only for small-signal operation. Under large-signal operation, the electron beam velocity was reduced near the output end of the r-f circuit, which shifted the response of the tube back upward in frequency and also caused "inverse saturation." This is a condition where the large-signal gain exceeds the small-signal gain. From the TW-143-A testing program it was concluded that:

A. Helical type tubes with appropriate r-f matching mechanisms can have very wide bandwidths. Bandwidths of at least 5 to 1 have been

demonstrated and useful gain may be obtainable over even wider bandwidths.

B. In low loss tubes such as TW-143-A, the stability depends primarily on the r-f matches and equipment connected to the input and output. Transparent tubes will require well-matched loads or isolators between the tube and load.

C. Tapered matching sections affect the phase velocity at each end of the helix. Depending on the particular tube, this could be either helpful or detrimental.

D. Lowering of the frequency band of a tube by overvoltage operation appears to be satisfactory for small-signal conditions only.

E. A low gain tube operated in an overvoltage condition will exhibit inverse saturation. This gain excursion can be on the order of 10 db or more. Systems personnel should be informed of this phenomenon.

F. The bandwidth characteristics of the inverse saturation phenomenon could not be concluded, but indications are that broad bandwidths should be obtainable.

A new tube design, designated TW-147, was generated which utilized the TW-143 electron gun. It was a compromise between the original TW-143 design and a design based on synchronized beam velocities. Helical couplers were chosen for the first two tubes of the TW-147 to further evaluate their characteristics. It was shown that helical couplers are not satisfactory for bandwidths of 3 to 1 or greater, when both low insertion loss and VSWR must be maintained. The third TW-147 tube utilized tapered matching sections which proved satisfactory. This tube developed 100 watts of output power over the frequency band,

thereby proving feasibility and fulfilling the requirements of the first part of the contract. However, this tube was centered higher in frequency than desired and exhibited some inverse saturation characteristics.

In order to correct these deficiencies, the design was adjusted and designated TW-148. Tubes of the TW-148 design have met or exceeded all contractual requirements, including electrical performance and environmental specifications. Three of these tubes were delivered to the Navy. These tubes are at present, solenoid focused, liquid cooled, and weigh about 35 pounds, with the focusing solenoid.

6. Recommendations

This program has been successfully concluded with the delivery of three tubes meeting the contractual requirements. In addition, this program resulted in a better understanding of traveling-wave tube operation and of the phenomenon termed "inverse saturation." From the program final results and from the original contract intent, it can be recommended that:

A. A 1000-watt or greater output power tube be developed for the 100- to 300-megacycle frequency range.

B. The 100-watt tube be refined to reduce the weight, use straight permanent magnet focusing, and incorporate a separate output r-f matching section and collector for more efficient depressed potential collection than is now possible.

C. The extremely wideband characteristics available from helical circuits and tapered matching sections be more thoroughly investigated. These bandwidths appear to be 5 to 1 or greater.

D. The phenomenon of inverse saturation be investigated thoroughly and presented to systems engineers who might be able to make use of it.

APPENDIX A
TENTATIVE SPECIFICATIONS
FOR TW-148

A.1 Absolute Maximum Ratings

| | | |
|----------------------------------|------------------|--------------------|
| Cathode Voltage | W.R.T. (ground) | -1500 volts |
| Cathode Current | | 600 mA |
| Helix Voltage | W.R.T. (ground) | -250 volts |
| Helix Current | | 25 mA |
| Repeller Voltage | W.R.T. (cathode) | 1700 volts |
| Repeller Current | | 15 mA |
| Anode Voltage | W.R.T. (cathode) | 850 volts |
| Anode Current | | 10 mA |
| Heater Current | | 4.0 Amperes |
| Solenoid Current | | 4.1 Amperes |
| Cooling - Collector and Solenoid | | 1 GPM water (min.) |

A.2 Typical Operating Conditions

| | | |
|------------------|------------------|-------------|
| Cathode Voltage | W.R.T. (ground) | -1130 volts |
| Cathode Current | | 500 mA |
| Helix Voltage | W.R.T. (ground) | -200 volts |
| Helix Current | | 0 mA |
| Repeller Voltage | W.R.T. (cathode) | 1500 volts |
| Repeller Current | | 2 to 12 mA |
| *Anode Voltage | W.R.T. (cathode) | 700 volts |
| Anode Current | | 3 mA |
| Heater Current | | 3.7 Amperes |
| Solenoid Current | | 3.7 Amperes |

*Adjust for 500 mA Cathode Current

APPENDIX B
 VIBRATION TESTS
 ENVIRONMENTAL LABORATORIES
TEST REPORT

REPORT NO. TR- 1011 DATE 15 Sep 64

PERFORMED FOR: Bendix Research Laboratories Division
 Southfield, Michigan

TEST: Sinusoidal Vibration

ITEM: Electron Tube, TWT-148-3R

TEST DATE: 2 Sep 64

PERFORMED AT: Space Laboratories

WORK ORDER NO: 82441-440-01-0100

AUTHORIZATION: P. O. 126668

REQUESTED BY: T. M. McKenzie

REPORT SENT TO: K. Earl
 A. G. Peifer

PREPARED BY: *R W Hyde*
 R. W. Hyde
 Test Engineer
 Systems Test Department

APPROVED BY: *R. H. Culpepper*
 R. H. Culpepper
 Project Test Engineer
 Systems Test Department

REFERENCE

(a) Paragraph 4.9.9 MIL-E-1 D March 31, 1958, paragraph B, Vibration (non operating).

INTRODUCTION

An electron tube, TWT-148-3R, manufactured by Bendix Research Laboratories Division, was subjected to a sinusoidal vibration test in accordance with Reference (a). The test was conducted in one axis as shown in Figure 1. The input levels are shown in Table 1.

SUMMARY OF RESULTS

No structural damage was observed as a result of the applied vibration.

METHODS AND DATA

The test item was assembled in a fixture supplied by Bendix Research Laboratories Division and mounted on the vibration exciter slip table as shown in Figure 1. A control accelerometer mounted on the fixture near the test item was the detector for a constant displacement/acceleration servo system. The output of this accelerometer was measured with a true rms voltmeter and recorded on an X-Y recorder. This recording is shown in Figure 2. The frequency of the vibration applied to the test item was cycled thru a range of 5-500-5 cps for 60 minutes.

The sensitivity of the accelerometer system was checked prior to the test by subjecting the accelerometer to a sinusoidal vibration of 0.25 in. double amplitude at a frequency of 44 cps, to give an acceleration of 25 g peak. Vibration displacement was measured with an optical wedge; frequency was measured with an electronic counter; and accelerometer system output was monitored with a true rms voltmeter. Calibration dates are shown on the attached list of test equipment.

The vibration test was witnessed by K. Earl and D. Rice of Bendix Research Laboratories Division, who retained the test item.

Environmental Laboratories
VIBRATION TEST LEVELS

| <u>Axis</u> | <u>Frequency- cps</u> | <u>Acceleration Level-g peak</u> | <u>Frequency Cycle Time-Minutes</u> | <u>Total Test Time-Minut</u> |
|--------------|---------------------------|--------------------------------------|---|----------------------------------|
| Longitudinal | 5-500-5 | 5* | 15 | 60 |

*Displacement limited to 0.12 in. da

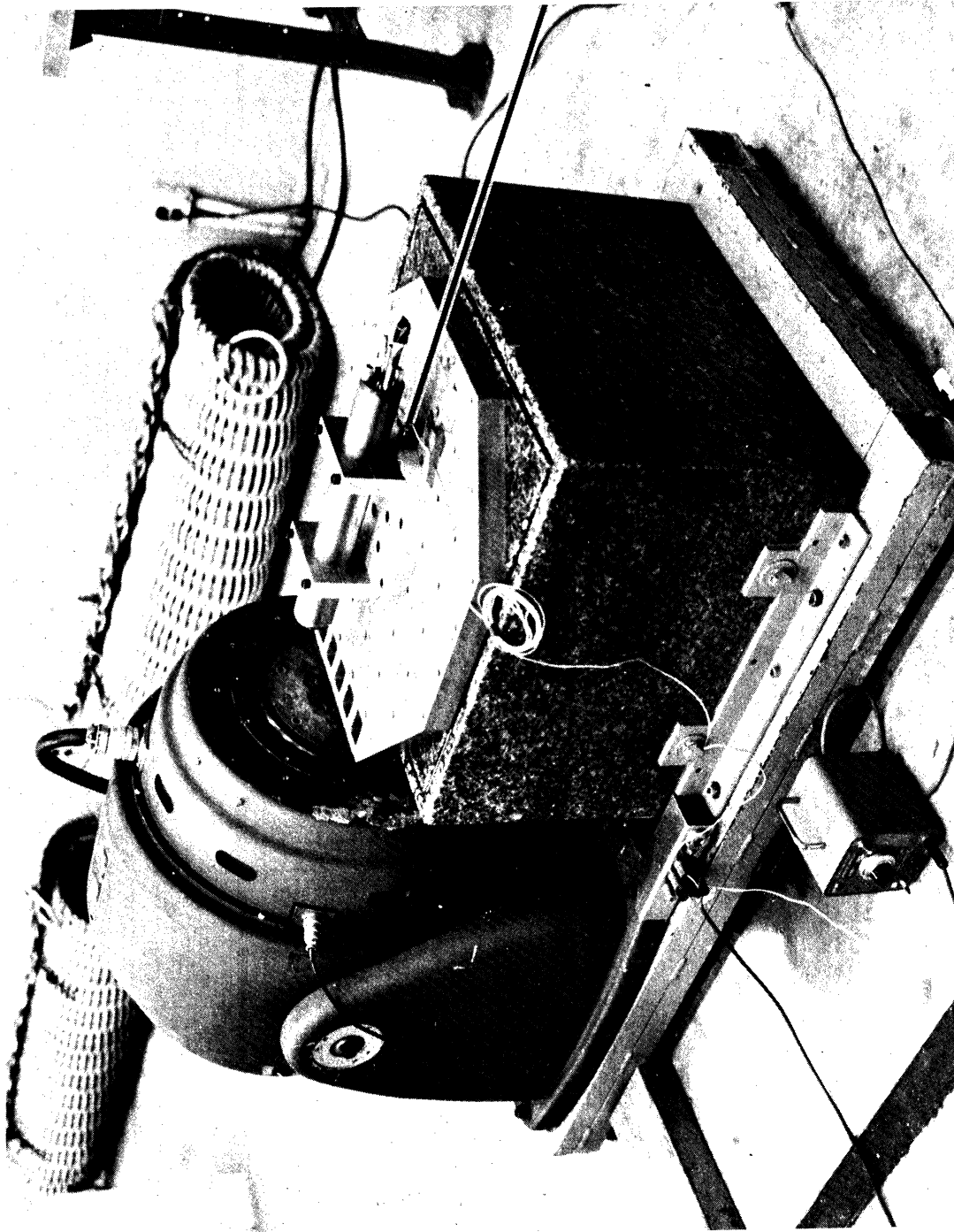


FIG. B.1 CONTROL ACCELEROMETER

Environmental Laboratories
VIBRATION LEVELS

Test Item: Electron Tube, TWT-148-3R
Test Date: 2 Sep 1964

Axis: Longitudinal

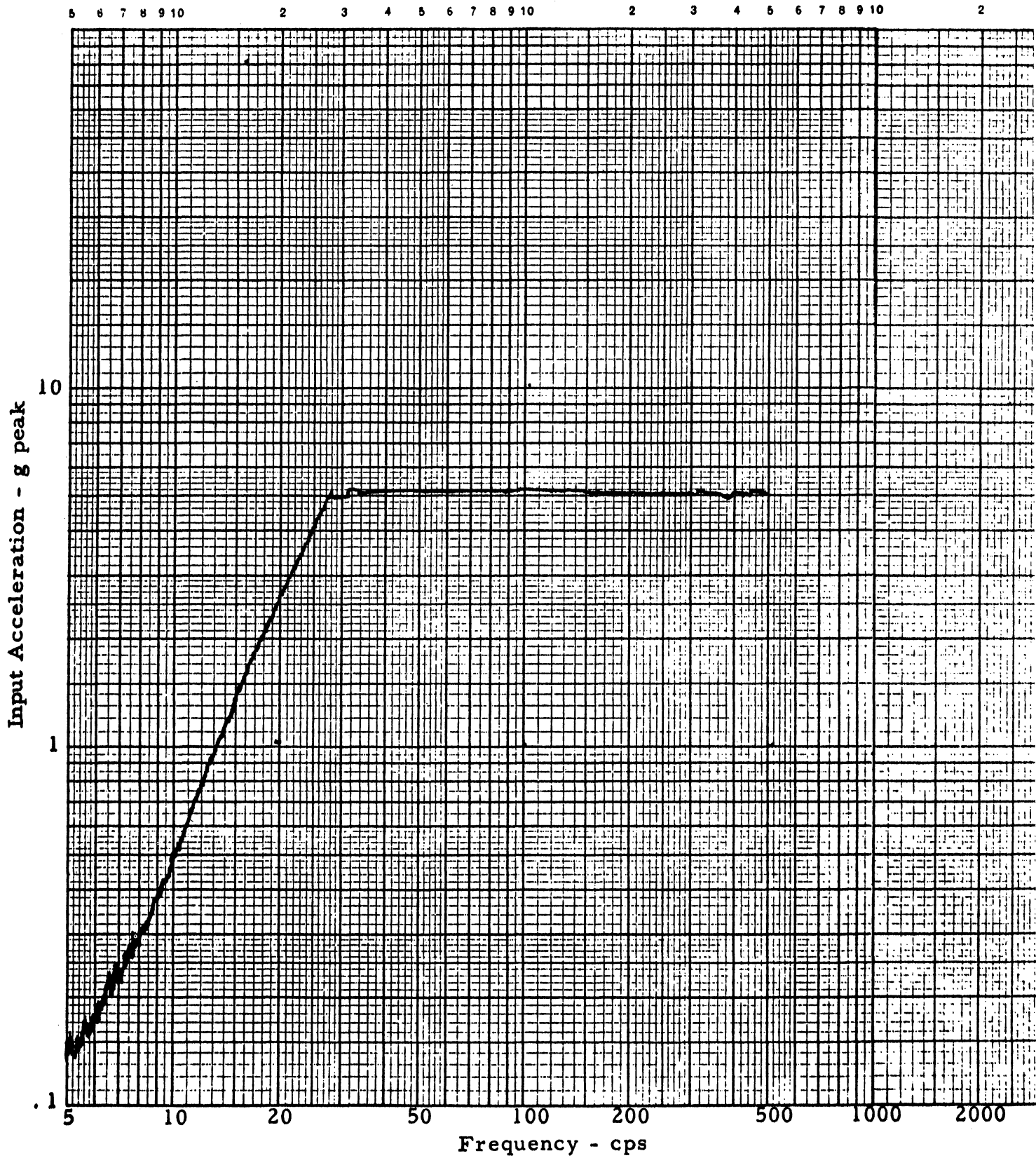


FIG. B.2 VIBRATION LEVELS

APPENDIX C
SHOCK TESTS
ENVIRONMENTAL LABORATORIES
TEST REPORT

REPORT NO. TR- 1012 DATE 8 Sep 64

PERFORMED FOR: Bendix Research Laboratories Division
20800 10 1/2 Mile Road
Southfield, Michigan

TEST: Shock

ITEM: Electron Tube, PN TWT-148-3R

TEST DATE: 4 Sep 64

PERFORMED AT: Space Laboratories

WORK ORDER NO: 82471-440-01-0100

AUTHORIZATION: P. O. 126744

REQUESTED BY: T. M. McKenzie

REPORT SENT TO: K. Earl

PREPARED BY: _____

R W Hyde
R. W. Hyde
Test Engineer
Systems Test Department

APPROVED BY: _____

R. H. Culpepper
R. H. Culpepper
Project Engineer
Systems Test Department

REFERENCE

- (a) Bendix Research Laboratories Division Test Plan (in accordance with MIL-E-1D, Paragraph 4.9.9, dated 31 March 1958), Paragraph C, Shock (nonoperating)

INTRODUCTION

An electron tube, PN TWT-148-3R, was shock tested in accordance with Reference (a). The test parameters are shown in Table 1.

SUMMARY OF RESULTS

No structural damage was observed as a result of the applied environment.

METHODS AND DATA

The test item was assembled in a fixture supplied by Bendix Research Laboratories Division and mounted on the shock test machine. An accelerometer was mounted near the base of the test item to measure the magnitude and duration of the shock pulse. The output of this accelerometer was connected to an oscilloscope with a polaroid camera attached. The test setup is shown in Figure 1.

Before mounting the test item, the drop height required to give a shock of 15 g at 11 msec was determined by trial drops.

The sensitivity of the accelerometer system was checked prior to the test by subjecting the accelerometer to a sinusoidal vibration of 0.25 in. double amplitude at a frequency of 44 cps, to give an acceleration of 25 g peak. Vibration displacement was measured with an optical wedge; frequency was measured with an electronic counter; and accelerometer system output was monitored with a true rms voltmeter. Calibration dates are shown on the attached list of test equipment.

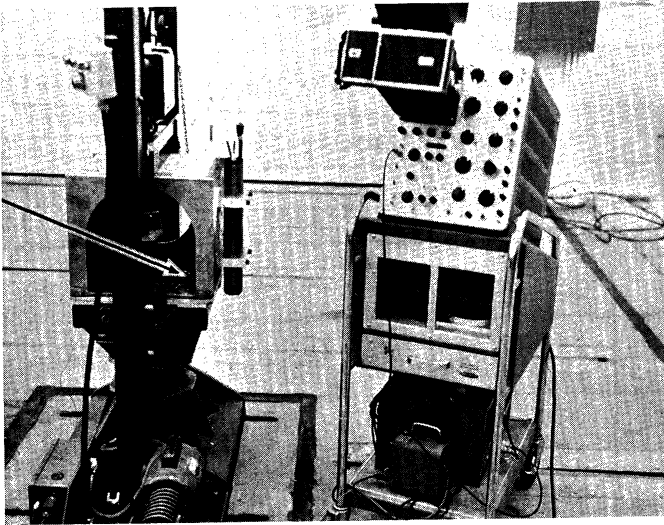
The tests were witnessed by K. Earl and D. Rice of the Bendix Research Laboratories Division who retained the test item.

Environmental Laboratories
SHOCK TEST PARAMETERS

| <u>No. of Shocks</u> | <u>Acceleration- Level-g</u> | <u>Pulse Duration- msec</u> | <u>Waveform</u> |
|----------------------|----------------------------------|---------------------------------|-----------------|
| 24* | 15 | 11 | Half-sine |

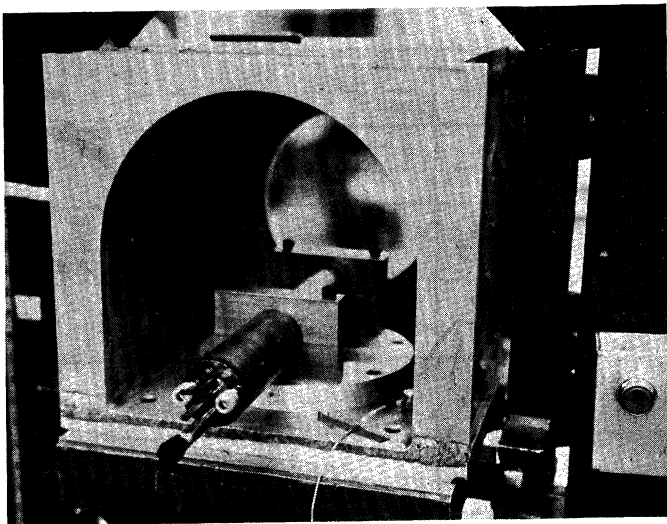
*6 shocks in each direction along the longitudinal axis
and 6 shocks along one direction of each of two lateral
axes.

Environmental Laboratories
SHOCK TEST

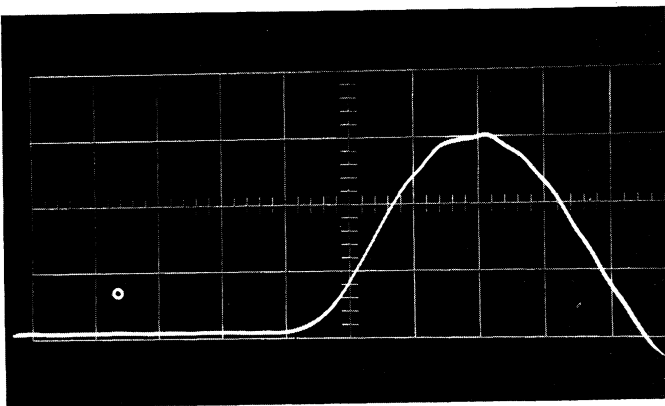


Longitudinal Axis
Test Setup

Showing Accelerometer
Location



Lateral Axis
Test Setup



Typical Shock Pulse

5 g/vertical division
2 msec/horizontal division

FIG. C.1 SHOCK TEST

APPENDIX D
R-F TEST SETUP

Figure D.1 shows a diagram of the power supply connections to the tube under test, while Figure D-2 shows a diagram of the r-f components in the test setup. For both the input and output networks, the meter readings are corrected by a factor which accounts for the insertion losses of the network components between the meter and the tube. The correction factors are determined from the calibration of

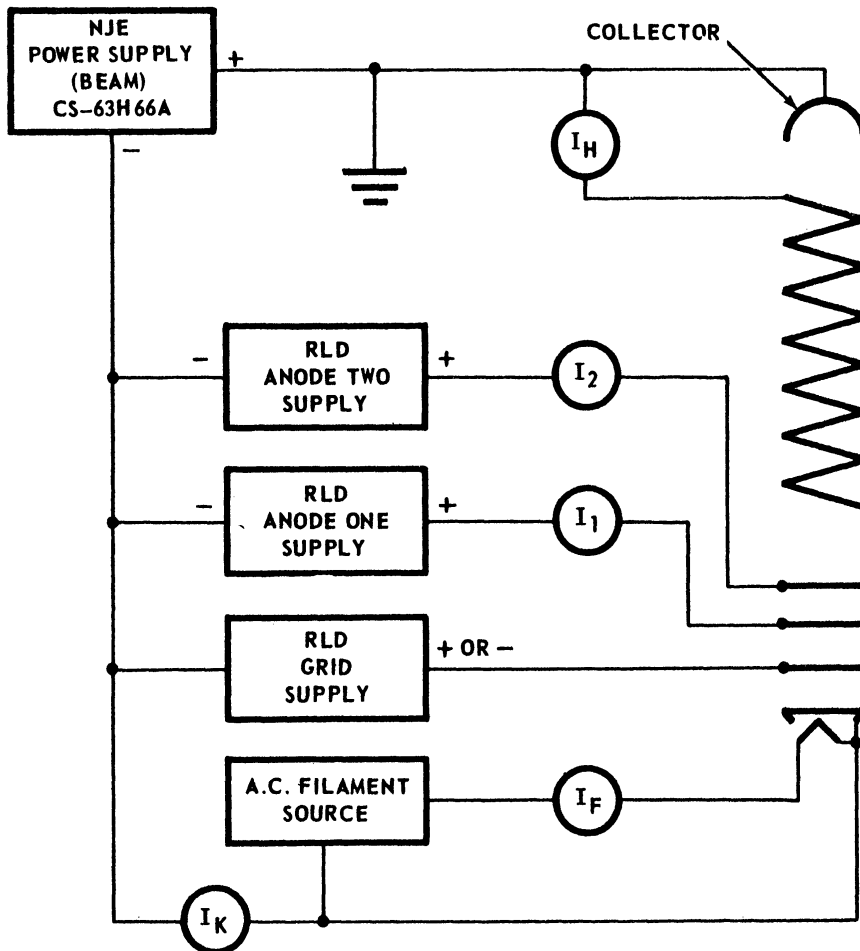


FIG. D.1 CRESTATRON D.C. POWER SUPPLY REQUIREMENTS.

components by a substitution method using a precision step attenuator as the substitute device.

Low pass filters, used in most measurements, are inserted between the tube output and the output power meter to eliminate harmonics from the measured power output.

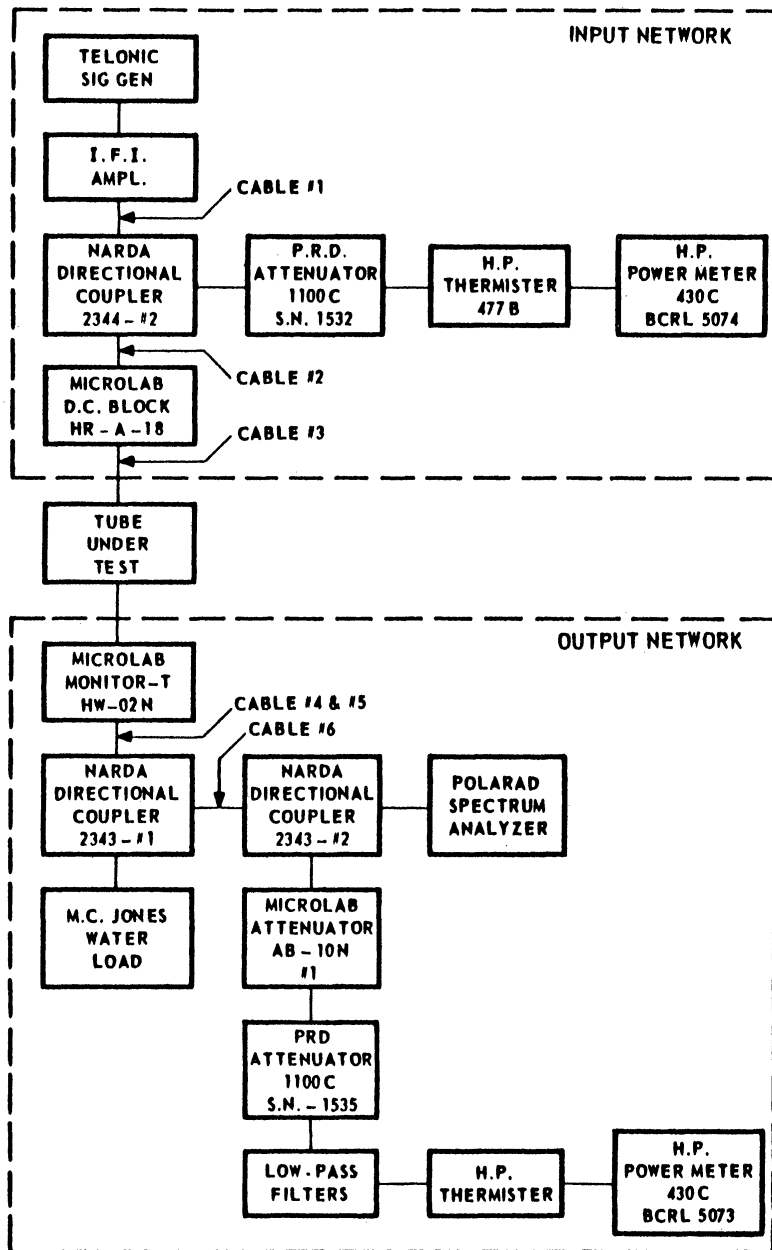


FIG. D-2 CRESTATRON R-F TEST EQUIPMENT (100-300 MC)

DISTRIBUTION LIST

| <u>No.</u> | <u>Copies</u> | <u>Agency</u> |
|------------|---------------|--|
| 1 | | Commanding Officer and Director, U. S. Navy Electronics Laboratory, San Diego 52, California |
| 2 | | Commander, Aeronautical Systems Division, Wright-Patterson Air Force Base, Ohio, Attn: ASRN |
| 1 | | Mr. J. Enright, ASRNET-1, Electronic Technology Laboratory, Aeronautical Systems Division, Wright-Patterson Air Force Base, Ohio |
| 1 | | Commanding Officer, Harry Diamond Laboratories, Electron Tube Branch, Washington 25, D. C. |
| 2 | | Commanding Officer, U. S. Army Electronics Research and Development Laboratory, Electron Devices Division, Fort Monmouth, New Jersey |
| 1 | | Commander, New York Naval Shipyard, Material Laboratory, Code 924, Naval Base, Brooklyn 1, New York |
| 2 | | Chief, Bureau of Naval Weapons, Department of the Navy, Washington 25, D. C., Attn: RAAV-4423 |
| 1 | | Chief, Bureau of Ships, Department of the Navy, Washington 25, D. C., Attn: Code 691A4 |
| 4 | | Chief, Bureau of Ships, Department of the Navy, Washington 25, D. C., Attn: Code 335 |
| 1 | | Director, U. S. Naval Research Laboratory, Washington 25, D. C., Attn: Code 5240, Dr. S. T. Smith |
| 1 | | Director, U. S. Naval Research Laboratory, Washington 25, D. C., Attn: Mr. L. A. Cosby, Code 5437 |
| 2 | | Director, U. S. Naval Research Laboratory, Washington 25, D. C., Attn: Library |
| 2 | | Advisory Group on Electron Tubes, 346 Broadway, 8th Floor, New York 13, New York |
| 1 | | Commanding General, Rome Air Development Center, Griffiss Air Force Base, Rome, New York, Attn: Documents Library RCOIL-2 |
| 1 | | Commander, Rome Air Development Center, Griffiss Air Force Base, Rome, New York, Attn: Mr. H. Chiosa, RCLRR-3 |
| 10 | | Commander, Defense Documentation Center, Cameron Station, Alexandria, Virginia |

| <u>No. Copies</u> | <u>Agency</u> |
|-------------------|---|
| 1 | Bendix Corporation, Systems Division, 3300 Plymouth Road, Ann Arbor, Michigan, Attn: Technical Library |
| 1 | Litton Industries, 960 Industrial Road, San Carlos, California, Attn: Technical Library |
| 1 | The University of Michigan, Willow Run Laboratories, Ypsilanti, Michigan, Attn: Dr. J. T. Wilson |
| 1 | Microwave Associates, Burlington, Massachusetts, Attn: Technical Library |
| 1 | Microwave Electronic Tube Company, Inc., Salem, Massachusetts, Attn: Technical Library |
| 1 | Radio Corporation of America, Power Tube Division, Harrison, New Jersey |
| 1 | Raytheon Company, Burlington, Massachusetts, Attn: Technical Library |
| 1 | S-F-D Laboratories, 800 Rahway Avenue, Union, New Jersey, Attn: Technical Library |
| 1 | Westinghouse Electric Corporation, P. O. Box 284, Elmira, New York, Attn: Technical Library |
| 2 | Scientific and Technical Information Facility Attn: NASA Representative (SAK/DL) P. O. Box 5700 Bethesda, Maryland 20014 |
| 1 | Dr. C. B. Sung, General Manager, Bendix Corporation, Research Laboratories, Northwestern Highway and 10-1/2 Mile Road, Southfield, Michigan |
| 1 | Dr. William Wiley, Manager, Applied Physics Dept., Bendix Corporation, Research Laboratories, Northwestern Highway and 10-1/2 Mile Road, Southfield, Michigan |

| | | | |
|---|--|---|--|
| <p>DD _____</p> <p>The University of Michigan, Electron Physics Laboratory, Ann Arbor, Michigan. RESEARCH AND DEVELOPMENT OF HIGH POWER CRESTATRONS FOR THE 100-300 MC FREQUENCY RANGE, by G. T. Konrad, September, 1965, 146 pp. incl. illus. (Contract No. N0bar-81403, Project Serial No. SF0100 201, Task No. 9294)</p> <p>Research and development work on VHF Crestatrons is described. Design parameters for both 100- and 1000-watt, cw, electrostatically focused tubes are presented. The 100-watt tube is described in much more detail, because it was completely tested. Details of the cold-test work, beam analyzer tests on the electron gun and focusing system, beam transmission tests and r-f tests are described fully.</p> <p>Digital computer programs are described, which were developed for the analysis of electrostatically focused beam systems. The gun region as well as the electrostatic focusing region can be analyzed. The designs of two $P_{\mu} = 20$ guns are checked with these computer programs.</p> <p>The details of design, construction and performance evaluation of a series of magnetically focused traveling-wave tubes for the 100-300 mc frequency region are presented. These tubes yield a minimum of 100 watts, cw at a minimum of 10 db gain throughout this frequency region. The three tubes to be delivered to the Navy were built so as to meet environmental specifications. Results of the environmental tests are presented.</p> | <p>UNCLASSIFIED</p> <p>PART I</p> <ol style="list-style-type: none"> 1. Electrostatically Focused Tubes Amplifiers 2. High Perveance Hollow-Beam Gun Studies <p>PART II</p> <ol style="list-style-type: none"> 1. Electrostatically Focused Tubes 2. Phase I--100-Watt Magnetically Focused Crestatron Feasibility Studies 3. Phase II--Development of Deliverable 100-Watt Magnetically Focused Crestatron <p>I. Konrad, G. T.</p> | <p>DD _____</p> <p>The University of Michigan, Electron Physics Laboratory, Ann Arbor, Michigan. RESEARCH AND DEVELOPMENT OF HIGH POWER CRESTATRONS FOR THE 100-300 MC FREQUENCY RANGE, by G. T. Konrad, September, 1965, 146 pp. incl. illus. (Contract No. N0bar-81403, Project Serial No. SF0100 201, Task No. 9294)</p> <p>Research and development work on VHF Crestatrons is described. Design parameters for both 100- and 1000-watt, cw, electrostatically focused tubes are presented. The 100-watt tube is described in much more detail, because it was completely tested. Details of the cold-test work, beam analyzer tests on the electron gun and focusing system, beam transmission tests and r-f tests are described fully.</p> <p>Digital computer programs are described, which were developed for the analysis of electrostatically focused beam systems. The gun region as well as the electrostatic focusing region can be analyzed. The designs of two $P_{\mu} = 20$ guns are checked with these computer programs.</p> <p>The details of design, construction and performance evaluation of a series of magnetically focused traveling-wave tubes for the 100-300 mc frequency region are presented. These tubes yield a minimum of 100 watts, cw at a minimum of 10 db gain throughout this frequency region. The three tubes to be delivered to the Navy were built so as to meet environmental specifications. Results of the environmental tests are presented.</p> | <p>UNCLASSIFIED</p> <p>PART I</p> <ol style="list-style-type: none"> 1. Electrostatically Focused Tubes Amplifiers 2. High Perveance Hollow-Beam Gun Studies <p>PART II</p> <ol style="list-style-type: none"> 1. Electrostatically Focused Tubes 2. Phase I--100-Watt Magnetically Focused Crestatron Feasibility Studies 3. Phase II--Development of Deliverable 100-Watt Magnetically Focused Crestatron <p>I. Konrad, G. T.</p> |
| <p>DD _____</p> <p>The University of Michigan, Electron Physics Laboratory, Ann Arbor, Michigan. RESEARCH AND DEVELOPMENT OF HIGH POWER CRESTATRONS FOR THE 100-300 MC FREQUENCY RANGE, by G. T. Konrad, September, 1965, 146 pp. incl. illus. (Contract No. N0bar-81403, Project Serial No. SF0100 201, Task No. 9294)</p> <p>Research and development work on VHF Crestatrons is described. Design parameters for both 100- and 1000-watt, cw, electrostatically focused tubes are presented. The 100-watt tube is described in much more detail, because it was completely tested. Details of the cold-test work, beam analyzer tests on the electron gun and focusing system, beam transmission tests and r-f tests are described fully.</p> <p>Digital computer programs are described, which were developed for the analysis of electrostatically focused beam systems. The gun region as well as the electrostatic focusing region can be analyzed. The designs of two $P_{\mu} = 20$ guns are checked with these computer programs.</p> <p>The details of design, construction and performance evaluation of a series of magnetically focused traveling-wave tubes for the 100-300 mc frequency region are presented. These tubes yield a minimum of 100 watts, cw at a minimum of 10 db gain throughout this frequency region. The three tubes to be delivered to the Navy were built so as to meet environmental specifications. Results of the environmental tests are presented.</p> | <p>UNCLASSIFIED</p> <p>PART I</p> <ol style="list-style-type: none"> 1. Electrostatically Focused Tubes Amplifiers 2. High Perveance Hollow-Beam Gun Studies <p>PART II</p> <ol style="list-style-type: none"> 1. Electrostatically Focused Tubes 2. Phase I--100-Watt Magnetically Focused Crestatron Feasibility Studies 3. Phase II--Development of Deliverable 100-Watt Magnetically Focused Crestatron <p>I. Konrad, G. T.</p> | <p>DD _____</p> <p>The University of Michigan, Electron Physics Laboratory, Ann Arbor, Michigan. RESEARCH AND DEVELOPMENT OF HIGH POWER CRESTATRONS FOR THE 100-300 MC FREQUENCY RANGE, by G. T. Konrad, September, 1965, 146 pp. incl. illus. (Contract No. N0bar-81403, Project Serial No. SF0100 201, Task No. 9294)</p> <p>Research and development work on VHF Crestatrons is described. Design parameters for both 100- and 1000-watt, cw, electrostatically focused tubes are presented. The 100-watt tube is described in much more detail, because it was completely tested. Details of the cold-test work, beam analyzer tests on the electron gun and focusing system, beam transmission tests and r-f tests are described fully.</p> <p>Digital computer programs are described, which were developed for the analysis of electrostatically focused beam systems. The gun region as well as the electrostatic focusing region can be analyzed. The designs of two $P_{\mu} = 20$ guns are checked with these computer programs.</p> <p>The details of design, construction and performance evaluation of a series of magnetically focused traveling-wave tubes for the 100-300 mc frequency region are presented. These tubes yield a minimum of 100 watts, cw at a minimum of 10 db gain throughout this frequency region. The three tubes to be delivered to the Navy were built so as to meet environmental specifications. Results of the environmental tests are presented.</p> | <p>UNCLASSIFIED</p> <p>PART I</p> <ol style="list-style-type: none"> 1. Electrostatically Focused Tubes Amplifiers 2. High Perveance Hollow-Beam Gun Studies <p>PART II</p> <ol style="list-style-type: none"> 1. Electrostatically Focused Tubes 2. Phase I--100-Watt Magnetically Focused Crestatron Feasibility Studies 3. Phase II--Development of Deliverable 100-Watt Magnetically Focused Crestatron <p>I. Konrad, G. T.</p> |

| | | | |
|--|---|---|---------------------|
| <p>DD</p> <p>The University of Michigan, Electron Physics Laboratory, Ann Arbor, Michigan. RESEARCH AND DEVELOPMENT OF HIGH POWER CRESTATrons FOR THE 100-500 MC FREQUENCY RANGE, by G.T. Konrad, September, 1965, 146 pp. incl. illus. (Contract No. N0bsr-81403, Project Serial No. SF0100 201, Task No. 9294)</p> <p>Research and development work on VHF Crestatrons is described. Design parameters for both 100- and 1000-watt, cw, electrostatically focused tubes are presented. The 100-watt tube is described in much more detail, because it was completely tested. Details of the cold-test work, beam analyzer tests on the electron gun and focusing system, beam transmission tests and r-f tests are described fully.</p> <p>Digital computer programs are described, which were developed for the analysis of electrostatically focused beam systems. The gun region as well as the electrostatic focusing region can be analyzed. The designs of two $\mu = 20$ guns are checked with these computer programs.</p> <p>The details of design, construction and performance evaluation of a series of magnetically focused traveling-wave tubes for the 100-500 mc frequency region are presented. These tubes yield a minimum of 100 watts, cw at a minimum of 10 db gain throughout this frequency region. The three tubes to be delivered to the Navy were built so as to meet environmental specifications. Results of the environmental tests are presented.</p> | <p>UNCLASSIFIED</p> <p>PART I</p> <ol style="list-style-type: none"> 1. Electrostatically Focused 100-Watt VHF Amplifiers 2. High Perveance Hollow-Beam Gun Studies <p>PART II</p> <ol style="list-style-type: none"> 1. Electrostatically Focused Tubes 2. Phase I--100-Watt Magnetically Focused Crestatron Feasibility Studies 3. Phase II--Development of Deliverable 100-Watt Magnetically Focused Crestatron <p>I. Konrad, G. T.</p> | <p>UNCLASSIFIED</p> <p>PART I</p> <ol style="list-style-type: none"> 1. Electrostatically Focused 100-Watt VHF Amplifiers 2. High Perveance Hollow-Beam Gun Studies <p>PART II</p> <ol style="list-style-type: none"> 1. Electrostatically Focused Tubes 2. Phase I--100-Watt Magnetically Focused Crestatron Feasibility Studies 3. Phase II--Development of Deliverable 100-Watt Magnetically Focused Crestatron <p>I. Konrad, G. T.</p> | <p>UNCLASSIFIED</p> |
| <p>DD</p> <p>The University of Michigan, Electron Physics Laboratory, Ann Arbor, Michigan. RESEARCH AND DEVELOPMENT OF HIGH POWER CRESTATrons FOR THE 100-500 MC FREQUENCY RANGE, by G.T. Konrad, September, 1965, 146 pp. incl. illus. (Contract No. N0bsr-81403, Project Serial No. SF0100 201, Task No. 9294)</p> <p>Research and development work on VHF Crestatrons is described. Design parameters for both 100- and 1000-watt, cw, electrostatically focused tubes are presented. The 100-watt tube is described in much more detail, because it was completely tested. Details of the cold-test work, beam analyzer tests on the electron gun and focusing system, beam transmission tests and r-f tests are described fully.</p> <p>Digital computer programs are described, which were developed for the analysis of electrostatically focused beam systems. The gun region as well as the electrostatic focusing region can be analyzed. The designs of two $\mu = 20$ guns are checked with these computer programs.</p> <p>The details of design, construction and performance evaluation of a series of magnetically focused traveling-wave tubes for the 100-500 mc frequency region are presented. These tubes yield a minimum of 100 watts, cw at a minimum of 10 db gain throughout this frequency region. The three tubes to be delivered to the Navy were built so as to meet environmental specifications. Results of the environmental tests are presented.</p> | <p>UNCLASSIFIED</p> <p>PART I</p> <ol style="list-style-type: none"> 1. Electrostatically Focused 100-Watt VHF Amplifiers 2. High Perveance Hollow-Beam Gun Studies <p>PART II</p> <ol style="list-style-type: none"> 1. Electrostatically Focused Tubes 2. Phase I--100-Watt Magnetically Focused Crestatron Feasibility Studies 3. Phase II--Development of Deliverable 100-Watt Magnetically Focused Crestatron <p>I. Konrad, G. T.</p> | <p>UNCLASSIFIED</p> <p>PART I</p> <ol style="list-style-type: none"> 1. Electrostatically Focused 100-Watt VHF Amplifiers 2. High Perveance Hollow-Beam Gun Studies <p>PART II</p> <ol style="list-style-type: none"> 1. Electrostatically Focused Tubes 2. Phase I--100-Watt Magnetically Focused Crestatron Feasibility Studies 3. Phase II--Development of Deliverable 100-Watt Magnetically Focused Crestatron <p>I. Konrad, G. T.</p> | <p>UNCLASSIFIED</p> |
| <p>DD</p> <p>The University of Michigan, Electron Physics Laboratory, Ann Arbor, Michigan. RESEARCH AND DEVELOPMENT OF HIGH POWER CRESTATrons FOR THE 100-500 MC FREQUENCY RANGE, by G.T. Konrad, September, 1965, 146 pp. incl. illus. (Contract No. N0bsr-81403, Project Serial No. SF0100 201, Task No. 9294)</p> <p>Research and development work on VHF Crestatrons is described. Design parameters for both 100- and 1000-watt, cw, electrostatically focused tubes are presented. The 100-watt tube is described in much more detail, because it was completely tested. Details of the cold-test work, beam analyzer tests on the electron gun and focusing system, beam transmission tests and r-f tests are described fully.</p> <p>Digital computer programs are described, which were developed for the analysis of electrostatically focused beam systems. The gun region as well as the electrostatic focusing region can be analyzed. The designs of two $\mu = 20$ guns are checked with these computer programs.</p> <p>The details of design, construction and performance evaluation of a series of magnetically focused traveling-wave tubes for the 100-500 mc frequency region are presented. These tubes yield a minimum of 100 watts, cw at a minimum of 10 db gain throughout this frequency region. The three tubes to be delivered to the Navy were built so as to meet environmental specifications. Results of the environmental tests are presented.</p> | <p>UNCLASSIFIED</p> <p>PART I</p> <ol style="list-style-type: none"> 1. Electrostatically Focused 100-Watt VHF Amplifiers 2. High Perveance Hollow-Beam Gun Studies <p>PART II</p> <ol style="list-style-type: none"> 1. Electrostatically Focused Tubes 2. Phase I--100-Watt Magnetically Focused Crestatron Feasibility Studies 3. Phase II--Development of Deliverable 100-Watt Magnetically Focused Crestatron <p>I. Konrad, G. T.</p> | <p>UNCLASSIFIED</p> <p>PART I</p> <ol style="list-style-type: none"> 1. Electrostatically Focused 100-Watt VHF Amplifiers 2. High Perveance Hollow-Beam Gun Studies <p>PART II</p> <ol style="list-style-type: none"> 1. Electrostatically Focused Tubes 2. Phase I--100-Watt Magnetically Focused Crestatron Feasibility Studies 3. Phase II--Development of Deliverable 100-Watt Magnetically Focused Crestatron <p>I. Konrad, G. T.</p> | <p>UNCLASSIFIED</p> |

UNIVERSITY OF MICHIGAN



3 9015 03466 2133